AN *IN VITRO* STUDY OF THE EFFECTS OF FREE FATTY ACIDS ON INSULIN MEDIATED GLUCOSE UPTAKE AND METABOLISM BY MYOCYTES AND FIBROBLAST DERIVED ADIPOCYTES

Sithandiwe Eunice Mazibuko

Student number: 022468

A thesis submitted in fulfilment of the requirements for the degree of MSc in Biochemistry in the Faculty of Biochemistry and Microbiology, University of Zululand

Supervisor: Dr Christo Muller

Co-supervisor: Prof Andy Opoku and Dr Carmen Pheiffer

January 2011

Declaration

I,……, hereby declare that the work on which this thesis is based is my original work (except where acknowledgements indicate otherwise), and that neither the whole work or part of it has been, is being, or is to be submitted for another degree in this or any other university.
I empower the University of Zululand to reproduce for the purpose of research either the whole or any portion of the contents in any manner whatsoever.

Signature: …….. Date: …….

Sithandiwe Eunice Mazibuko (student number: 022468)

ABSTRACT

Introduction

The incidence of type 2 diabetes (T2D) is increasing at an alarming rate, especially in developing countries, including South Africa. In developing countries, changes in lifestyle, especially the increase in the consumption of a westernized diet, rich in fats and sugar, is associated with hyperlipidemia, obesity and development of T2D. Skeletal muscle and adipose tissues are the major tissues involved with post-prandial peripheral glucose disposal in response to insulin. Insulin resistance reduces the ability to clear glucose from the circulation resulting in hyperinsulinemia and hyperglycemia with the development of T2D. High levels of plasma free fatty acids (FFAs), particulary saturated FFAs such as palmitate, are associated with insulin resistance in muscle and adipose tissue. Monounsaturated FFAs, such as oleate and essential FFAs such as omega 3 and omega 6 are claimed to be beneficial and to improve insulin sensitivity.

Aim

This study aims to determine the *in vitro* effect of the free fatty acids (FFAs) palmitate, oleate, omega 3 and omega 6 on insulin-stimulated glucose metabolism in myocytes and adipocytes.

Materials and methods

Mouse C2C12 and rat L8 cells were differentiated into myocytes and myotubules by serum deprivation, while mouse 3T3-L1 fibroblasts were differentiated into adipocytes by culturing in 3-isobutyl-1-methylxanthine (IBMX), dexamenthasone and insulin. Myocytes and adpipocytes were cultured in DMEM containing 5.5 mM or 20 mM glucose supplemented with 0.75 mM of each of the respective FFAs (i.e. palmitate, oleate, omega 3 and omega 6) for 24 hours. Thereafter media was replaced with fresh media containing 0.75 mM of each of the FFAs with or without insulin stimulation in the last hour.

Glucose uptake was measured using a 2-deoxy-[^{3}H]-D-glucose method. Glycogen and glucose-6-phosphate (G6P) concentrations were determined using commercial kits. Glucose oxidation was measured by $^{14}CO_2$ release from cells incubated with glucose D-[^{14}C(U)]. Cell viability and mitochondrial dehydrogenase activity was assessed using the 3-(4, 5-dimethylthiazol-2-yl)-2, 5-diphenyl tetrazolium bromide method. Quantitative real-time PCR was used to measure messenger RNA levels of selected genes involved in the insulin signaling pathway.

Results

The different FFAs tested had varying effects in C2C12 and L8 myocytes, and 3T3-L1 adipocytes cultured in media containing 5.5 mM or 20 mM glucose. Palmitate decreased both basal and insulin-stimulated glucose uptake in C2C12 myocytes cultured in 5.5 mM and 20 mM glucose. Oleate decreased insulin stimulated glucose uptake in cells cultured in 5.5 mM glucose but had no effect at 20 mM glucose. The essential FFAs had no effect on glucose uptake.

In L8 myocytes, palmitate decreased both basal and insulin-stimulated glucose uptake at 5.5 mM glucose, while only insulin-stimulated glucose uptake was reduced at 20 mM glucose. Neither oleate, omega 3 nor omega 6 affected basal glucose uptake in cells cultured in 5.5 mM or 20 mM glucose. However, at 20 mM glucose these three FFAs reduced insulin-stimulated glucose uptake.

In contrast to myocytes, none of the FFAs affected basal or insulin-stimulated glucose uptake in 3T3-L1 adipocytes cultured at 5.5 mM glucose. However at 20 mM glucose only palmitate reduced both basal and insulin-stimulated.

In terms of glucose metabolism, palmitate decreased basal and insulin-stimulated G6P concentrations in C2C12 myocytes cultured in 5.5 mM and 20 mM glucose. Oleate increased basal G6P concentrations at 5.5 mM glucose, but had no effect at 20 mM glucose. Omega 3 increased and omega 6 decreased basal G6P

concentrations at both 5.5 mM and 20 mM glucose. At 5.5 mM glucose, oleate had no effect on insulin-stimulated G6P concentrations, while omega 3 and omega 6 decreased G6P concentrations. At 20 mM glucose these three FFAs increased insulin-stimulated G6P concentrations. In L8 myocytes palmitate, oleate and omega 3 reduced basal G6P concentrations, while omega 6 increased basal G6P concentrations when cultured in 5.5 mM glucose. At 20 mM glucose palmitate and oleate decresed both basal and insulin-stimulated G6P concentrations, while only insulin-stimulated G6P concentrations were decreased by omega 3 and omega 6. In 3T3-L1 adipocytes basal G6P was not affected by all the FFAs at 5.5 mM glucose. However, insulin-stimulated G6P was reduced by palmitate and omega 3. All of the FFAs increased basal G6P concentrations at 20 mM glucose in 3T3-L1 adipocytes. Only oleate decreased insulin-stimulated G6P at 20 mM glucose.

In C2C12 myocytes none of the FFAs had an affect on basal or insulin-stimulated glycogen concentrations at 5.5 mM or 20 mM glucose. In L8 myocytes cultured in 5.5 mM glucose palmitate, oleate and omega 3 increased basal glycogen concentrations. Palmitate, oleate and omega 6 decreased insulin-stimulated glycogen concentrations. At 20 mM glucose, oleate, omega 3 and omega 6 increased basal glycogen concentrations while none of the FFAs had an effect on insulin stimuated glycogen concentration. In 3T3-L1 adipocytes cultured in 5.5 mM glucose only omega 3 and omega 6 reduced basal glycogen concentrations. None of the FFAs effected glycogen concentrations at 20 mM glucose.

In C2C12 myocytes cultured in 5.5 mM glucose, none of the FFAs affected basal glucose oxidation. Palmitate decreased and oleate inceased insulin-stimulated glucose oxidation. In L8 myocytes only palmitate decreased basal glucose oxidation. Palmitate, oleate and omega 6 reduced insulin-stimulated glucose oxidation at 5.5 mM glucose. In 3T3-L1 adipocytes none of the FFAs affected basal glucose oxidation at 5.5 mM glucose. At 20 mM glucose all of the FFAs reduced both basal and insulin-stimulated glucose oxidation in all three cell lines used.

In C2C12 myocytes, palmitate downregulated insulin-stimulated mRNA expression of Irs1, Pi3k and Glut4 although this was not statistically significant.

Conclusion

At equimolar concentrations, palmitate exerted the worse effect on basal and insulin-stimulated glucose uptake compared to oleate, omega 3 and omega 6 in all cell lines used. In terms of glucose metabolism, all the FFAs tested had a minimal effect on glycogen storage, while all FFAs decreased glucose oxidation especially at the 20 mM glucose concentration.

These findings are in agreement with previous studies where FFAs compete with glucose for substrate oxidation. However, palmitate has additional effects on glucose uptake which could be related to the accumulation of lipid metabolites such as diacylglycerol and ceramide. In 3T3-L1 adipocytes palmitate reduced glucose uptake only at 20 mM glucose. This supports the hypothesis that adipocytes in contrast to myocytes retain their insulin sensitivity at normoglycemic conditions (5.5 mM glucose) but not at at hyperglycemic conditions (20 mM glucose).

Although not statistically significant, palmitate treatment of C2C12 myocytes decreased the mRNA expression of genes involved in the insulin signalling pathway. Taken together our results confirm that saturated FFA such as palmitate could contribute to and exacerbate insulin resistance

ACKNOWLEDGEMENTS

I would like to express my sincere gratitude and appreciation to my supervisor Dr CJF Muller and co-supervisors, Professor A Opoku and Dr C Pheiffer, for their assistance and guidance throughout the project.

In addition, I would like to thank Dr J Louw of the Diabetes Discovery Platform for giving me the opportunity to study in his unit. I would also like to thank my colleagues of the Diabetes Discovery Platform for technical assistance.

Special thanks go to my husband Mduduzi Mbeje, my son Lwandle and my family for their constant encouragement and support during this study.

Most of all I would like to thank God almighty for the strength He gave me to finish this project.

Financial support for this study was provided by the Diabetes Discovery Platform of the South African Medical Research Council and the University of Zululand.

TABLE OF CONTENTS

ABBREVIATIONS

β-cells	Beta cells
Act B	Beta actin
ADP	Adenosine-5-diphosphate
Akt	Threonine kinase B
ATCC	American Type Culture Collection
ATP	Adenosine-5- triphosphate
BSA	Bovine serum albumin
CD36/FAT	Fatty acid translocase
cDNA	Complementary deoxyribonucleic acid
CO_2	Carbon dioxide
CPM	Counts per minute
CPTI	Carnitine palmitoyltransferase one
DAG	Diacylglycerol
DMEM	Dulbecco's Modified Eagle's Medium
DMSO	Dimethyl sulfoxide
DOG	2-deoxy-[^{3}H]-D-glucose
DPBS	Dulbecco's phosphate buffered saline
DPM	Disintegrations per minute
EFFAs	Essential free fatty acids
EtOH	Ethanol
F6P	Fructose-6-phosphate
FABP	Fatty acid binding protein
FABPc	Cytoplasmic fatty acid binding protein
FABPpm	Plasma membrane fatty acid binding protein
FATP	Fatty acid transporter protein
FATP1	Fatty acid transporter one
FBP	Fructose-1,6-biphosphate
FCS	Fetal calf serum
FFA	Free fatty acid
FOXO1	Forkhead box protein O1

G6P	Glucose-6-phosphate
G6PD	glucose-6-phosphate dehydrogenase
GLUT	Glucose transporter
GLUT1	Glucose transporter one
GLUT2	Glucose transporter two
GLUT3	Glucose transporter three
GLUT4	Glucose transporter four
GSK3	Glycogen synthase kinase three
Gsy	Glycogen synthase
HDL	High density lipoprotein
HS	Horse serum
HSL	Hormone sensitive lipase
IBMX	3-isobutyl-1-methylxanthine
IDDM	Insulin-dependent diabetes mellitus
IR	Insulin receptor
IRS	Insulin receptor substrate
IRS 1 and IRS 2	Insulin receptor substrate one and two
JNK	c-Jun N-terminal kinases
LCFA	Long chain fatty acids
LPL	Lipoprotein lipase
MAPK	Mitogen activated protein kinase
MAPK	Mitogen-activated protein kinase
mRNA	Messenger ribonucleic acid
MTT	3-(4, 5-dimethylthiazol-2-yl)-2, 5-diphenyl tetrazolium bromide
MUFFAs	Monounsaturated free fatty acids
$NaHCO_3$	Sodium bicarbonate
NaOH	Sodium hydroxide
NFκB	Nuclear factor kappa beta
OD	Optical density
PCA	Perchloric acid
PDK-1	Pyruvate dehydrogenase kinase, isozyme 1
PEP	Phosphoenolpyruvate

PFK	Phosphofructokinase
PI3k	Phosphatidylinositol 3 kinase
PIP_3	Phosphatidylinositol (3, 4, 5)-triphosphate
PKC	Atypical protein kinase C
PKCθ.	Protein kinase theta
PPARs	Peroxisome proliferator-activated receptors
qRT-PCR	Quantitative real-time polymerase chain reaction
SDS	Sodium dodecyl sulphate
SFFAs	Saturated free fatty acids
SH2	Src homology 2 domain
SHC	Src homologous and collagen protein
STZ	Streptozotocin
T2D	Type 2 diabetes
TCA	Tricarboxylic citric acid
TG	Triglycerides
UFFAs	Unsaturated free fatty acids
VLDL	Very low density lipoproteins
WHO	World Health Organisation

LIST OF TABLES

LIST OF FIGURES

Chapter 1

Literature review

1.1 Introduction

There are two main types of diabetes, type 1 and type 2 diabetes mellitus. Type 1 diabetes mellitus is also referred to as insulin-dependent diabetes mellitus (IDDM), and is due to the inability of the pancreas to secrete insulin (Skyler, 2007). Type 2 diabetes (T2D), also called non-insulin dependent diabetes (NIDDM) or adult-onset diabetes, is the most common form of diabetes accounting for approximately 90% of cases worldwide (Nolan *et al.,* 2006). T2D, a disorder of glucose and insulin metabolism is characterised by high blood glucose levels and reduced insulin sensitivity (Thevonod, 2008; Prashanth *et al.,* 2009). The World Health Organisation (WHO) classifies an individual with fasting plasma glucose levels of ≥7.0 mmol/l as diabetic (Davidoff, 1997; Seino *et al.,* 2010). T2D is a multifactorial disease that occurs primarily in adults and is associated with insulin resistance, dyslipidemia and obesity. However, T2D is becoming prevalent amongst children, particulary in obese children. It is essentially a lifestyle disease that can be managed by exercise and diet. Early detection is crucial to improve the management of T2D (Rosenbloom *et al.,* 2009).

T2D is a major cause of morbity and mortality. An estimated 285 million adults are affected with T2D worldwide. Predictions are that this figure is expected to rise to between 366 and 439 million individuals by 2030 (Wild *et al.,* 2004; Kumar and Singh, 2010, Shaw *et al.,* 2010). Traditionally, T2D was considered a disease of developed nations, however, the prevalence of T2D is increasing at alarming rates in developing countries. In Sub-Saharan Africa the prevalence of T2D is estimated at 7.1 million and expected to rise to 18.6 million by 2030. Reasons for the high incidence of T2D in developing countries include, amongst the others, increased prosperity, urbanisation and a shift towards a “westernized lifestyle” (Wild *et al.,* 2004).

1.2 Risk factors associated with type 2 diabetes

A number of risk factors associated with the development of T2D have been identified. These include, amongst others, genetics, lifestyle, nutrition, lack of physical activity and obesity (Hays *et al.,* 2008; Räisänen *et al.,* 2008). There is a strong correlation between the development of metabolic syndrome and T2D. Insulin resistance, increased waist circumference, increased triglycerides, reduced high density lipoprotein (HDL) cholesterol, increased blood pressure and increased fasting glucose are features of the metabolic syndrome (Imai *et al.,* 2010).

The development of insulin resistance is associated with diet, specifically a westernized, high fat diet that is rich in saturated fats and sugar (Hu, 2001). Insulin resistance affects the body's ability to maintain normoglycemia resulting in hyperglycemia. The resultant chronic hyperglycemia and associated hyperlipidemia further exacerbates insulin resistance and the progression towards T2D (Goalstone and Draznin, 1997; Youngren, 2007; Prashanth *et al.*, 2009).

1.3 Glucose

Glucose is a simple sugar (monosaccharide) that cells use for energy. It is essential for normal cell function. The naturally occurring stereoisomer of glucose is D-glucose or dextrose ($C_6H_{12}O_6$) (Schenck, 2006). Glucose is used as a biological fuel during aerobic and anaerobic respiration or fermentation. Aerobic respiration is the most efficient means of glucose utilization, yielding 32 molecules of adenosine-5'-triphosphate (ATP) during the processes of glycolysis and oxidative phosphorylation. Anaerobic respiration yields only 2 molecules of ATP (Mauseth, 2009, Van der Heiden *et al.,* 2009).

1.4 The glucose transporters

Due to the hydrophilic nature of glucose, cell membranes are effectively impermeable to glucose, therefore it must be transported actively across the plasma membrane by specific carrier proteins referred to as the glucose transporter (GLUT) family of facilitative glucose transporters (Calvo *et al.,* 2010). The glucose transporters or solute carrier family 2 (GLUT or SLC2) are a family of proteins that facilitate the transport of glucose into the cell (Gorovits and Charron, 2003). The transport of glucose across the plasma membrane is controlled by various factors, one of which is the expression of appropriate glucose transporters at the surface of the cell. The synthesis, post-transcriptional modifications and subsequent translocation of the glucose transport proteins is under hormonal regulation and play an essential role in glucose homeostasis (Brown, 2000).

The glucose transporters are integral membrane proteins that contain 12 membrane-spanning α-helices with both the amino and carboxyl termini exposed on the cytoplasmic side of the plasma membrane (Figure 1). Active transport of glucose across the plasma membrane by the relevant glucose transporter involves the binding of glucose to the extracellular side of the glucose transporter. This leads to conformational changes to the glucose transporter complex, whereafter the glucose is transported to the cytoplasmic side of the plasma membrane. Thereafter, glucose is released into the cytoplasm from the binding site. Once the glucose is released from the transporter, the unoccupied transporter changes back to its original conformation with its binding site at the cell surface (Kahn, 1992). It is generally accepted that five of these α-helixes form the hydrophilic pore through which glucose is transported (Mueckler, 1994; Olson and Pessin 1996).

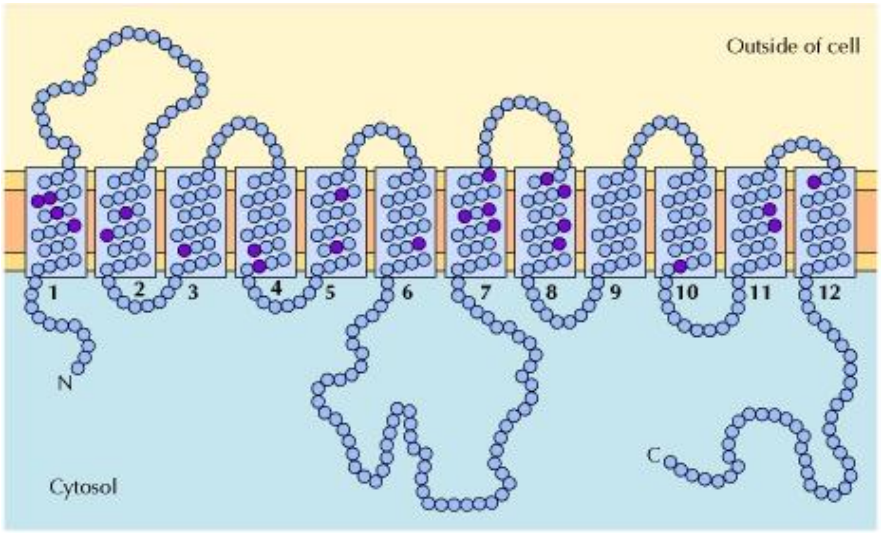

Figure 1. Structure of the glucose transporter.
The mammalian facilitated glucose transporters have 12 transmembrane spanning α-helices with both the amino and carboxy-terminal domains exposed on the same side of the plasma membrane. Figure taken from Cooper, 2000

To date, 13 members of the glucose transport family, each with different tissue distribution and kinetic properties have been identified. Currently, the best characterized members of the GLUT family are the class I glucose transporters (GLUT1-4) (Khan and Pessin, 2002; Medina and Owen, 2002; Calvo *et al.,* 2010). Each of these members will be discussed in more detail below.

1.4.1 Glucose transporter 1

Glucose transporter 1 (GLUT1) is also called erythrocyte, brain or HepG2-type transporter (Calvo *et al.,* 2010). This high affinity glucose transporter is the main isoform expressed in fetal tissue and is expressed in most adult tissues and cell types. It is the main glucose transporter involved in basal glucose uptake from the extracellular environment and most importantly, transports glucose across epithelial and endothelial barrier tissues (Calvo *et al.,* 2010). Basal glucose uptake appears to be more complex than first suggested. It is regulated by glucose-6-phosphate (G6P) and cytoplasmic ATP concentrations (Mueckler,

1994, Nedachi and Kanzaki 2006). GLUT1 levels are inversely correlated with extracellular glucose concentrations with maximal expression during starvation and decreased levels observed after re-feeding (Heilig *et al.,* 1997).

Although GLUT4 is the insulin-responsive glucose transporter, studies have demonstrated that long-term stimulation of skeletal muscle with insulin increases Glut1 mRNA expression and protein levels, and the translocation of GLUT1 to the plasma membrane. These studies have also demonstrated that long-term insulin stimulation does not activate Glut4 mRNA expression (Thorell *et al.,* 1999; Kanzaki and Pessin, 2001). This was supported by Koivisto *et al.,* 1991; Yamamoto et al*.,* 2000 who showed that prolonged insulin treatment increased Glut1 mRNA expression in L6 and 3T3-L1 cells, without affecting Glut4 mRNA expression.

1.4.2 Glucose transporter 2

The glucose transporter 2 (GLUT2) isoform is primarily expressed in pancreatic β-cells, hepatocytes and in the basolateral membrane of intestinal and renal epithelial cells (Li *et al.,* 2007; Nair and Wilding, 2010). GLUT2 has a low affinity for glucose but has high transport capacity to allow natural flux of glucose into or out of the cell. In combination with glucokinase, GLUT2 serves as a glucose sensor that responds to changes in blood glucose by increasing the rate of glucose uptake into the cells. Glucokinase activity is the rate limiting step for the uptake of glucose into cells (Mueckler, 1994; Broydell *et al.,* 1998; Watson and Pessin, 2007; Bouche *et al.,* 2004).

1.4.3 Glucose transporter 3

Glucose transporter 3 (GLUT3) is a low capacity glucose transporter that is responsible for glucose uptake in neurons (Gomez *et al.,* 2010). It is expressed during fetal development and in adult neurons, and functions to ensure a constant movement of the glucose into these cells. Although GLUT3 expression is restricted to nervous tissue in the mouse, Glut3 mRNA and proteins have been

detected in human tissues such as the placenta, liver and kidney (Nualart *et al*., 2009).

1.4.4 Glucose transporter 4

Glucose transporter 4 (GLUT4) is a high affinity glucose transporter predominantly expressed in insulin sensitive tissues such as muscle and adipocytes (Watson and Pessin, 2006; Karnieli and Armoni, 2008; Montel-Hagen *et al.,* 2009). In the basal or unstimulated state, GLUT4 is internally sequestered, and its movement from intracellular storage vesicles to the cell surface and back is low. Studies have shown that only 4 to 10% of GLUT4 is located at the cell surface with more than 90% of GLUT4 stored in intracellular compartments during the unstimulated state (Foster, 2001). Activation of the insulin-signaling pathway results in translocation of GLUT4 from intracellular vesicles to the cell surface where it facilitates glucose uptake (Yang, 2010). Studies in transgenic mice have demonstrated that expression of GLUT4 is crucial for glucose homeostasis (Tsao *et al.,* 1999; Treadway, 1994) and that a diabetic phenotype can be alleviated by increasing the expression of GLUT4 (Tozzo et al.,1997). Glut4 mRNA expression is downregulated during insulin deficiency such as streptozotocin (STZ)-induced diabetes (Olson and Knight, 2003). Furthermore, Glut4 gene expression is regulated in a tissue-specific manner. For example, Glut4 mRNA expression decreases more rapidly in adipose tissue compared to skeletal muscle in response to STZ-induced diabetes (Knight *et al.,* 2003; Saini, 2010).

Apart from insulin, other stimuli have been shown to increase in the translocation of GLUT4 to the plasma membrane (Figure 2). These include hypoxia and exercise (Tortella and Pilch, 2002; Gorovits and Charron, 2003; Watson and Pessin, 2007). Furthermore, it has been reported that Glut4 mRNA is increased with exercise but decreased during insulin deficiency (Knight *et al.,* 2003).

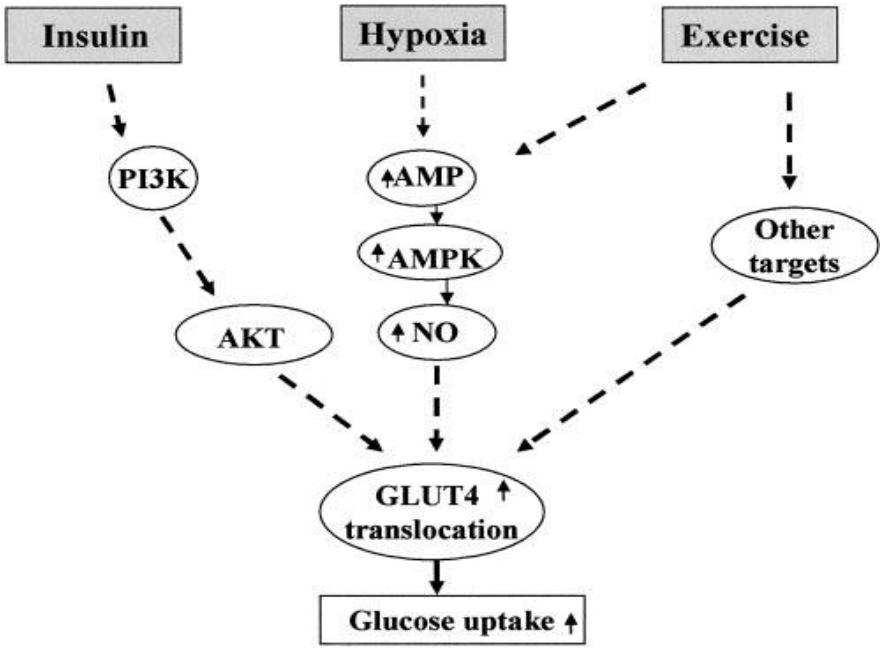

Figure 2. Pathways leading to GLUT4 translocation.
Insulin, hypoxia and exercise increase the translocation of GLUT4 to the plasma membrane resulting in increased glucose uptake. Figure adapted from Klip, 2001.

1.5 Glucose metabolism

Glucose metabolism is a major source of energy in all living organisms. After entering the cell, glucose can be converted to ATP, glycogen or fatty acids (Da Poian *et al.,* 2010). The fate of glucose in the cell is tightly regulated and is dependent on a number of factors such as the concentrations of ATP, glycogen and fat energy stores.

1.5.1 Glycolysis

Glycolysis is a metabolic pathway in which glucose is broken down to pyruvate in the cytoplasm (Figure 3). The first step of glycolysis is phosphorylation of glucose to glucose-6-phosphate (G6P) by hexokinase in muscle and adipocytes and glucokinase in the liver and pancreas (Blin, 1999; Buchakjian and Kornbluth 2010). This is an irreversible, rate-limiting step and ensures that glucose does not diffuse out of the cell (Seki *et al.,* 2005). G6P can be broken down by

glucose-6-phosphate dehydrogenase (G6PD) and converted to glycogen during glycogenesis or it can be utilized as an energy source during glycolysis (O'Boyle and Beamish, 1977). During glycolysis G6P is converted to fructose-6-phosphate (F6P) by phosphohexose, and then to fructose-1,6-biphosphate (FBP) by phosphofructokinase. This reaction is irreversible and is a major point of regulation during glycolysis. FBP is broken down into two molecules of phosphoenolpyruvate (PEP) during a number of reversible processes. Pyruvate kinase then converts PEP into pyruvate. Glycolysis is represented by the reaction:

Glucose + 2 NAD^+ + 2 ADP + 2P_i $\rightarrow$ 2 pyruvate + 2 NADH + 2 H^+ + 2 ATP + 2 H_2O

A simplified schematic diagram of the glycolytic pathway is illustrated in Figure 3.

The enzyme pyruvate decarboxylase converts pyruvate to oxaloacetic acid or the enzyme pyruvate dehydrogenase converts pyruvate to acetyl-CoA and CO_2 in the mitochondria. Acetyl-CoA and oxaloacetic acid enters the TCA cycle where it is fully oxidised to CO_2 yielding 12 molecules of ATP and water. The proton gradient generated during this process allows more ATP generation during oxidative phosphorylation. Acetyl CoA can also be used as a substrate for fatty acid and cholesterol synthesis (Dietschy and Spady, 1984).

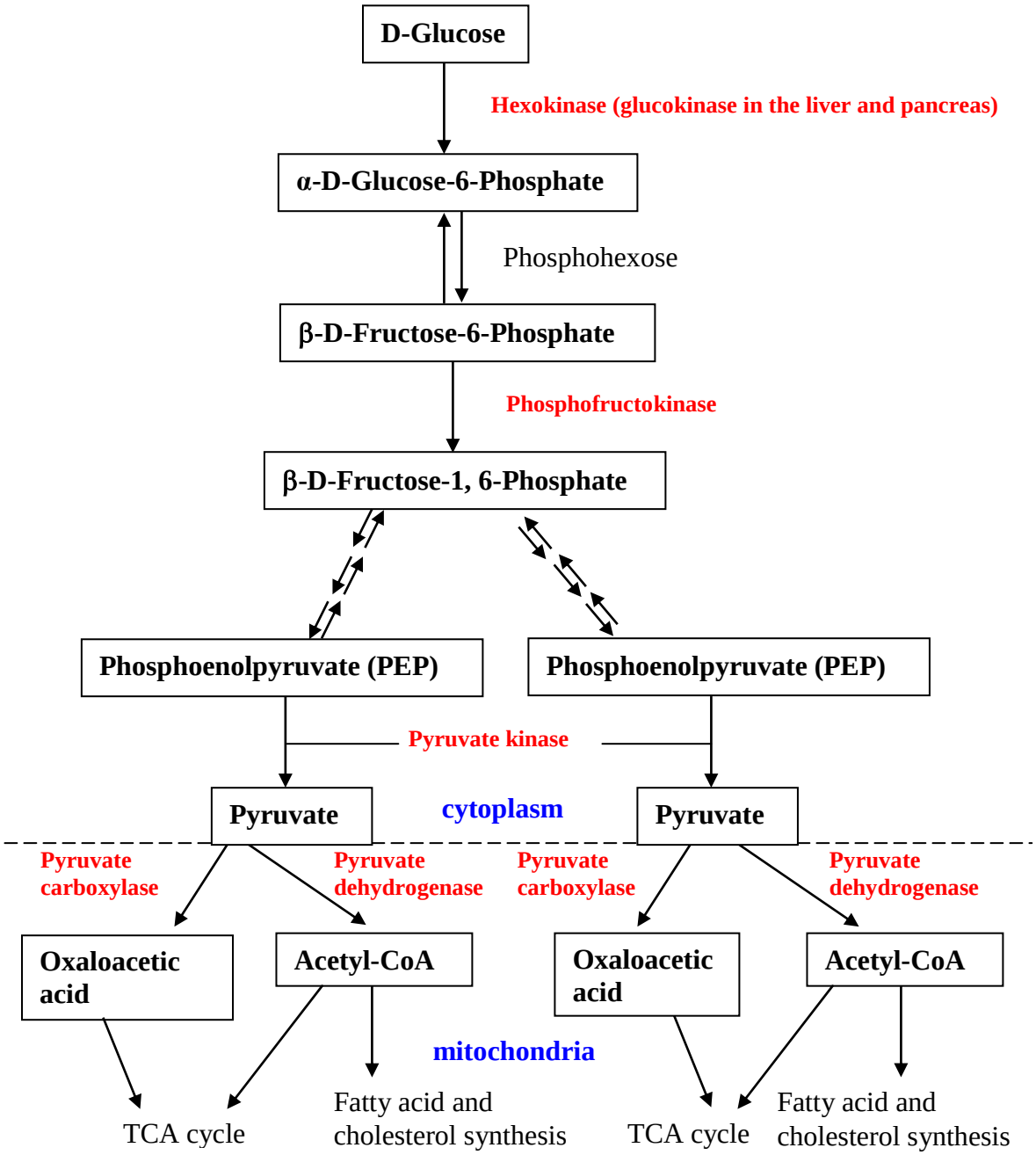

Figure 3. Illustration of glycolysis in muscle and adipose tissue.
One molecule of glucose is converted to two molecules of pyruvate which can be utilsed in anaerobic respiration, the TCA cycle or fatty acid and cholesterol synthesis. Irreversible reactions are indicated by single arrows. The enzymes catalysing these reactions are shown in red.

1.6 Insulin and insulin signaling

1.6.1 Insulin

Insulin is an anabolic hormone that is secreted by beta cells (β-cells) present in the pancreatic islets, in response to increased concentrations of glucose and amino acids after a meal (Aronoff *et al.,* 2004). The action of insulin is vital for tissue development, growth, and maintenance of glucose homeostasis. Insulin regulates blood glucose levels by stimulating glucose uptake, utilization and storage in insulin-responsive tissues such as muscle and adipocytes, while suppressing hepatic gluconeogenesis (Bouche *et al.,* 2004).

Once inside the cell, glucose is metabolised resulting in an increase in the adenosine triphosphate:adenosine diphosphate (ATP:ADP) ratio. This results in depolarization of the cell membrane, an influx of calcium ions and exocytotic release of insulin from storage granules (Odegaard, 2009). The ability to secrete insulin depends on β-cell function, β-cell mass and β-cell/insulin receptor interactions (Pessin and Saltiel, 2000; White, 2006; Prashanth *et al.*, 2009).

1.6.2 The insulin receptor

The insulin receptor (IR) is encoded by a single gene located on the short arm of chromosome 19 and consists of 22 exons and 21 introns (Youngren, 2007). It is a heterotetrameric protein, consisting of two identical extracellular α-subunits and two identical transmembrane β-subunits that are linked by disulphide bonds (Figure 4). The binding of insulin to the α-subunits of the IR induces a conformational change that causes autophosphorylation of distinct tyrosine residues on the β-subunits. Activation of the IR results in a number of intracellular phosphorylation events that regulate various biological pathways. Impairments in IR function have been implicated in insulin resistance, obesity, hyperinsulinemia, glucose intolerance and hyperlipidemia (Moller *et al.,* 1996). The transcription factor, Forkhead box protein O1 (FOXO1) has been shown to downregulate IR gene expression in the presence of insulin (Puig and Tjian, 2005).

1.6.3 Insulin receptor substrate proteins

The insulin receptor substrate (IRS) proteins are a family of proteins that are phosphorylated by the activated IR. Six different IRS proteins (IRS1-6) have been identified (Wauman *et al.,* 2008). The IRS proteins are highly homologous with overlapping and differential tissue distribution and function. IRS1 is the major substrate of the IR, leading to stimulation of glucose transport in muscle and adipose tissue (Dupont *et al.,* 2009). Lack of IRS1 is associated with impaired coupling of glucose sensing to insulin secretion suggesting that it is important in β-cell functioning. Reduced insulin stimulated IRS1 phosphorylation has been reported in insulin resistant models (Kido *et al*., 2001; Youngren, 2007).

IRS2 is the main isoform expressed in the liver (Buzzi *et al.,* 2010). It has been shown that activation of IRS2 boosts insulin production by the β-cells of the pancreas. Disruption of the *Irs2* gene in mice causes peripheral insulin resistance and dysregulated hepatic gluconeogenesis (Kido *et al.,* 2001; White, 2006).

IRS3 expression is restricted to the brain, liver, adipocytes and fibroblasts. IRS4 is expressed mainly in embryonic tissues and muscle (Schreyer *et al.,* 2003). The functions of the IRS3 to IRS6 proteins are not clear, although studies have reported that they are able to compensate for the lack of IRS1 and IRS2 in certain cases (Taniguchi *et al.,* 2006; Chan and Lee, 2008).

1.6.4 Insulin resistance

Insulin resistance is defined as the condition where insulin-responsive tissues fail to respond properly to normal levels of circulating insulin (Watson and Pessin, 2007). This can be due to the inability of insulin to bind to its receptors or post-IR, signaling defects (Nandi *et al.,* 2010). Insulin resistance is characterized by decreased uptake of glucose in muscle and adipose tissue, and increased hepatic gluconeogenesis (Weigert *et al.,* 2003; Bouzakri *et al.,* 2006; Prasanth *et al.*, 2009). Insulin resistance predisposes individuals to significant health risks in addition to its role in the pathogenesis of T2D (Youngren, 2007).

Pancreatic β-cells initially compensate for peripheral insulin resistance by increasing insulin secretion to maintain normal blood glucose levels. This leads to hyperinsulinemia, impaired glucose tolerance and ultimately the β-cells become exhausted and lose their ability to secrete insulin (Nandi *et al.,* 2010). At this stage, end-stage T2D has developed, and can only be managed by exogenous insulin injections (Zmuda *et al.,* 2010).

Insulin resistance affects the action of insulin in major target tissues such as muscle, adipocytes and hepatocytes, leading to increased circulating fatty acids and hyperglycemia. In turn, the raised concentrations of glucose and fatty acids in the bloodstream worsen both insulin secretion and insulin resistance (Goalstone and Draznin, 1997; Prashanth *et al.*, 2009).

1.6.5 Insulin signalling

Insulin initiates its biological action by binding to the tyrosine kinase insulin receptor (IR) located in the plasma membrane of insulin-responsive tissues. Autophosphorylation of the IR results in the activation of a number of signalling cascades that regulate a number of biological processes (Figure 4).

Once phosphorylated, the activated IR initiates intracellular phosphorylation events that include the phosphorylation of IRS1/2 and Shc, that serve as docking molecules for a number of other molecules. IRS1/2 recruits the phosphatidylinositol 3-kinases (PI3k) regulatory and catalytic subunits p85 and p110, respectively. Activated PI3k phosphorylates phosphoinisitol-(4,5)-biphosphate (PI-4,5-P2) to phosphoinisitol-(3,4,5)-triphosphate to (PIP3). PIP3 interacts with phosphoinositide dependent kinase (PDK-1), which phosphorylates Akt (protein kinase B) and protein kinase C-γ. This results in the translocation of GLUT4 from intracellular vesicles to the plasma membrane where it facilitates glucose uptake into the cell (Khan and Pessin, 2002). A number of studies using

chemical inhibitors of PI3k, such as Wortmannin (Wymann, 1996; Khan and Pessin, 2002) have confirmed the pathway of insulin-stimulated GLUT4 translocation.

In addition to GLUT4 translocation, activation of the IR initiates various other pathways. For example, the phosphorylation of Shc recruits the proteins Grb2 and SOS, which in turn phosphorylate a number of proteins, ultimately activating mitogen-activated protein kinase (MAPK) and resulting in cell growth and protein synthesis (Figure 4).

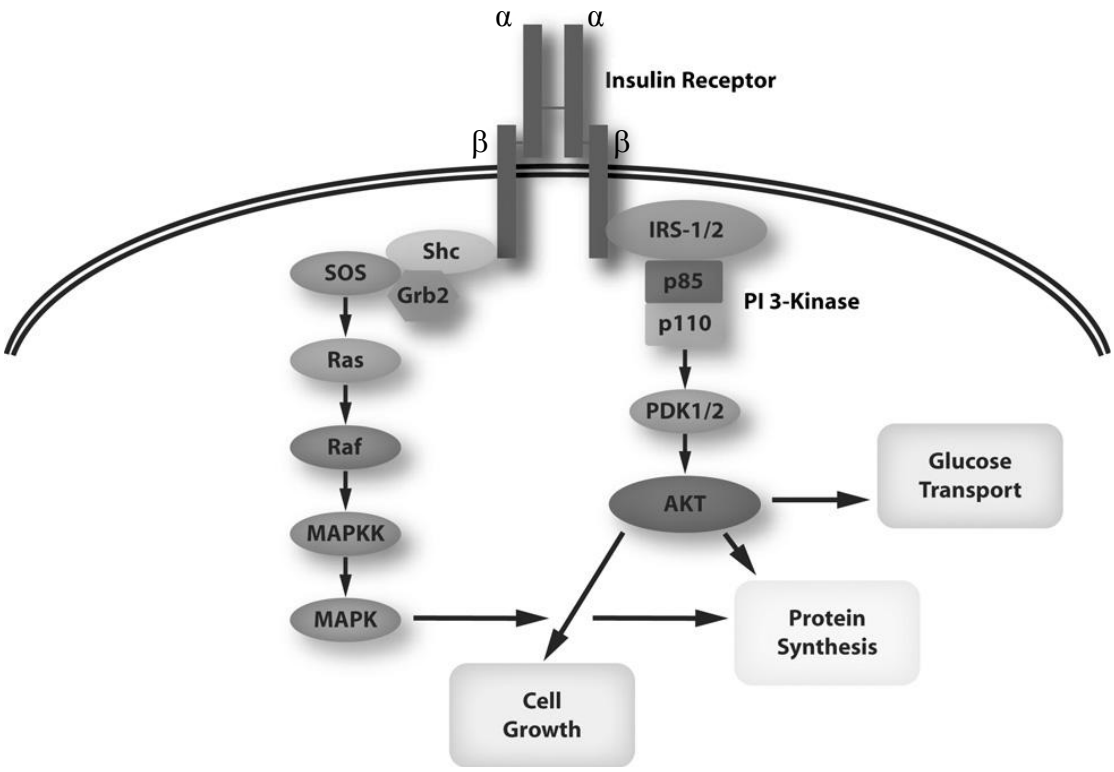

Figure 4.The insulin signalling pathway.
Insulin initiates its biological action by binding to the α-subnuits of the insulin receptor resulting in the autophosphorylation of the β-subunits and the tyrosine phosphorylation of the insulin receptor substrates (IRS1/2) and other intracellular substrates such as Shc. Activated IRS1/2 serves as docking proteins for PI3-kinase (PI3k) ultimately resulting in activation of Akt which stimulates cell growth, protein synthesis and glucose transport. Activation of MAPK by the insulin receptor results in cell growth and protein synthesis. Figure taken from Youngren, 2007.

1.7 Free fatty acids

Free fatty acids (FFAs) particularly long chain fatty acids (LCFAs) serve a variety of functions and are an essential source of energy (Dutta-Roy, 2000). They play an important role in mammalian homeostasis, particularly in the formation of biological membranes, and as fuel for energy production in tissues such as the heart and skeletal muscle. However, high levels FFAs may also be toxic to the cell and cause cell injury, therefore FFAs transport needs to regulated (Glatz *et al.,* 2010; Criddle, 2006). High levels of FFAs in plasma is commonly associated with impaired insulin-mediated glucose uptake in skeletal muscles and often coexist with obesity and T2D (Wang *et al.,* 2004; Gao, 2009; Han *et al.,* 2009).

1.7.1 Saturated free fatty acids

Saturated free fatty acids (SFFAs) have no double bonds between adjacent carbon atoms and therefore are saturated with hydrogen atoms (Marcel and Suzue, 1972). They have the general formula $CH_3(CH_2)nCOO$. One of the most common SFFAs found in plants and animals is palmitate (C16:0). Palmitate has been shown to adversely affect insulin signaling and promote glucose intolerance (Belfort *et al.,* 2005; Piro *et al.,* 2010). Studies have shown that replacing SFFAs with monounsaturated or polyunsaturated fatty acids improves insulin sensitivity and reduce the risk of developing T2D (Gao *et al.,*2009; Risérus *et al.,*2008; Montel-Hagen *et al.,* 2009).

1.7.2 Unsaturated free fatty acids

Unsaturated or monounsaturated free fatty acids (UFFAs and MUFFAs, respectively) have one or more double bond between adjacent carbon atoms. This type of FFA is considered to be healthier than SFFAs (Mozaffarian *et al.,* 2004). MUFFAs have been shown to enhance glucose uptake resulting in an increase in glucose oxidation and glycogen sythesis, suggesting that a diet rich in MUFFAs may facilitate glucose uptake and utilization in normal and insulin

resistant skeletal muscle (Coll *et al.,* 2008; Gao *et al.,* 2009; Ragheb *et al.,* 2009). The most common MUFFA, oleic acid (C18:0) is commonly found in ground nuts and olives. Oleic acid has been reported to protect against cardiovascular disease and improve insulin resistance (Dimopoulos *et al.,* 2006).

1.7.3 Essential free fatty acids

Essential fatty acids (EFFAs) are polyunsaturated fatty acids and are the parent compounds of the omega 3 (linolenic acid (C18:3)) and omega 6 (linoleic acid (C18:2)) FFA. They are essential in the human diet because they cannot be synthesized by the body and are required to maintain health. Humans can easily make saturated fatty acids or monounsaturated fatty acids with a double bond at the omega 9 position, but do not have the enzymes necessary to introduce a double bond at the omega 3 or omega 6 position (De Santa Olalla *et al.,* 2009).

Omega 3 has been reported to have anti-obesity effects and to protect against metabolic syndrome and T2D*. In vitro* studies have shown that omega 3 is able to increase glucose and lipid uptake, and β-oxidation (Haag *et al.,* 2009). Risérus *et al.,* 2008 reported that both omega 3 and omega 6 improve insulin sensivity and reduce the risk of developing T2D.

1.8 Uptake and metabolism of free fatty acids

FFAs are stored as triglycerides (TGs) in adipose tissue and released into the circulation by lipolysis (Teusink *et al.,* 2003). Two different lipase enzymes mediate the release of FFAs into the circulation. Lipoprotein lipase (LPL), on the surface of the endothelium, hydrolyses TGs in chylomicrons and very low density lipoproteins (VLDL) yielding FFAs and glycerol (Vakili and Coudilli, 2007). Hormone sensitive lipases (HSL), present in the cytoplasm of adipocytes, catalyses the release of FFAs from stored triglycerides (Sztalryd *et al.,* 1995). These FFAs then enter the bloodstream where they bind to albumin and are

transported to target tissues to be taken up by the cells either by diffusion or by transport proteins in the plasma membrane (Rasmussen and Wolfe, 1999).

Free fatty acids are hydrophobic molecules that easily dissociate from their blood transporter protein, albumin, and cross the plasma membrane by simple diffusion (Glatz *et al.,* 2010). Alternatively, FFAs are taken up by cells using transport proteins, such as the plasma membrane fatty acid binding protein (FABPpm), fatty acid translocase (CD36/FAT), fatty acid transporter protein (FATP), and caveolin (Koonen, 2005).

In the cytoplasm, FFAs are transported by a number of FABPs, such as the cytoplasmic fatty acid binding protein (FABPc) and fatty acid transporter 1 (FATP1) (Binnert *et al.,* 2000; Glatz *et al.,* 2010). FATP1 has been identified as the transporter that allows rapid activation of LCFAs by acyl coenzyme A (acyl-coA) synthetase to form FA acyl-CoAs (Thompson *et al.,* 2009). The mitochondrial transmembrane protein, carnitine palmitoyltransferase I (CPTI) transports FA acyl-CoAs across the outer mitochondrial membrane (Sebastián *et al.,* 2009) (Figure 5). This is the rate-limiting step in β-oxidation CPTI also catalyzes the trans-esterification of acyl-CoA to acyl-carnitine. Acyl-carnitine is translocated through the inner mitochondrial membrane by carnitine:acyl-carnitine translocase. CPTII, located on the matrix side of the inner mitochondrial membrane, catalyses the reaction with coenzyme A to release carnithine and produce acyl-CoA for β-oxidation (Kerner and Hoppel, 2000).

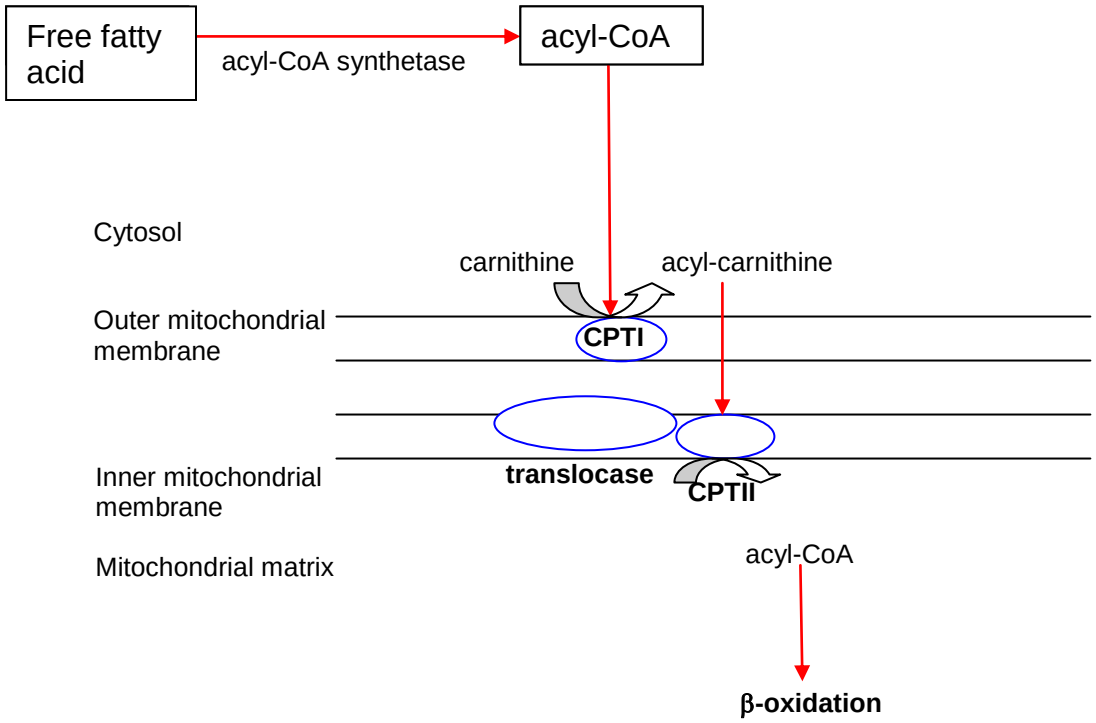

Figure 5. Activation of long-chain fatty acids and their transport into the mitochondria for β-oxidation.
Acyl-CoA synthetase is located on the outer mitochondrial membrane and activates long chain fatty acids to form acyl-CoA. CPTI exhanges the CoA moiety with carnithine. Acyl-carnithine is translocated through the inner mitochondrial membrane by translocase. CPTII located on the matrix side of the inner mitochondrial membrane converts acyl-carnithine to acyl-CoA that is utilised in β-oxidation. Figure adapted from Mursula 2002.

1.9 Fatty acid oxidation

Fatty acid oxidation or β-oxidation refers to the metabolism of FFAs in the mitochondria to produce energy. After entering the mitochondria as acyl-CoAs, β-oxidation enzymes degrade FFAs to acetyl-CoA. Acetyl-CoA is oxidised in the tricarboxylic acid (TCA) or Krebs cycle to produce the reducing equivalents, NADH and $FADH_2$ NADH and $FADH_2$ will subsequently enter the mitochondrial respiratory or electron transport chain. Here, oxidation of the reducing equivalents generates an electrochemical proton gradient ($\Delta\mu H^+$) across the inner mitochondrial membrane. The oxidation of free fatty acids yields

significantly more energy per carbon atom than the oxidation of carbohydrates (Garrett and Grisham, 2005).

1.10 Relationship between fatty acid and glucose metabolism

Muscle utilizes both glucose and free fatty acid as fuel sources for energy production (Figure 6). Glucose entering the cell is broken down into pyruvate, which is converted to acetyl-CoA, by the enzyme pyruvate dehydrogenase in the mitochondria. Free fatty acids circulating in the bloodstream are transported into the mitochondria where they are converted to acetyl-CoA during β-oxidation. Acetyl-CoA is converted to energy (ATP) in the TCA cycle and during oxidative phosphorylation. The ability of muscle to switch from fat oxidation during fasting to glucose oxidation after a meal is referred to as metabolic flexibility (Corpeleijn *et al.,* 2009).

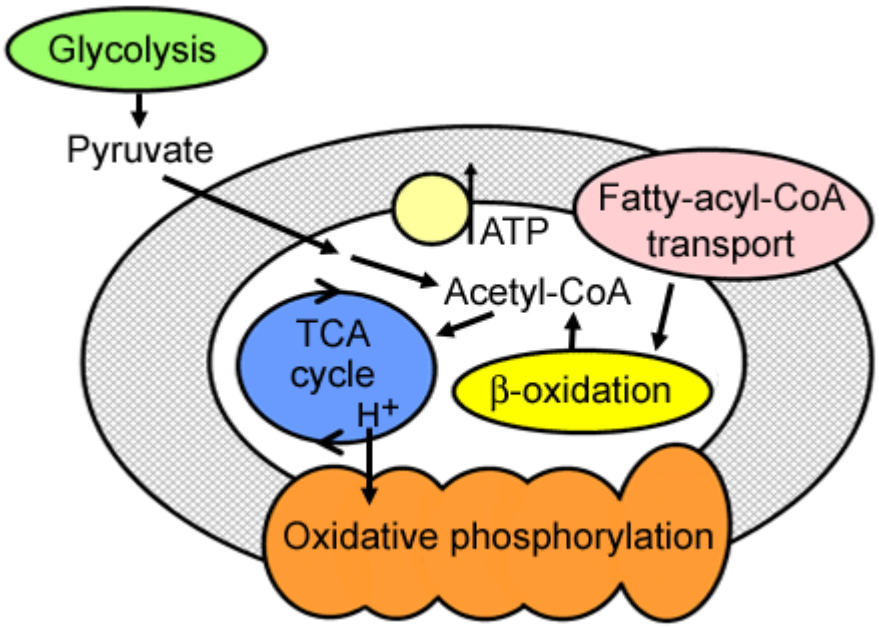

Figure 6. The utilisation of glucose and fatty acids as energy.
During glycolysis glucose is broken down to pyruvate in the cytoplasm, which is converted to acetyl-CoA in the mitochondria. Fatty acids are converted to acetyl-CoA during β-oxidation. Acetyl-CoA is converted to energy (ATP) in the TCA cycle and during oxidative phopshorylation**.**

During the fasting state, glucose uptake is low and plasma FFA concentrations are high. Therefore, during this period FFAs serve as the principal fuel source for energy production in muscle. After a meal, an increase in plasma glucose concentration stimulates insulin secretion from the β-cells in the pancreas. The resultant hyperinsulinemia suppresses lipolysis resulting in a decrease in plasma FFA concentration and a subsequent decrease in the rate of FFA oxidation. Therefore, insulin simultaneously stimulates glucose uptake and metabolism, while reducing lipid metabolism in muscle cells (Abdul-Ghani and DeFronzo, 2010).

Randle *et al.,* 1998 proposed that high levels of FFAs inhibit glucose metabolism due to increased FFA oxidation and inhibition of glucose oxidation (Figure 7). They demonstrated that FFAs compete with glucose for substrate oxidation in rat heart muscle. According to their hypothesis, increased FFA oxidation increases the mitochondrial ratio of acetyl-CoA to coenzyme A and NADH to NAD^+. An increase in these ratios, inactivates pyruvate dehydrogenase and therefore glucose oxidation, resulting in an increase in citrate levels. This in turn inhibits glycolysis by reducing phosphofructokinase activity leading to the accumulation of G6P and glycogen levels.

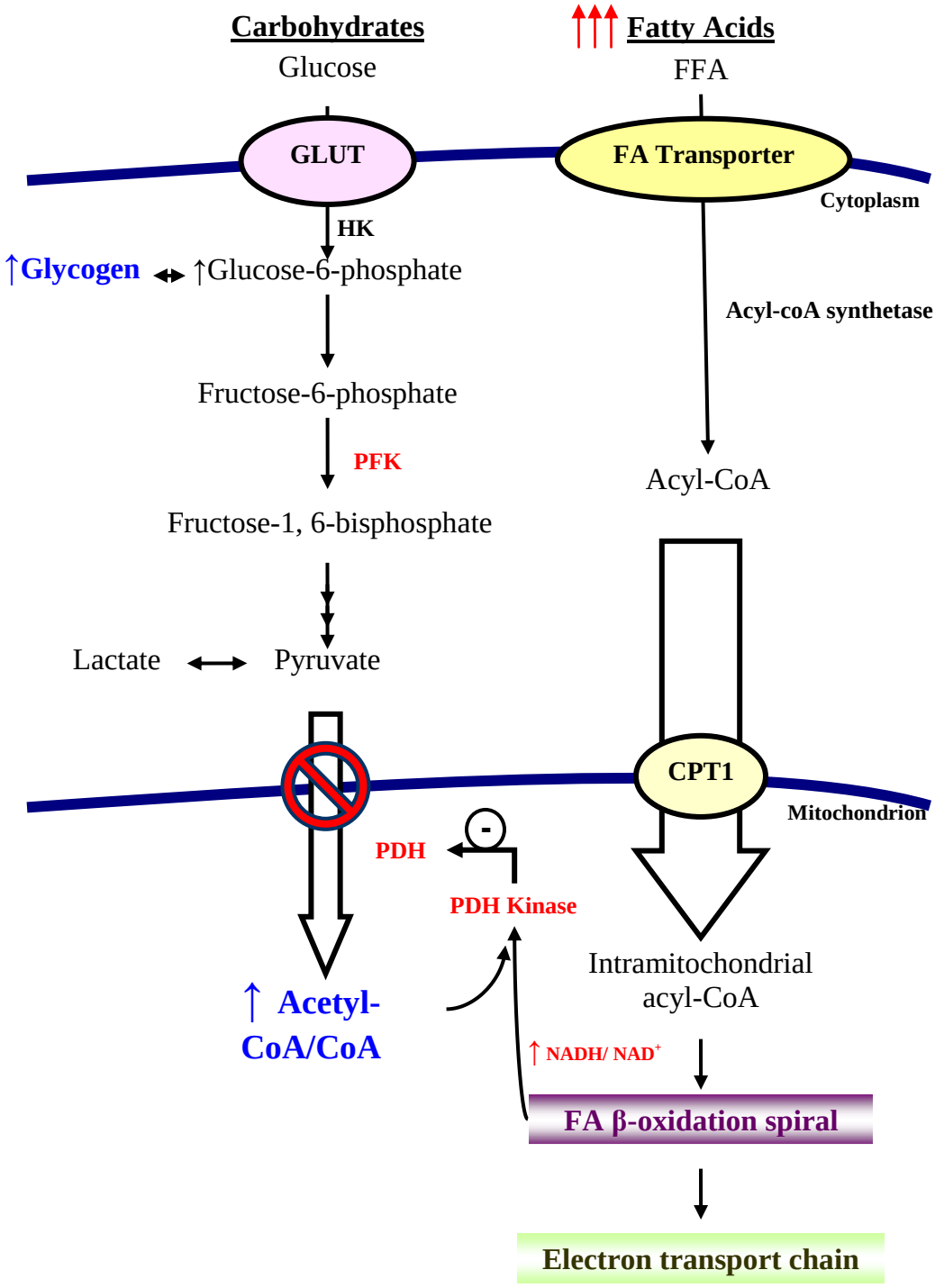

Figure 7. Schematic diagram of the relationship between fatty acid and glucose oxidation. Increased free fatty acid uptake leads to elevated rates of FA oxidation. This increases the mitochondrial ratio of NADH to NAD^+ and acetyl-CoA to coenzyme A. An increase in these ratios, stimulates the activity of pyruvate dehydrogenase (PDH) kinase which in turn inactivates PDH, causing inhibition of glucose oxidation and increased citrate levels. This in turn downregulates PFK activity leading to the accumulation of glucose-6-phosphate and increased glycogen levels. Figure taken from Chan, 2006.

1.11 Relationship between fatty acid metabolism and insulin signalling

Elevated concentrations of FFAs, especially in skeletal muscle, which is a major site of peripheral glucose uptake, has been associated with insulin resistant states such as obesity and T2D (Kelley and Mandarino, 2000; Koonen, 2005; Watt *et al.,* 2006; Glatz, 2010). However, the underlying mechanisms are still unclear (Ragheb *et al.,* 2009). Roden *et al.,* 1996, suggested that high levels of FFAs reduce insulin sensitivity and inhibit insulin-mediated glucose uptake in skeletal muscle. They proposed that when FFA uptake exceeds oxidation capacity, intracellular FFA metabolites such as acyl-CoAs, diacylglycerol (DAG) and ceramides accumulate in the cell. These metabolites activate PKC and a downstream serine/threonine kinase cascade, which in turn leads to increased serine phosphorylation of IRS1, thereby blocking IRS1 tyrosine phosphorylation and inhibiting the activity of PI3k and Akt/PKB, major stimulators of GLUT4 translocation (Cooney *et al.,* 2004; Chavez and Summers, 2003). This inhibition results in impaired insulin-mediated glucose transport (Figure 8).The study by Corpeleijn, 2009 found similar results. These authors showed that the FFA metabolites acyl-CoAs, diacylglycerol (DAG) and ceramides activate serine/threonine kinases, including PKC, JNK and NFκB which phosphorylate serine residues of IRS1. This decreases activation of downstream signaling molecules such as PI3k and AKT, which ultimately results in a decrease in GLUT4 translocation and consequently a decrease in glucose uptake into the cell.

Excessive accumulation of intramyocellular FFAs and their metabolites is results in lipotoxicity which is a main contributor to the pathophysiology of insulin resistance and dysfunctioning of the heart and skeletal muscle (Holland, 2007). A number of *in vitro* models have been developed to aid the understanding of how FFAs cause insulin resistance. In C2C12 muscle cells, the SFFA palmitate has been shown to reduce insulin-stimulated glucose uptake and glycogen synthesis by inhibiting protein kinase B (Dimopoulos *et al.,* 2006; Isharwal *et al.,* 2009, Hommelberg, 2010). Similar results were observed in L6 muscle cells (Montel-

Hagen *et al.,* 2009, Chavez and Summers, 2003, Gao *et al.,* 2009). Ragheb *et al.,* 2009 showed that both palmitate and the MUFFA, oleate inhibit the PKC signaling pathway resulting in increased serine/threonine phosphorylation of IRS1 in C2C12 myocytes. These pathways, together with the NFκB pathway and the stress kinases, JNK and p38MAPK are believed to be involved in FFA-induced insulin resistance (Roden *et al.,* 1996; Shulman, 2000). However, the precise mechanism whereby FFA and their metabolites induce insulin resistance still needs to be elucidated.

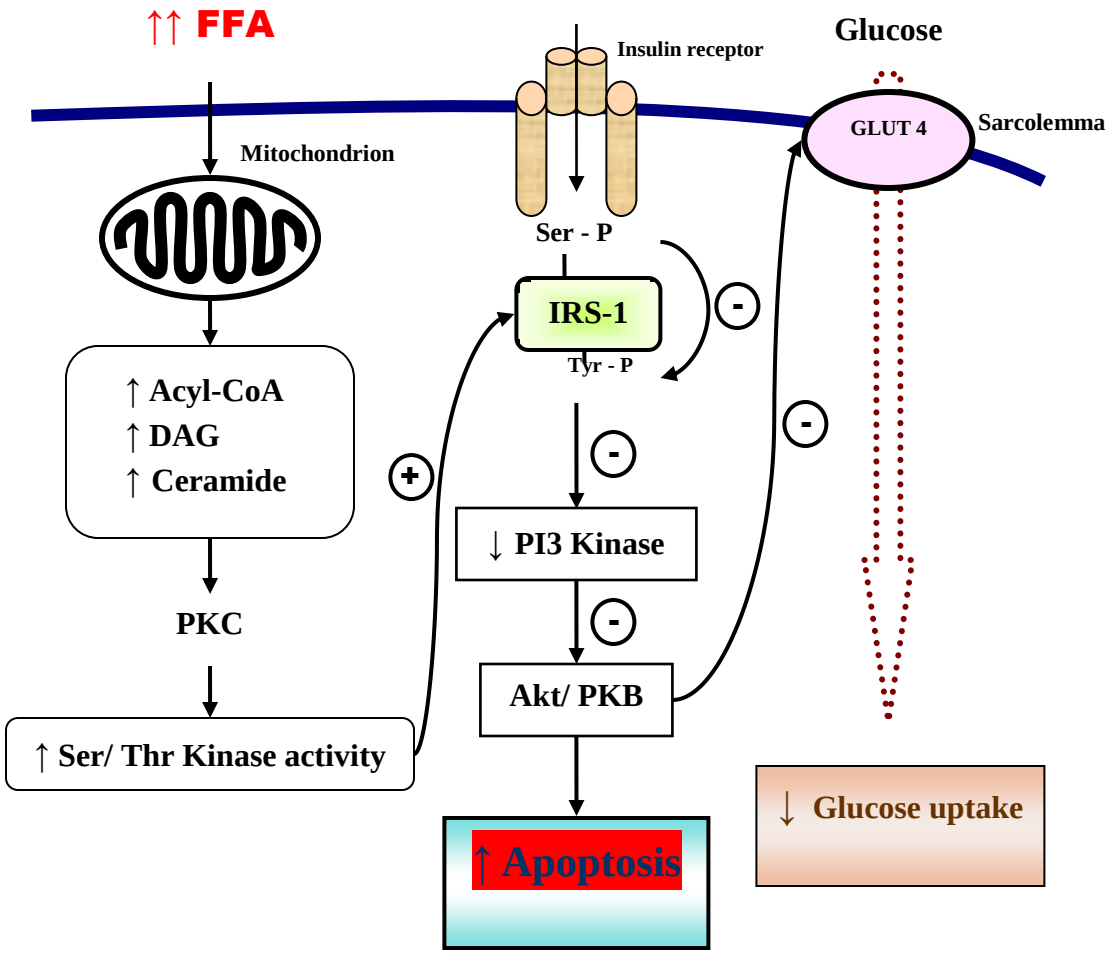

Figure 8. The relationship between fatty acid metabolism and insulin signalling.
Elevated levels of free fatty acids and increased levels of uptake results in high levels of intracellular fatty acids that exceed the oxidation capacity of a cell, leading to accumulation of fatty acid metabolites such as acyl-CoAs, diacylglycerol (DAG) and ceramides. These metabolites activate PKC and a downstream serine/ threonine kinase cascade, which in turn leads to increased serine phosphorylation of IRS1, thereby blocking IRS1 tyrosine phosphorylation and inhibiting the activity of PI3 kinase and AKT/PKB, major stimulators of GLUT4 translocation. Figure reproduced from Chan, 2006.

1.12 The role of insulin on glucose and fatty acid uptake and metabolism

In skeletal muscle, insulin and contraction are the main physiological stimuli able to induce fatty acid and glucose uptake and metabolism (Bouche *et al.,* 2004; Jain *et al.,* 2009). After a meal, insulin stimulates both glucose and FFA uptake by simultaneously increasing translocation of GLUT4 and the FFA transporter proteins, CD36/FAT and/or FABPpm, and FATP1. In both cases, activation of PI3k is required (Watson and Pessin, 2007; Jain *et al.,* 2009; Glatz, 2010).

CD36 mRNA and protein increases rapidly, within hours, after insulin stimulation in human skeletal muscle (Corpeleijn *et al.,* 2008). CD36 plays an important role in LCFA uptake into skeletal muscle in rodents and humans, and its concentration and activity is increased by exercise. However, the transport of LCFA by CD36 into skeletal muscle does not seem to regulate the rate of LCFA oxidation. The CD36 content and LCFA transport capacity have been reported to be increased in obese and T2D individuals and correlate with increased muscle triglyceride content, while fat oxidation is decreased.

Recent studies have found that insulin failed to stimulate fatty acid and glucose transport in skeletal muscle of Akt-2 null mice, and failed to induce the translocation of CD36 and FATP1, as well as GLUT4, while the translocation of FABPpm and FATP4 was not impaired (Jain *et al.,* 2009). These observations indicate that insulin stimulated GLUT4 translocation and the insulin-stimulated translocation of some fatty acid transporters (CD36 and FATP1) are similarly regulated via the PI3K-Akt2 signaling pathway (Jain *et al.,* 2009; Abdul-Ghani and DeFronzo, 2010).

1.13 Hypothesis

FFAs are an important energy source for the body. Despite this, a number of studies have demonstrated that elevated levels of free fatty acids reduce insulin sensitivity and glucose utilization.

We hypothesized that high levels of the saturated and monounsaturated free fatty acids reduces insulin sensitivity and glucose disposal in C2C12 and L8 skeletal muscle cells, but not in 3T3-L1 derived adipocytes.

1.14 Aim

To investigate basal and insulin-stimulated glucose uptake, glycogen synthesis and glucose oxidation in C2C12 and L8 myocytes, and 3T3-L1 adipocytes cells cultured with saturated, monounsaturated and essential fatty acids in low and high glucose culture conditions. Furthermore, we investigated the expression of genes involved in insulin signaling and glucose uptake in C2C12 myocytes cultured with the SFFA, palmitate.

Chapter 2

Cell models used in this study

2.1 *In vitro* models

Immortalized muscle cell lines can be used as experimental models for studying physiological and pathophysiological process relevant to clinical conditions such as insulin resistance and T2D (Chan *et al.,* 2008). Muscle cell lines, C2C12 mouse satellite/myoblast cells and L8 rat myoblast cells, and adipocytes derived from 3T3-L1 cells are commonly used for glucose uptake and insulin resistance studies (Mann *et al.,* 2003; Wang *et al.,* 2004). Using cell lines is an ethical way of studying cell metabolism, as well as genotypic and phenotypic responses to external stimuli such as FFAs and hormones at a cellular level (Hartshorne, 2009).

2.2 Muscle cells

Muscle cell differentiation is controlled by a complex set of interactions between tissue restricted transcription factors, ubiquitously expressed transcription factors, and cell cycle regulatory proteins (Guo *et al.,* 2003). During the process, the morphology and physiology of the cell may change dramatically, but the genetic make up usually remains the same.

2.2.1 C2C12 cells

The C2C12 muscle cell line is a subclone of a myoblast cell line derived from normal adult C3H mouse leg (Silberstein *et al.,* 1986). C2C12 cells differentiate rapidly to form myotubules expressing muscle proteins. These cells have been used as *in vitro* models to study myogenesis and cell differentiation (Diel *et al.,* 2008), glucose metabolism and insulin signalling (Kumar, and Dey, 2003).

When sub-culturing these cells, it is important to avoid 100% confluence, as this will deplete the myoblastic population in the culture (www.lonzabio.com). A number of studies have reported that C2C12 cells have a defective insulin signaling pathway (Nedachi *et al.,* 2006). Ragheb *et al.,* 2009 reported that insulin-stimulation increases glucose uptake by 50% in C2C12 cells.

2.2.2 L8 cells

In contrast to C2C12 myoblasts, L8 myoblasts originate from newborn rat skeletal muscle (Mau *et al.,* 2008). After differentiation of L8 cells into myotubules, they express several proteins typical of skeletal muscle (López-Solache *et al.,* 2002).

2.3 3T3-L1 cells

3T3-L1 cells are derived from the 3T3-Swiss albino mouse through clonal isolation and have a fibroblast-like morphology (Rosen *et al.,* 2000). 3T3-L1 cells can be differentiated into adipocytes using adipogenesis inducing media. Fully differentiated adipocytes have most of the biochemical and morphological characteristics of adipocytes, and are used as an *in vitro* model to study insulin pathways, obesity and cardiovascular diseases (Morganstein *et al.,* 2008).

Chapter 3

Material and methods

3.1.1 Materials

The materials used in this study, together with their suppliers and product numbers are listed in Appendix 1.

3.1.2 Cell lines

Murine C2C12 myoblast (ATCC CRL 1722, Maryland, USA), rat L8 myoblast (ATCC CRL1458, Maryland, USA) and 3T3-L1 (CCL 92, Maryland, USA 1) mouse fibroblast originating from the American Type Culture Collection, were purchased from Highveld biologicals (Jhb, SA).

3.2 Cell Culture

3.2.1 Thawing of cells

Cryopreserved cells, stored in freezing media containing Dulbecco's Modified Eagle's Medium (DMEM), 10% fetal calf serum (FCS) and 7% (v/v) dimethyl sulfoxide (DMSO) as cryoprotectant, were thawed by placing cells in a 37°C water bath. Immediately after thawing, cell suspensions were transferred from cryotubes to 15 ml tubes containing 10 ml of pre-warmed 37°C growth media (DMEM supplemented with 10% FCS). Cells were pelleted by centrifugation at 800 g for 5 minutes. The supernatant was gently removed by aspiration and the cell pellet was lightly vortexed. Cells were resuspended in 5 ml growth media and gently mixed by pipetting. For consistency between experiments and to prevent depletion of specific cell line phenotypes by excessive passaging, for all assays, only cell sub-cultures of less than 20 passages were used.

3.2.2 Counting of cells

A sample of the cell suspension was stained with 0.1% (w/v) trypan blue in Dulbecco's phosphate buffered saline (DPBS) and counted using a hemocytometer. Briefly, 50 µl trypan blue solution was added to 50 µl of the cell suspension and mixed. Thereafter, 10 µl of the trypan blue/cell suspension was

pipetted into the counting chambers of a hemocytometer (Figure 9). The cells were counted using the 10x magnification lens of an inverted light microscope (Olympus ck x31) using phase contrast. Six squares of the counting chambers were counted (three in each chamber), averaged, multiplied by a factor of two (cells were diluted 1:2 in media), and by 1 x 10^4 (surface area of hemocytometer) to determine cells/ ml.

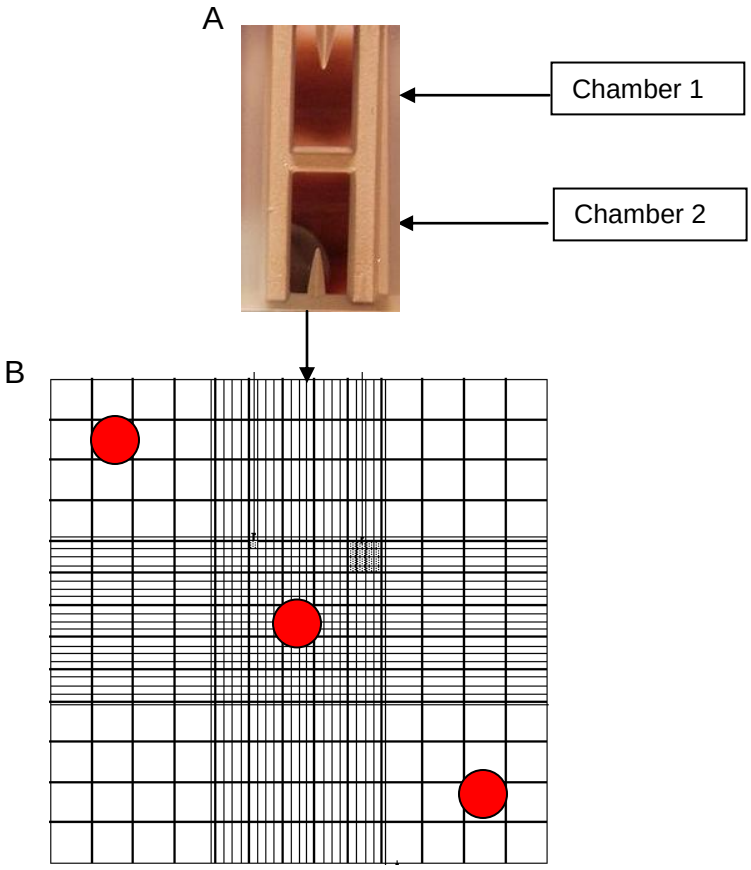

Figure 9. An illustration of one of the counting chambers.
The two counting chambers (A). The number of cells in three squares were counted in each counting chamber (indicated by red dots) and averaged to obtain the total number of cells (B).

3.2.3 Sub-culture

After counting, cells were seeded in 75 cm^2 flasks at a density of 2.5 x 10^4 cells/ml for C2C12 and L8 cells and 2.0 x 10^4 cells/ml for 3T3-L1 cells. A total volume of 18 ml of pre-warmed growth media was added to the cells. Cells were

incubated at 37°C in 5% CO_2 and humidified air for three days until they were approximately 70% confluent. Media was refreshed on the second day.

3.2.4 Differentiation

When cells were approximately 70% confluent, media was removed by aspiration and cells were rinsed with 8 ml of warm (37°C) DPBS. Cells were trypsinized by adding 2 ml trypsin/versene to the cell culture and incubation at 37°C in 5% CO_2 and humidified air for seven minutes to allow cells to dislodge from the flask. A light microscope was used to confirm that cells have dislodged. Trypsinization was stopped by adding 8 ml of growth media. To ensure a single cell suspension and minimise clumping, the cell suspension was mixed by pipetting up and down against the growth surface. The cells were counted as previously described in section 3.2.2. Cells were seeded into multi-well plates at the densities listed in Table 1. Cells were incubated at 37°C in 5% CO_2 and humidified air for three days until 80-90% confluence was reached.

Table 1. Cell densities used for seeding different plate types.

Cell type	Plate type*	Cell concentration	Volume (µl)	Cell density
C2C12 and L8 cells	96 well	2.5×10^4 cells/ml	200 µl	5×10^3 cells/ml
	24 well	2.5×10^4 cells/ml	1000 µl	2.5×10^4 cells/ml
	6 well	2.5×10^4 cells/ml	3000 µl	7.5×10^4 cells/ml
3T3-L1 cells	96 well	2.0×10^4 cells/ml	200 µl	4×10^3 cells/ml
	24 well	2.0×10^4 cells/ml	1000 µl	2.0×10^4 cells/ml
	6 well	2.0×10^4 cells/ml	3000 µl	6.0×10^4 cells/ml

*96 well plates were used for the colourometric glucose uptake and MTT assays
24 well plates were used for the 2-deoxy-[3H]–D-glucose assays
6 well plates were used for the glucose-6-phosphate, glycogen and glucose oxidation assays, and RNA extraction.

3.2.5 Myoblast differentiation (C2C12 and L8 cells)

To induce differentiation of myoblasts into myocytes, 80-90% confluent cells were cultured in DMEM containing 2% horse serum (HS) (growth factor poor media). Hourse serum lacks growth factors found in FCS, thus cell proliferation is arrested and the myoblasts undergo myocytic differentiation and start to form multinucleate myotubules. Cells were incubated at 37°C in 5% CO_2 and humidified air for two days until myotubules were observed by phase contrast microscopy (Olympus ck x31).

3.2.6 Adipocyte differentiation (3T3-L1 cells)

To ensure induction of the adipogenic phenotype, 3T3-L1 cells need to be subjected to two cell divisions in the presence of adipogenic inducing media. Therefore, when 3T3-L1 fibroblasts reached 80-90 % confluence, the growth media was replaced with adipogenic inducing media consisting of DMEM supplemented with 10% FCS, 0.6 µM dexamethasone, 0.1 mM IBMX and 16 µM insulin. Cells were incubated at 37°C in 5% CO_2 and humidified air for five days during which media was refreshed daily. After adipocyte induction, cells were cultured in adipogenesis maintenance media containing DMEM with 10% FCS and 16 µM insulin for a further two days. The extent of adipocyte differentiation was assessed by fat droplet formation and was visualized under phase contrast using an inverted light microscope.

3.2.7 Free fatty acid treatment

To determine the optimal concentration of FFAs that induce the maximal effect on glucose uptake in C2C12 myocytes and 3T3-L1 adipocytes, FFAs were tested at four different concentrations (Table 2). One hundred millimolar stock solutions of FFAs were prepared by dissolving the FFA in ethanol heated to 100°C. The working FFA solutions were prepared in DMEM containing 5.5 mM glucose and supplemented with 2% bovine serum albumin (BSA). Working solutions were

kept at 37°C for an hour to allow FFAs to conjugate with the BSA. The presence of the FFA did not affect the pH of the solution which remained between 7.4 and 7.5.

Table 2. Different concentrations of FFAs tested in the study

Free fatty acid	Working concentrations (mM)
Palmitate (FW 256.43)	1.0, 0.75, 0.5 and 0.25
Oleate (FW 282.47)	1.0, 0.75, 0.5 and 0.25
Omega 3 (FW 278.44)	1.0, 0.75, 0.5 and 0.25
Omega 6 (FW 280.46)	1.0, 0.75, 0.5 and 0.25

3.3 Experimental outline

Myocytes and adipocytes were treated with FFAs as indicated in Figure 10. Three independent experiments were conducted with either 5.5 mM or 20 mM glucose containing media. To measure basal glucose uptake cells were cultured in 5.5 mM or 20 mM glucose media only (Figure 10A). Insulin-stimulated glucose uptake was measured by culturing cells in 5.5 mM or 20 mM glucose media supplemented with 1 μM insulin (Figure 10B).

To assess the effect of the FFAs on glucose uptake, media containing 5.5 mM or 20 mM glucose (Figure 10C), and low or high glucose containing 1 μM insulin (Figure 10D) were supplemented with 0.75 mM of palmitate, oleate, omega 3 and omega 6. As a solvent control, 0.1% (v/v) ethanol was added to the 5.5 mM or 20 mM glucose containing media (Figure 10E).

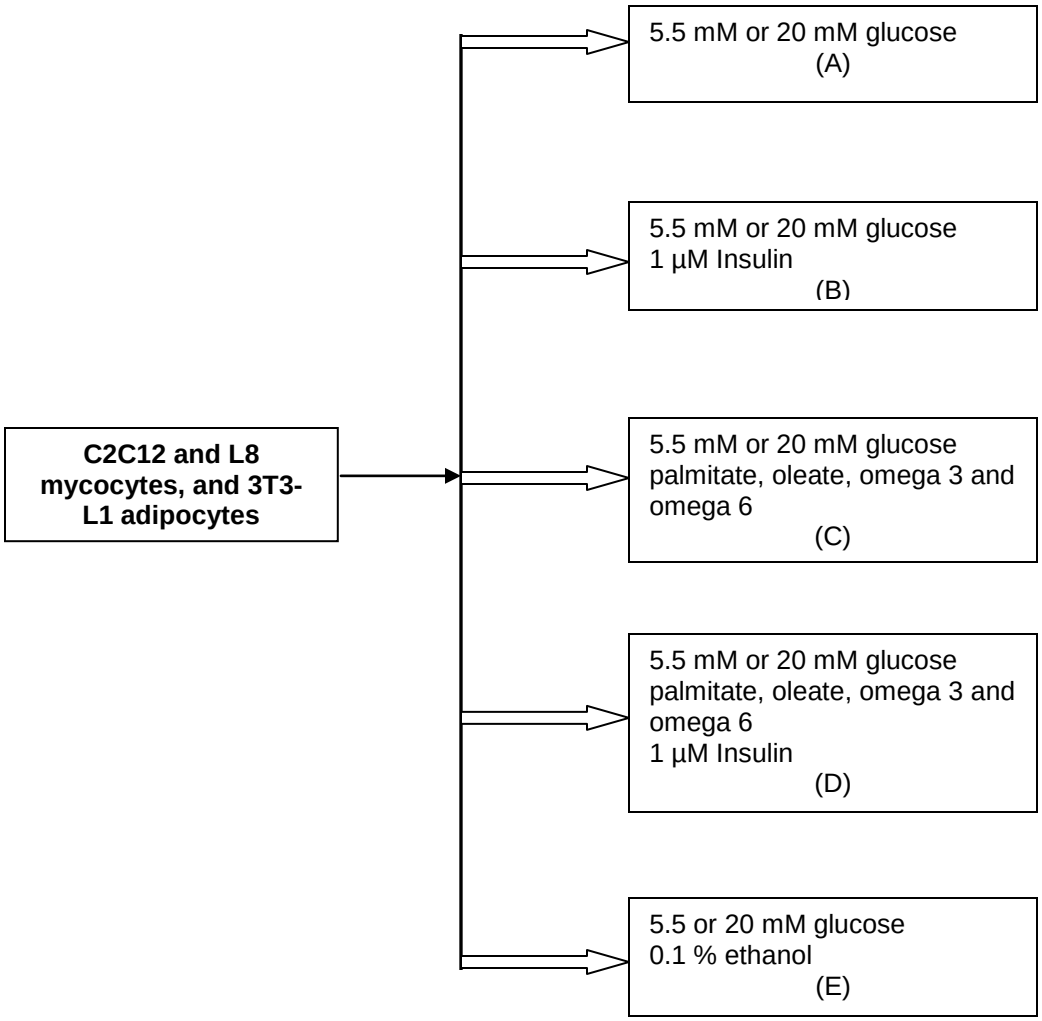

Figure 10. Experimental outline to determine the effect of FFAs on basal and insulin stimulated glucose uptake.

3.3.1 Experimental design

Differentiated myocytes and adipocytes were pre-exposed to FFA by culturing in DMEM supplemented with palmitate, oleate, omega 3 and omega 6 for 24 hours. Thereafter, cells were glucose and serum starved by incubating with DPBS at 37°C in 5% CO_2 and humidified air for 30 minutes. After serum starvation, the media was replaced with DMEM (without phenol red, L-glutamine and pyruvate)

containing 5.5 mM or 20 mM glucose, 2% BSA and 0.75 mM of the relevant FFA. Cells were incubated for six hours at 37°C in 5% CO_2 and humidified air. Insulin (1 μM) was added in the last hour (after five hours of incubation with FFA). Cells were returned to the incubator for the last hour of incubation Figure 11.

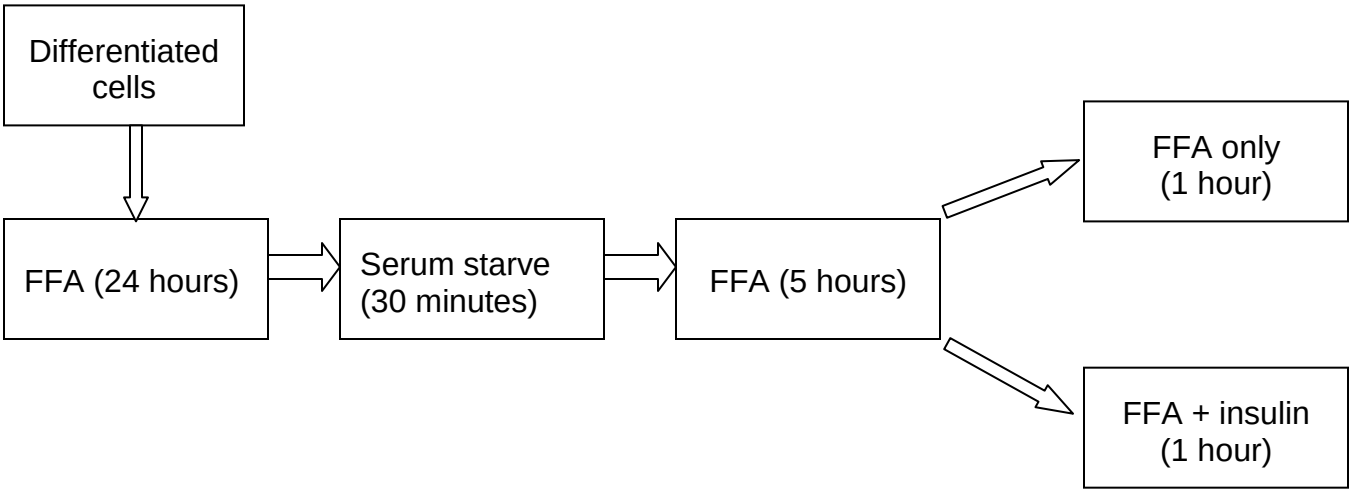

Figure 11. Experimental design to determine the effect of FFAs on basal and insulin stimulated glucose uptake.

3.4 Colourimetric glucose uptake assay to determine the optimal concentration of free fatty acids.

To determine the concentration of FFAs that exerts the maximal effect on glucose uptake in C2C12 myocytes and 3T3-L1 adipocytes, an indirect method that quantifies glucose uptake by measuring the amount of glucose remaining in the media after incubation was used.

After pre-exposure of C2C12 myocytes and 3T3-L1 adipocytes to FFAs as described in section 3.3, culture media was removed and cells were washed with warm (37°C) DPBS to remove excess glucose and media. Thereafter, cells were glucose and serum starved by incubating with DPBS at 37°C in 5% CO_2 and humidified air for 30 minutes. After serum starvation, cells were cultured in DMEM (without phenol red, L-glutamine and pyruvate) containing 5.5 mM glucose and 2% BSA, with or without FFA as described in section 3.3. Cells were incubated at 37°C in 5% CO_2 and humidified air for two hours. Thereafter, the concentration of glucose remaining in the media was measured by transferring 6 µl of culture media to a new 96 well plate. The medium sample was diluted by adding 194 µl of deionised water, and the glucose concentration was determined using a commercial kit according to the manufacturer's instructions (Biovision Glucose Assay kit).

A standard curve was prepared by pipetting 0, 2, 4, 6, 8, and 10 µl nM/well of glucose standard in a 96 plate and adjusted to 50 µl using glucose reaction buffer. Fifty microlitres of diluted media samples were added to the 96 well plate. Thereafter, 50 µl of glucose reaction mix consisting of colourimetric dye, glucose oxidase and reaction buffer was added to the wells. The plate was incubated at 37^{o}C for 30 minutes, thereafter the plate was read at an optical density of 570 (OD_{570}) in a BioTek® plate reader ELX 800 using Gen 5® software. Glucose uptake was calculated by subtracting the glucose concentration remaining in the media after incubation from the initial glucose concentration. To adjust for cell variations in cell density, a 3(4,5-dimethylthiazol-2-yl)-2,5-diphenyl tetrazolium

bromide (MTT) assay, as described in section 3.5, was done on the cells after the glucose uptake experiments.

3.5 The MTT assay

The MTT assay is a colourimetric assay based on the conversion of the tetrazolium salt, MTT, to formazan by mitochondrial dehydrogenases. The assay is commonly used to determine mitochondrial activity and cell viability. After exposing the cells to the relevant FFA, the media was aspirated and 200 µl of DMEM containing either 5.5 mM or 20 mM glucose and 2% BSA was added. As phenol red absorbs at the same wavelength as formazan, DMEM without phenol red was used for the MTT assay. Fifty microlitres of MTT in PBS was added to each well and the cells were incubated at 37^{o}C in 5% CO_2 and humidified air for an hour. The resultant formazan product was dissolved in 200 µl DMSO and 25 µl Sorensen's phosphate buffer (pH 10.5). The plate was read at an OD_{570} in a BioTek® plate reader ELX 800 using Gen 5® software.

3.6 The 2-deoxy-[^{3}H]-D-glucose uptake method

The determination of 2-deoxy-[^{3}H]-D-glucose uptake involves adding radioactively labelled 2-deoxy-[3H]-D-glucose to cells and then measuring the concentration of intracellular 2-deoxy-[^{3}H]-D-glucose (DOG) using a scintillation counter.

To quantify glucose uptake, cells were treated as described in section 3.3, media was removed and cells were washed twice with 1 ml of warm DPBS. Thereafter, 250 µl of DMEM containing 5.5 mM glucose, 2% BSA and 0.5 µCi/ml DOG was added to each well. Cells were incubated at 37^{o}C in 5% CO_2 and humidified air for 15 minutes. After incubation, 2-deoxy-[^{3}H]-D-glucose uptake was stopped by washing the cells twice with 1 ml of ice cold DPBS. Cells were lysed by adding 1 ml of 0.3 M sodium hydroxide (NaOH)+1% sodium dodecyl sulfate (SDS) solution and incubated at 37°C for 45 minutes. Lysed cells were mixed into suspension by

pipetting up and down ten times. Five microlitres of the cell lysate was used for protein determination using the Bradford method as described in section 3.7.

The remainder of the lysate (995 µl) was aliquoted into Eppendorf tubes and stored at -20°C. For scintillation analysis, the cell lysate was thawed at room temperature and the entire suspension was added to a scintillation vial containing 1 ml distilled water. Thereafter, 8 ml of Ready Gel Ultima Gold was added to the vials and the samples were mixed by vigorous shaking until it formed a whitish gel. Vials were placed into a liquid scintillation analyzer (2200 CA, Parkard Tricarb series) and left in the analyzer overnight to allow samples to equilibrate to room temperature and darkness. The following day, the samples were read with a program for quantifying the ^{3}H-isotope. Results were calculated using the counts per minute (CPM) to determine DOG uptake, and disintegrations per minute (DPM) to determine counter efficiency. The specific radioactivity of DOG and the counter efficiency were used to determine cpm/fmol. The averaged CPM and protein values were used to determine the fmol/mg. Results were reported as fmol 2-deoxy-[^{3}H]-D-glucose /mg protein using the GraphPad radioactivity calculator (GraphPad software).

3.7 Protein determination

Protein concentrations were determined using the Bradford protein determination method, according to the manufacturer's instructions. A BSA protein standard curve was included in the 96 well plate by adding, 5 µl of BSA standards (0.125, 0.25, 0.5, 0.75, 1, 1.5 and 2.0 mg/ml) into the first row. Thereafter, 5 µl of samples prepared in section 3.6 were added to the remaining wells of the 96 well plate. Two hundred and fifty microlitres of Bradford reagent was then added to each well containing standards or samples and mixed by pipetting up and down twice. The plate was incubated at room temperature for ten minutes and the absorbance was read at OD_{570} in a BioTek® ELX800 plate reader. The amount of protein in the sample was quantified by subtracting the absorbance of the blank

from the standard and sample absorbance values. A standard curve was graphed by plotting absorbance values of the BSA standards against their concentrations. The protein concentrations of samples were determined from the BSA standard curve. Protein concentration expressed as mg/ml was used to normalise 2-deoxy-[^{3}H]-D-glucose uptake results.

3.8 Deproteinizing samples for the glucose-6-phosphate and glycogen assays

As the presence of proteins and their enzymatic activities may interfere with the analysis of small molecules in biological samples. Samples for the G6P and glycogen determination assays were deproteinized using the perchloric acid (PCA) precipitation method.

Cells were treated as described in section 3.3. Thereafter, cells were trypsinized, rinsed with PBS, spun down and the pellet was frozen at -80°C. The frozen pellet was deproteinized using the deproteinizing sample preparation kit according to the manufacturer's recommendations. A volume of 250 µl of distilled water and 50 µl of ice cold PCA was added to the cell pellet. The pellet was dissolved by pipetting up and down ten times. Thereafter, cells were centrifuged at 4°C for two minutes at 13 000 g. A total of 240 µl of supernatant was transferred to a new tube, 10 µl of neutralizing solution was added and mixed by pipetting up and down. Thereafter, samples were placed on ice for five minutes, centrifuged at 13 000 g for two minutes and the G6P and glycogen assays were performed.

3.9 The glucose-6-phosphate assay

The G6P assay was done to investigate the effect of FFAs on G6P, a key intermediate of glucose metabolism. After cells were deproteinized, G6P concentrations were determined using a commercial kit according to the manufacturer's instructions (Glucose-6-phosphate kit, Biovision). To estimate the actual G6P concentrations in the cells, a glucose standard curve was prepared

by pipetting 0, 2, 4, 6, 8, and 10 µl nM of G6P standard into the wells of a 96 well plate and adjusted to 50 µl with a G6P assay buffer. Fifty microlitres of the samples (section 3.8) were added into the remaining wells of the 96 well plate. Thereafter, 50 µl of reaction mix consisting of G6P assay buffer, G6P enzyme mix and G6P substrate mix was added to the wells containing the standards and samples. The plate was incubated at 37°C for 30 minutes, and the plate was read at OD_{450} in the BioTek® plate reader ELX 800 using Gen 5® software. Absorbance values were divided by 0.8 to correct for sample dilution during deproteinization. The concentrations of G6P in samples were determined from the standard curve. Results were reported as nM G6P/µl, calculated as follows:

nM G6P/µl = Amount of G6P in sample (nM)/total sample volume (µl)

3.10 The glycogen assay

After deproteinization as described in section 3.8, the glycogen assay was done to determine the effect of FFA on glycogen synthesis. Glycogen concentrations were determined using a commercial kit according to the manufacturer's instructions (Glycogen assay kit, Biovision).

To estimate the actual glycogen concentration, a glycogen standard curve was prepared by pipetting 0, 2, 4, 6, 8, and 10 µl µg of glygocen standards into the wells of a 96 well plate and adjusted to 50 µl with hydrolysis buffer. Fifty microlitres of samples were added to the remaining wells of the 96 well plate, and 2 µl of hydrolysis enzyme mix was added to the wells containing the standards and samples. The plate was incubated at room temperature for 30 minutes, thereafter 50 µl of reaction mix consisting of development buffer, development enzyme mix and OxiRed probe was added to the wells containing the standards and samples. The plate was incubated at room temperature, protected from light, for 30 minutes, the plate was read at OD_{570} in the BioTek® plate reader ELX 800 using Gen 5®software. Absorbance values were divided by 0.8 to correct for sample dilution during deproteinization. The concentrations of glycogen in samples were determined from the standard curve. Results were reported as µg

glycogen/µl which was calculated as follows: **µg glycogen/µl = Amount of glycogen in sample (µg)/total sample volume (µl)**

3.11 Glucose oxidation

Glucose oxidation refers to the process whereby glucose is broken down into CO_2 and H_2O with the release of energy as ATP. In this study, glucose oxidation was measured using the method described by Kraft and Johnson (1972), with slight modifications. Cells were treated as described in section 3.3. After six hours of incubation, media was removed and cells were washed twice with 1 ml of warm DPBS. Thereafter, glucose oxidation was initiated by adding 500 µl of DMEM containing 5.5 mM glucose and 0.5 µCi/ ml glucose D-[^{14}C (U)] to each well. Few drops of 0.1 M NaOH were added to the filter paper (to ensure that CO_2 is absorbed onto the membrane) was placed onto the bottom of individual lids of the 6 well plates. After closing the plates, cells were incubated for one hour at 37°C in 5% CO_2 and humidified air. After an hour, filter paper was removed, placed in a scintillation vial containing 10 ml of scintillation fluid and mixed. Vials were placed in the scintillation counter and left overnight to equilibrate in the dark. The samples were read using a programme for quantifying ^{14}C. Results were calculated using the counts per minute (CPM) to determine ^{14}C release, and disintegrations per minute (DPM) to determine counter efficiency. The specific radioactivity of glucose D-[^{14}C (U)] and the counter efficiency were used to determine cpm/fmole. The averaged CPM and protein values were used to determine the fmol/mg. Results were reported as fmol/mg protein using the GraphPad radioactivity calculator.

3.12 RNA extraction

Total RNA was extracted from C2C12 myocytes and 3T3-L1 adipocytes cultured in 5.5 mM glucose and 0.75 mM palmitate. One millilitre of Tri reagent was added to a well of a six well plate, the cells were scraped off the surface of the well, and

the Tri-reagent and cells mixture was transferred to the next replicate well. This was done to facilitate the pooling of triplicate wells. Finally, the cells were transferred to 2 ml Eppendorf tubes containing stainless steel beads and stored at -80°C. Cells were thawed, lysed and homogenised in a TissueLyser (Qiagen) for two minutes at 20 Hz. The lysate was centrifuged at 12 000 g for ten minutes at 4°C and the supernatant was transferred to a new Eppendorf tube. Thereafter, 0.2 ml of chloroform was added to each tube, mixed intermittently for three minutes and centrifuged at 12 000 g for 15 minutes at 4°C. The upper aqueous phase was transferred to a new 1.5 ml Eppendorf tube without disturbing the interphase or organic phase. Thereafter, 0.5 ml of isopropanol was added and mixed thoroughly. For RNA precipitation, samples were incubated at -20°C overnight. The following day, the RNA was pelleted by centrifuging at 12 000 g for 20 minutes at 4°C. The supernatant was discarded, the RNA pellet was washed with 1 ml 75% ethanol and centrifuged at 12 000 g for 15 minutes at 4°C. This wash step was repeated. After the final wash, the fluid was drained from the Eppendorf tubes by blotting on paper towel and the pellet in the tube was allowed to air dry for 15 minutes. The RNA pellet was resuspended by adding 100 µl RNase free water, mixed by pipetting up and down ten times and then incubated at 55°C for ten minutes. Thereafter, RNA was cleaned up using the RNeasy Mini kit according to the manufacturer's instructions.

A volume of 350 µl of RLT lysis buffer was added to the RNA solution, followed by 250 µl of 96% ethanol and mixing by pipetting up and down. The samples were transferred to an RNeasy spin column in a 2 ml collection tube and centrifuged at 12 000 g for 15 seconds. The flow-through was discarded and 500 µl RPE buffer was added to the RNeasy spin column, centrifuged at 12 000 g for 15 seconds and the flow-through discarded. Thereafter, 500 µl RPE buffer was added to the spin column, centrifuged at 12000 g for two minutes and the flow-through discarded. The RPE wash step was repeated. Hereafter, the RNeasy spin column was placed in a new 2 ml collection tube and centrifuged at 12 000 g for one minute to ensure that the membrane was completely dry. To elute the

RNA, the RNeasy spin column was placed in a new 1.5 ml collection tube and 40 µl of RNase free water was added directly to the spin column membrane. Samples were allowed to stand at room temperature for one minute before RNA was eluted by centrifugation at 12 000 g for one minute. The elution step was repeated to ensure that all RNA was retrieved from the spin column. Another 40 µl RNase free water was added directly to the spin column membrane. Samples were allowed to stand at room temperature for one minute and RNA was eluted by centrifugation at 12 000 g for one minute. The two RNA eluates were pooled and placed on ice for RNA quantification.

3.13 RNA quantification and purity

Nucleic acids (RNA and DNA) absorb at 260 nm (A_{260}), while proteins and other contaminants absorb at 280 nm (A_{280}). Thus, the ratio of 260 nm to 280 nm is used to assess the purity of a sample. A ratio of two is generally accepted as pure for RNA. The ratio of A_{260} to A_{230} is used as a secondary measure of purity, and indicates contaminants that absorb at or near 230 nm.

RNA concentration and purity was determined by measuring the absorbance at $A_{260,}$ A_{280} and A_{230} in a Nanodrop 1000 spectrophotometer. The spectrophotometer was initialised by pipetting 2 µl distilled water onto the pedestal of the spectrophotometer, and blanked with 2 µl RNase free water. Thereafter, 2 µl sample was pipetted onto the pedestal and the absorbance determined. Each sample was read in triplicate.

3.14 DNase treatment

RNA samples were DNase treated to remove contaminating genomic DNA from RNA preparations. Samples were DNase treated using the Turbo DNase kit as recommended by the manufacturers. Briefly, 5 µl of 10x DNase buffer and 1.5 µl of DNase was added to 20 µg of RNA and RNase-free water in a total reaction volume of 50 µl. Samples were mixed and incubated at 37°C for 30 minutes, after which another 1.5 µl of DNase was added and incubated at 37°C for a further 30

minutes. The reaction was stopped by adding 10 µl DNase inactivation reagent and mixed by placing tubes on an orbital shaker for two minutes. Thereafter, the tubes were centrifuged at 10 000 g for 1.5 minutes and the supernatant transferred to a new tube. RNA concentrations were determined using a Nanodrop 1000 spectrophotometer.

3.15 Reverse transcription

Total RNA was reverse transcribed into cDNA using the High-Capacity cDNA kit according to the manufacturer's instructions. One microgram DNase treated RNA sample was added to 10 µl RNase-free water and placed on ice. A reaction mix consisting of reaction buffer, dNTPs, random primers, RNase-inhibitor (5000 units/ml), reverse transcriptase and nuclease-free water was prepared into two separate tubes labelled RT plus and RT minus. The RT minus reaction mix tube (negative control) contained the same reaction mix as the RT plus tube, but with the reverse transcription enzyme replaced by water (Table 3). After adding the RT plus and RT minus mix components, the prepared reaction mixes were mixed by pipettting and the tubes centrifuged briefly.

Table 3. Reaction components for the reverse transcription reaction.

Component	Volume (µl)	
	Plus RT	**Minus RT**
1 µg DNase-treated RNA in RNase-free water	10	10
10 x RT buffer	2	2
25 x dNTP mix	0.8	0.8
10 x random primers	2	2
RNase inhibitor	1	1
Nuclease-free water	3.2	4.2
Reverse Transcriptase	1	0
Total volume	20	20

Ten microlitres of plus or minus RT reaction mixes were added to 0.2 ml tubes containing RNA samples. The tube contents were mixed, briefly centrifuged and placed in a 2720 thermal cycler. Reactions were incubated at 25°C for 10

minutes, 37°C for 120 minutes, and 85°C for five seconds to inactivate the reverse transcriptase enzyme. Samples were stored at -20°C until gene expression analysis. The RT minus tube (negative control) was used to calculate the amount of genomic DNA contamination.

3.15.1 Quantitative Real-time PCR to assess genomic DNA contamination

To assess the extent of genomic DNA contamination in RNA samples, cDNA generated from plus and minus reverse transcription reactions were amplified with exon spanning primers that would amplify both mRNA and genomic DNA. A reaction mix consisting of 12.5 μl SYBR Green mix, 1 μl of 10 μM ActB Forward Primer (400 nM), 1 μl of 10 μM ActB Reverse Primer (400 nM) and H_2O to a final volume of 24 μl was prepared. The reaction mix was scaled up according to the number of test samples. The reaction mix is indicated in Table 4.

Twenty four microlitres of reaction mix was aliquoted into the PCR plate, followed by 1 μl (50 ng) of undiluted cDNA (plus or minus RT reactions). The plate was sealed with adhesive film, mixed on a plate shaker for ten minutes and then briefly centrifuged at 3 000 g. The PCR reactions were conducted on the ABI 7500 Sequence Detection System Instrument (Applied Biosystems) using the Absolute Quantification (AQ) Software (SDS V1.4). Universal cycling conditions; 50ºC for two minutes and 95ºC for ten minutes, followed by 40 cycles of 95ºC for 15 seconds and 60ºC for one minute were used. A dissociation curve was added for secondary product detection. Data was acquired during the extension step (60°C for one minute). After the run, default settings for the threshold cycle (Ct) and baseline were used and Ct values were exported to Microsoft Excel for analysis.

Table 4. Reaction mix for quantification of genomic DNA contamination

Component	Volume (µl)	Final Concentration
2x master mix	12.5	1X
ActB Forward primer (10 µM)	1	400 nM
ActB Reverse Primer (10 µM)	1	400 nM
Water	9.5	-
cDNA	1	50 ng
Final volume	25	-

3.15.2 Gene expression analysis

Quantitative real-time PCR (qRT-PCR) is one of the most sensitive and commonly used techniques to study gene expression. In this study Taqman® gene expression assays from Applied Biosystems were used. Taqman® gene expression assays consists of a Taqman® probe with a FAM™ or VIC® dye label and minor groove binder (MGB) moiety on the 5' end, and non-fluorescent quencher (NFQ) dye on the 3' end.

For qRT-PCR, a reaction mixture consisting of 5 µl of Taqman® universal PCR master mix, 0.5 µl of pre-developed Taqman® gene expression assays, and water to a final volume of 9 µl was prepared (Table 5).

Table 5. Reaction components for PCR reaction.

Component	Volume (µl)	Final Concentration
2x master mix	5	1X
Taqman Gene Expression Assay	0.5	
Water	3.5	
cDNA	1	5 ng
Final volume	10	

Standard curve was prepared from Total Rat Liver RNA (Ambion). The reaction mix was scaled up according to the number of samples to be analysed. Nine microlitres of the reaction mix was aliquoted into a well of the PCR plate, followed by 1 µl of a 10-fold dilution series of the standard curve or test samples cDNA. A no template control (NTC) using water instead of cDNA was used as a negative control in all PCR reactions. All samples were analysed in duplicate. PCR plates were covered with adhesive film and briefly centrifuged. Thereafter, plates were placed in a shaker for 10 minutes and briefly centrifuged at 3 000 g. The PCR reactions were conducted on the ABI 7500 Sequence Detection System Instrument (Applied Biosystems) using universal cycling conditions as described before. Data generated on the ABI 7500 Instrument was analysed with the ABI Standard Quantification (AQ) software (SDS V1.4) using a Ct of 0.1 and a baseline of between 3 and 15 cycles. Taqman® gene expression assays, Beta actin (ActB) and glyceraldehyde-3-phosphate dehydrogenase (Gapdh) (Table 6) were used as endogenous controls to normalize mRNA levels in test samples. Data was normalised to the average of the two endogenous controls. The Taqman® gene expression assays that were used in this study are listed in Table 6. The suffix _m represents an assay whose probe spans an exon-exon junction of the associated gene and therefore will not detect genomic DNA.

Table 6. Taqman® gene expression assays that were used in the study.

Probes	Assay ID
Insulin receptor substrate 1 (Irs1)	Mm01278327_m1
Insulin receptor substrate 2 (Irs2)	Mm03038438_m1
Phosphatidylinositol 3 Kinase (Pi3k)	Mm00803160_m1
Glucose transporter 4 (Glut4)	Mm01245502_m1
Glycogen synthase (Gsy)	Mm00523953_m1
Beta actin (ActB)	4352339E
Glyceraldehyde-3-phosphate dehydrogenase (Gapdh)	4352341E

3.17 Statistical analyses

All results are expressed as the mean ± standard deviation (SD). Statistical analyses of the data was done with the student t-test or one-way ANOVA where appropriate. Data with a p-value <0.05 was considered statistically significant. GraphPad Prism (version 5.02) or GraphPad Instat software version 5.02 was used for analyses.

Chapter 4

Results

4.1 Reporting of Results

Results will be reported under the following sub-headings:

- Differentiation of C2C12, L8 and 3T3-L1 cell lines.
- Determination of the optimal free fatty acid concentrations in C2C12 and 3T3-L1 cells.
- Glucose uptake by C2C12, L8 and 3T3-L1 cells exposed to FFAs (palmitate, oleate, omega 3 and omega 6) in culture with media containing 5.5 mM and 20 mM glucose.
- Glucose-6-phosphate concentrations in C2C12, L8 and 3T3-L1 cells exposed to FFAs (palmitate, oleate, omega 3 and omega 6) in culture with media containing 5.5 mM and 20 mM glucose.
- Glycogen concentrations in C2C12, L8 and 3T3-L1 cells exposed to FFAs (palmitate, oleate, omega 3 and omega 6) in culture with media containing 5.5 mM and 20 mM glucose.
- Glucose oxidation % in C2C12, L8 and 3T3-L1 cells exposed to FFAs (palmitate, oleate, omega 3 and omega 6) in culture with media containing 5.5 mM and 20 mM glucose.
- Summary of cell culture results.
- mRNA expression of Irs1, Irs2, Glut4, Pi3k and Gsy in C2C12 myocytes and 3T3-L1 adipocytes exposed to palmitate in media containing 5.5 mM glucose.
- Summary of mRNA results.

4.2 Myotubule formation

After two days of culture in DMEM supplemented with 10% FCS, C2C12 and L8 cells had grown to 80-90% confluence. At this stage the 10% FCS media was replaced by media containing 2% HS. Two days after transferring cells to the low serum medium, myotubule formation was observed. Compared to C2C12 cells (Figure 12A and B), L8 cells (Figure 13A and B) were less efficient at forming myotubules.

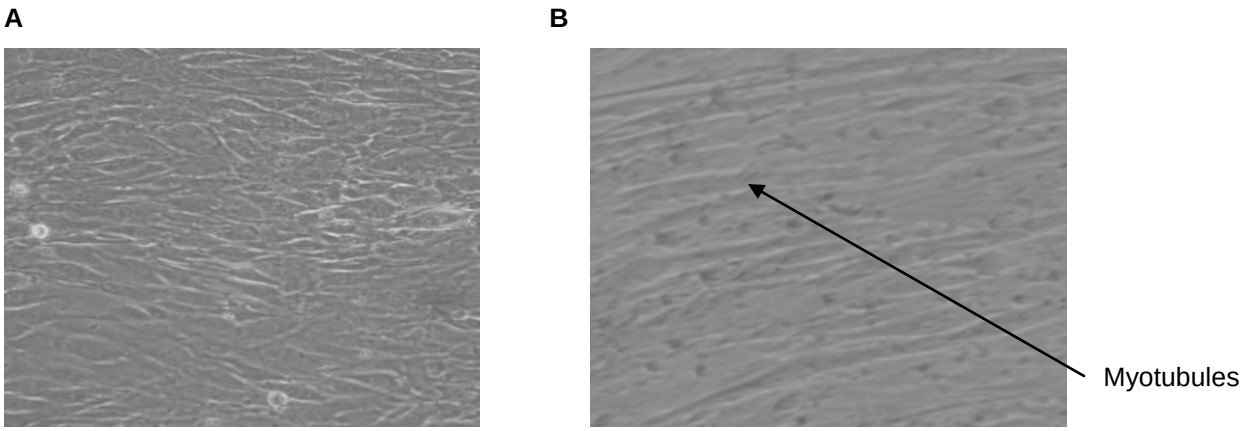

Figure 12. Myotubule formation in C2C12 cells.
A phase contrast photomicrograph of 80-90% confluent C2C12 cells (A). Spindle-shaped myotubules, indicated by the arrow, were formed after transferring confluent C2C12 cells to media supplemented with 2% HS (B).

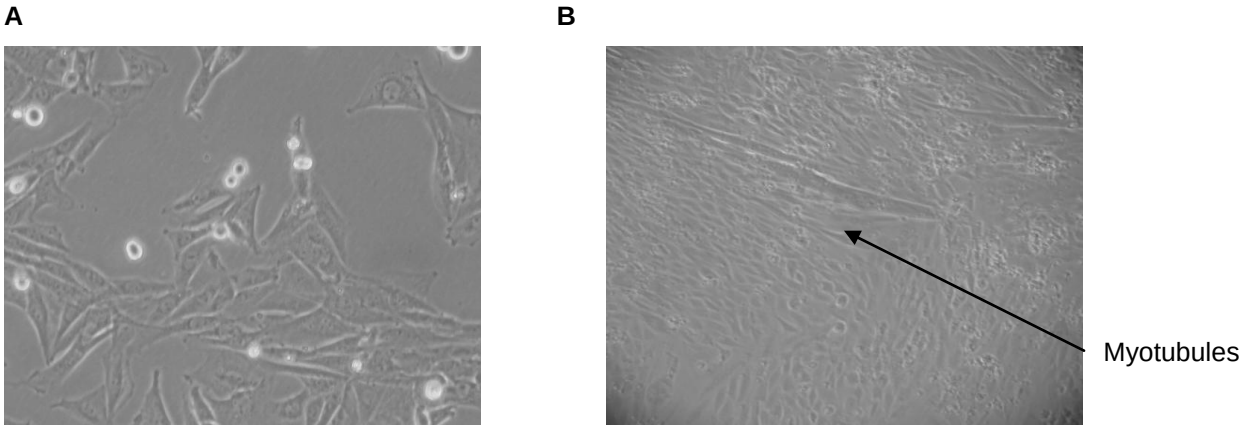

Figure 13. Myotubule formation in L8 cells.
A phase contrast photomicrograph of 50-60% confluent L8 cells (A). Spindle-shaped myotubules, indicated by the arrow, were formed after transferring confluent L8 cells to media supplemented with 2% HS (B).

4.3 Adipocyte formation

After three days of culture in DMEM supplemented with 10% FCS, 3T3-L1 cells had grown to 80-90% confluence. Adipocytic differentiation of the 3T3-L1 cells with visible intracellular fat accumulation was observed five days after exposure to adipogenic media (Figure 14A and B).

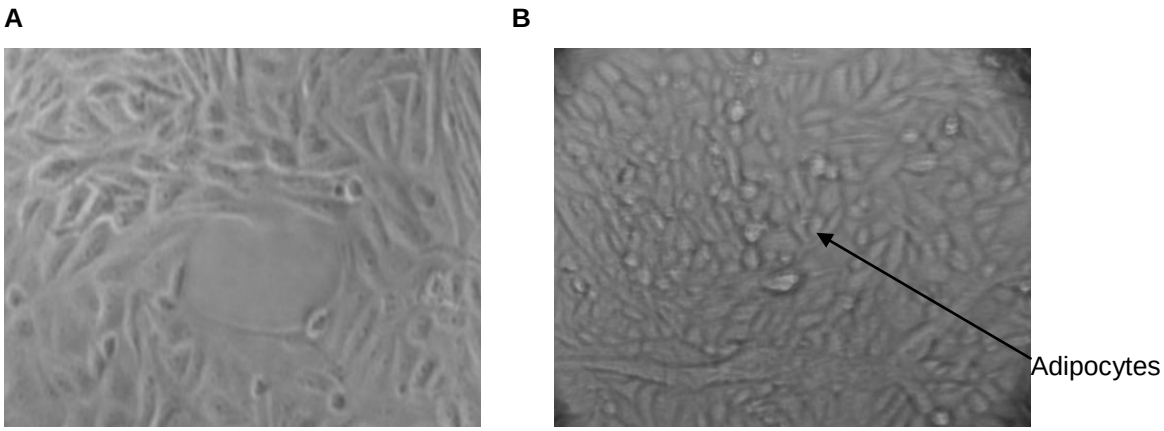

Figure 14. Adipogenesis in 3T3-L1 cells.
A phase contrast photomicrograph of 80-90% confluent 3T3-L1 cells (A). Fat accumulating adipocytes, indicated by the arrow, were formed after transferring confluent 3T3-L1 cells to adipogenesis inducing media (B).

4.4 Determining the optimal concentration of free fatty acid

A colourimetric glucose assay that measures the amount of glucose taken up from the culture media by cells, was used to determine the concentration of FFA that exerted the maximal effect on glucose uptake. C2C12 myocytes and 3T3-L1 adipocytes were cultured in 5.5 mM of glucose containing five different concentrations of FFAs (0, 0.25, 0.5, 0.75 and 1 mM) for two hours, and the effect on glucose uptake was assessed. Furthermore, the MTT assay, commonly used to determine mitochondrial activity and cell viability, showed that 0.75 mM FFA did not affect mitochondrial dehydrogenase activity when cells were exposed to the various FFAs for two hours.

4.4.1 Palmitate

In C2C12 myocytes, palmitate at the highest concentration tested (1 mM) reduced both glucose uptake and mitochondrial activity, suggestive of possible lipid cytotoxicity. Palmitate at the concentration of 0.5 mM and 0.75 mM reduced glucose uptake without affecting mitochondrial activity. In 3T3-L1 cells addition of palmitate had no effect on glucose uptake or mitochondrial activity at any of the concentrations tested (Table 7).

Table 7. The effect of palmitate on glucose uptake and mitochondrial dehydrogenase activity.

	Palmitate concentration				
	0 mM	**0.25 mM**	**0.5 mM**	**0.75 mM**	**1 mM**
C2C12 myocytes					
% glucose uptake‡	100.0 ± 14.1	105.5 ±1 2.0	57.1 ± 7.0**	52.1 ± 12.0*	54.6 ± 14.0*
P value		0.67	**0.006**	**0.01**	**0.03**
% formazan production#	100.0 ± 17	115.5 ± 13.4	92.2 ± 9.9	96.1 ± 14.4	38.7 ± 9.2**
P value		0.1	0.1	0.7	**0.002**
3T3-L1 adipocytes					
% glucose uptake‡	100.0 ± 21.1	62.9 ± 17.4	60.8 ± 30.6	69.9 ± 24.6	67.2 ± 1.7
P value		0.6	0.5	0.7	0.6
%formazan production#	100.0 ± 1.9	95.7 ± 8.2	93.6 ± 26.1	87.4 ± 22.1	83.6 ± 23.9
P value		0.2	0.5	0.1	0.1

‡Glucose uptake was calculated by subtracting the glucose concentration remaining in the media after incubation with palmitate, from the initial glucose concentration (5.5 mM glucose) and the percentage glucose uptake was calculated and normalised against the control without FFA

#Formazan production is an indicator of mitochondrial dehydrogenase activity and cell viability. The formazan concentration following exposure to palmitate at various concentrations was calculated and normalised against the control without FFA.

Results are expressed as the average of three independent experiments ± standard deviation;*P<0.05, **P<0.005

4.4.2 Oleate

In C2C12 myocytes, 0.5 mM and 0.75 mM oleate stimulated glucose uptake, however, this increase was not statistically significant. None of the concentrations of oleate tested affected mitochondrial activity (Table 8). Oleate did not affect glucose uptake in 3T3-L1 adipocytes. However, 1.0 mM oleate decreased mitochondrial activity in adipocytes (Table 8).

Table 8. The effect of oleate on glucose uptake and mitochondrial dehydrogenase activity.

	Oleate concentration				
	0 mM	**0.25 mM**	**0.5 mM**	**0.75 mM**	**1.0 mM**
C2C12 myocytes					
% glucose uptake‡	100.0 ± 14.1	107.5 ± 18.0	145.8 ± 45.0	142.0 ± 45.0	92.6 ± 10.0
P value		0.6	0.3	0.3	0.1
% formazan production#	100.0 ± 17.0	116.0 ± 8.3.0	92.2 ± 24.6	99.2 ± 14.5	91.5 ± 14.4
P value		0.1	0.5	0.9	0.4
3T3-L1 adipocytes					
% glucose uptake‡	100.0 ± 4.1	76.6 ± 13.1	77.3 ± 4.9	78.3 ± 6.1	59.3 ±1 5.9
P value		0.7	0.7	0.7	0.5
% formazan production#	100.0 ± 1.9	85.7 ± 19.4	95.3 ± 5.5	97.7 ± 11.7	81.3 ± 18.5*
P value		0.1	0.08	0.7	**0.04**

‡Glucose uptake was calculated by subtracting the glucose concentration remaining in the media after incubation with oleate, from the initial glucose concentration (5.5 mM glucose) and the percentage glucose uptake was calculated and normalised against the control without FFA (0mM)

#Formazan production is an indicator of mitochondrial dehydrogenase activity and cell viability. The formazan concentration following exposure to oleate at various concentrations was calculated and normalised against the control without FFA.

Results are expressed as the average of three independent experiments ± standard deviation;*P<0.05

4.4.3 Omega 3

Omega 3 had opposing effects on glucose uptake in C2C12 myocytes and 3T3-L1 adipocytes. In C2C12 myocytes all concentrations of omega 3 decreased glucose uptake, although this was not significant. None of the concentrations tested affected mitochondrial dehydrogenase activity (Table 9). In 3T3-L1 myocytes, all concentrations of omega 3 increased glucose uptake, without affecting mitochondrial dehydrogenase activity (Table 9).

Table 9. The effect of omega 3 on glucose uptake and mitochondrial dehydrogenase activity.

	Omega 3 concentrations				
	0 mM	**0.25 mM**	**0.5 mM**	**0.75 mM**	**1 mM**
C2C12 myocytes					
% glucose uptake‡	100.0 ± 14.3	92.6 ± 10.0	84.5 ± 6.0	68.3 ± 25.0	79.2 ±19.0
P value		0.5	0.1	0.2	0.3
% formazan production#	100.0 ± 16.3	92.3 ± 11.2	99.0 ± 19.1	100.9 ± 11.7	93.3 ±9.0
P value		0.5	0.9	0.9	0.5
3T3-L1 adipocytes					
% glucose uptake‡	100.0 ± 21.1	126.0 ± 5.6**	135.6 ± 9.9**	130.1 ± 21.5	141.5 ± 6.7*
P value		**0.001**	**0.004**	0.083	**0.01**
% formazan production#	100.0 ± 1.99	93.9 ± 41.6	107.0 ± 21.3	107.1 ± 41.3	103.9 ± 14.3
		0.6	0.3	0.6	0.4

‡Glucose uptake was calculated by subtracting the glucose concentration remaining in the media after incubation with omega 3, from the initial glucose concentration (5.5 mM glucose) and the percentage glucose uptake was calculated and normalised against the control without FFA (0mM)

#Formazan production is an indicator of mitochondrial dehydrogenase activity and cell viability. The formazan concentration following exposure to omega 3 at various concentrations was calculated and normalised against the control without FFA.

Results are expressed as the average of three independent experiments ± standard deviation;*P<0.05, **P<0.005

4.4.4 Omega 6

As with omega 3, omega 6 had opposing effects on glucose uptake in C2C12 myocytes and 3T3-L1 adipocytes. In C2C12 cells the 0.25 mM and 0.5 mM omega 6 increased glucose uptake while 0.75 mM and 1.0 mM omega 6 decreased glucose uptake. Mitochondrial activity was reduced by 1.0 mM omega 6 only (Table 10). In 3T3-L1 adipocytes, omega 6 at 0.5 mM, 0.75 mM and 1.0 mM concentrations increased glucose uptake. Mitochondrial activity was decreased by 0.75 mM and 1 mM omega 6 (Table 10).

Table 10. The effect of omega 6 on glucose uptake and mitochondrial dehydrogenase. activity.

	Omega 6 concentrations				
	0 mM	**0.25 mM**	**0.5 mM**	**0.75 mM**	**1 mM**
C2C12 myocytes					
% glucose uptake‡	100.0 ± 14.3	117.1 ± 9.0	123.2 ±9.0*	66.6 ± 3.0	71.4 ±3.0**
P value		0.1	**0.04**	0.3	**0.003**
% formazan production#	100.0 ± 16.3	111.6 ± 11.3	118.6 ± 23.2	100.2 ± 8.4	61.6 ± 8.4*
P value		0.3	0.2	0.9	**0.01**
3T3-L1 adipocytes					
% glucose uptake‡	100.0 ± 21.1	127.6 ± 32.8	134.2 ± 13.1*	130.4 ± 7.5**	134.1 ± 16.9*
P value		0.2	**0.01**	**0.003**	**0.02**
% formazan production#	100.0 ± 1.9	94.7 ± 34.8	91.8 ± 11.7	84.7 ± 11.8*	83.2 ± 13.8*
P value		0.6	0.1	**0.02**	**0.02**

‡Glucose uptake was calculated by subtracting the glucose concentration remaining in the media after incubation with omega 6, from the initial glucose concentration (5.5 mM glucose) and the percentage glucose uptake was calculated and normalised against the control without FFA (0mM)
#Formazan production is an indicator of mitochondrial dehydrogenase activity and cell viability. The formazan concentration following exposure to omega 6 at various concentrations was calculated and normalised against the control without FFA.
Results are expressed as the average of three independent experiments ± standard deviation;*P<0.05, **P<0.005

4.5 Selection of a single optimal concentration of free fatty acid for glucose uptake and metabolism experiments

As illustrated previously (Tables 7-10), different concentrations of the FFAs, palmitate, oleate, omega 3 and omega 6, exerted differing effects on glucose uptake and mitochondrial activity in C2C12 myocytes and 3T3-L1 adipocytes. It was decided to use 0.75 mM for each of the FFAs as this would allow a direct comparison of the FFA effect and potency on glucose uptake and metabolism in the different cells used in the study.

4.6 Glucose metabolism: C2C12 and L8 myocytes, and 3T3-L1 adipocytes

4.6.1The effect of FFAs on glucose uptake in C2C12 myocytes

The 2-deoxy-[^{3}H]-D-glucose uptake method was used to investigate the effect of FFA on the rate of basal and insulin-stimulated glucose uptake. Myocytes and adipocytes were cultured in media containing 5.5 mM or 20 mM glucose, 0.75 mM FFA (palmitate, oleate, omega 3 and omega 6), with or without 1 µM insulin stimulation, as described in section 3.3. Thereafter, cells were washed and exposed to media containing 5.5 mM glucose with 0.5 µCi of 2-deoxy-[^{3}H]-D-glucose for 15 minutes. After 15 minutes the cells were washed, lysed and intracellular 2-deoxy-[^{3}H]-D-glucose was measured using a liquid scintillation counter.

Palmitate reduced basal glucose uptake in C2C12 myocytes cultured in 5.5 mM (12.7 ± 3.0 fmol/mg vs. 4.5 ± 0.1 fmol/mg; p=0.03) and 20 mM (8.2 ± 1.4 fmol/mg vs. 5.0 ± 0.4 fmol/mg; p=0.02) glucose. Neither oleate nor the essential FFAs omega 3 and omega 6, significantly affected basal glucose uptake when cells were cultured in either 5.5 mM or 20 mM glucose (Figure 15).

Palmitate reduced insulin-stimulated glucose uptake in C2C12 myocytes cultured in 5.5 mM (20.5 ± 3.11 fmol/mg vs. 7.2 ± 5.8 fmol/mg; p=0.02) and 20 mM (9.2 ± 2.2 fmol/mg vs 5.3 ± 1.3 fmol/mg; p=0.05) glucose. Oleate decreased insulin-stimulated glucose uptake in cells cultured in 5.5 mM glucose (20.5 ± 3.1 fmol/mg vs. 11.2 ± 2.7 fmol/mg; p=0.01), but had no affect on glucose uptake when cells were cultured in 20 mM glucose. The essential FFAs, omega 3 (20.5 ± 3.1 fmol/mg vs. 12.6 ± 3.5 fmol/mg; p=0.1) and omega 6 (20.5 ± 3.1 fmol/mg vs. 8.7 ± 3.2 fmol/mg; p=0.08) decreased insulin-stimulated uptake, although not statistically significant, when cells were cultured in 5.5 mM glucose but not when cells were cultured in 20 mM glucose (Figure 16).

A

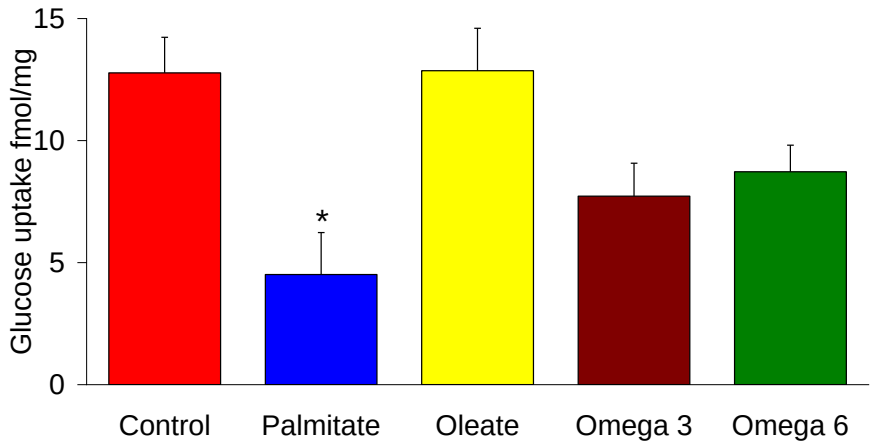

B

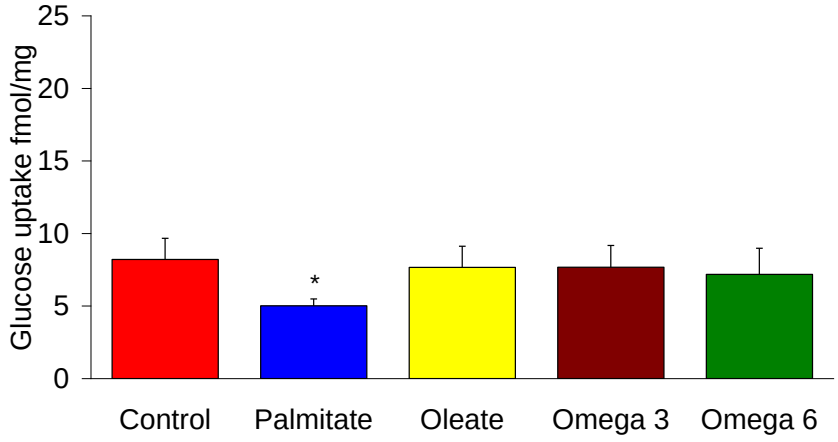

Figure 15. The effect of FFAs on basal glucose uptake in C2C12 myocytes.
Myocytes were cultured in 5.5 mM (A) or 20 mM (B) glucose and exposed to the indicated FFAs for six hours. Glucose uptake was measured using the 2-deoxy-[^{3}H]-D-glucose method. Results are expressed as the mean of three independent experiments ± SD; *P < 0.05.

A

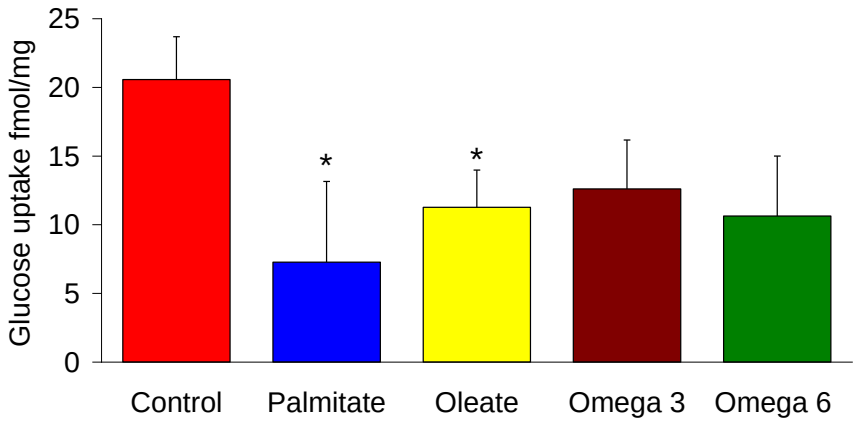

B

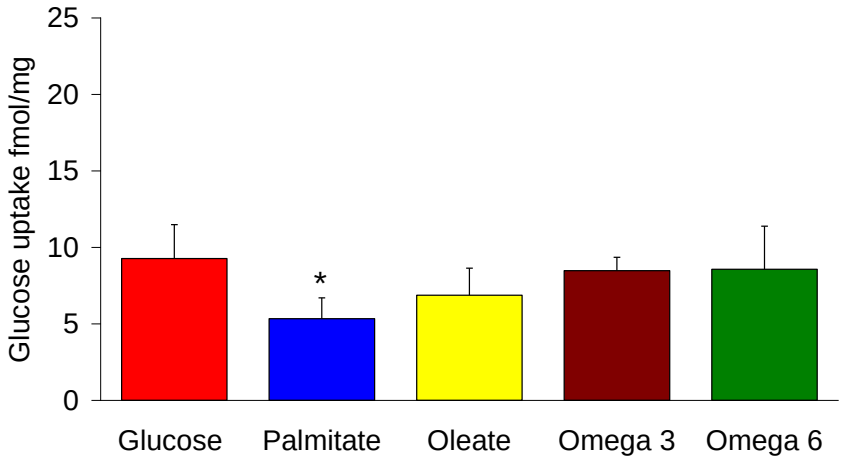

Figure 16. The effect of FFAs on insulin-stimulated glucose uptake in C2C12 myocytes. Myocytes were cultured in 5.5 mM (A) or 20 mM (B) glucose and exposed to the indicated FFAs for six hours, with insulin stimulation in the last hour. Glucose uptake was measured using the 2-deoxy-[^{3}H]-D-glucose method. Results are expressed as the mean of three independent experiments ± SD; *P < 0.05.

4.6.2 The effect of FFAs on glucose uptake in L8 myocytes

Palmitate reduced basal glucose uptake in L8 myocytes cultured in 5.5 mM glucose (4.39 ± 0.24 fmol/mg vs. 2.0 ± .0.5 fmol/mg; p=0.03), however it had no effect on cells cultured in 20 mM glucose. Neither oleate nor the essential FFAs omega 3 and omega 6, significantly affected basal glucose uptake when cells were cultured in either 5.5 mM or 20 mM glucose (Figure 17).

Palmitate reduced insulin-stimulated glucose uptake in L8 myocytes cultured in 5.5 mM glucose (5.3 ± 0.7 fmol/mg vs. 2.5 ± 0.6 fmol/mg; p=0.01). Neither oleate nor the essential FFAs omega 3 and omega 6, significantly affected insulin stimulated glucose uptake when myocytes were cultured in 5.5 mM glucose. However in myocytes cultured in 20 mM glucose, palmitate (12.4 ± 2.1 fmol/mg vs. 2.5 ± 0.7 fmol/mg; p= 0.001), oleate (12.4 ± 2.1 fmol/mg vs. 7.4 ± 0.6 fmol/mg; p=0.01), omega 3 (12.4 ± 2.1 fmol/mg vs. 8.4 ± 0.3 fmol/mg; p= 0.02) and omega 6 (12.4 ± 2.1 fmol/mg vs. 8.7 ± 0.7 fmol/mg; p=0.04) reduced insulin-stimulated glucose uptake (Figure 18).

A

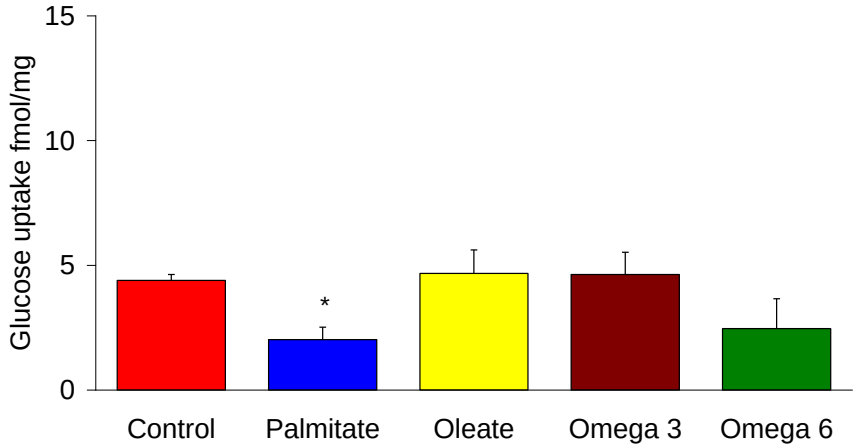

B

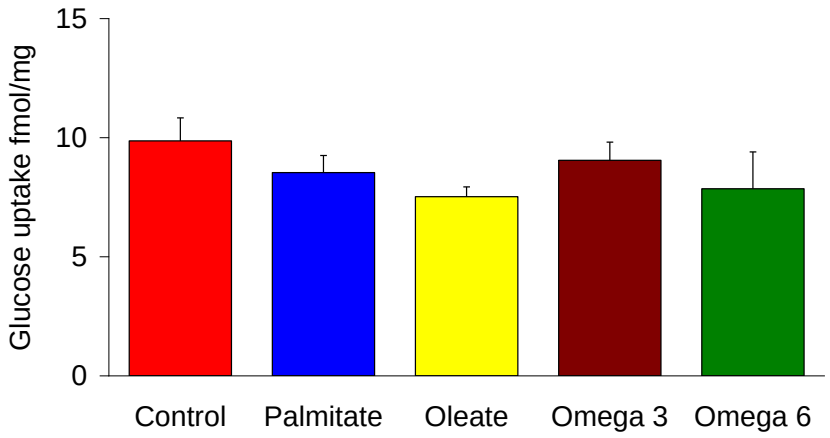

Figure 17. The effect of FFAs on basal glucose uptake in L8 myocytes.
Myocytes were cultured in 5.5 mM (A) or 20 mM (B) glucose and exposed to the indicated FFAs for six hours. Glucose uptake was measured using the 2-deoxy-[^{3}H]-D-glucose method. Results are expressed as the mean of three independent experiments ± SD; *P < 0.05.

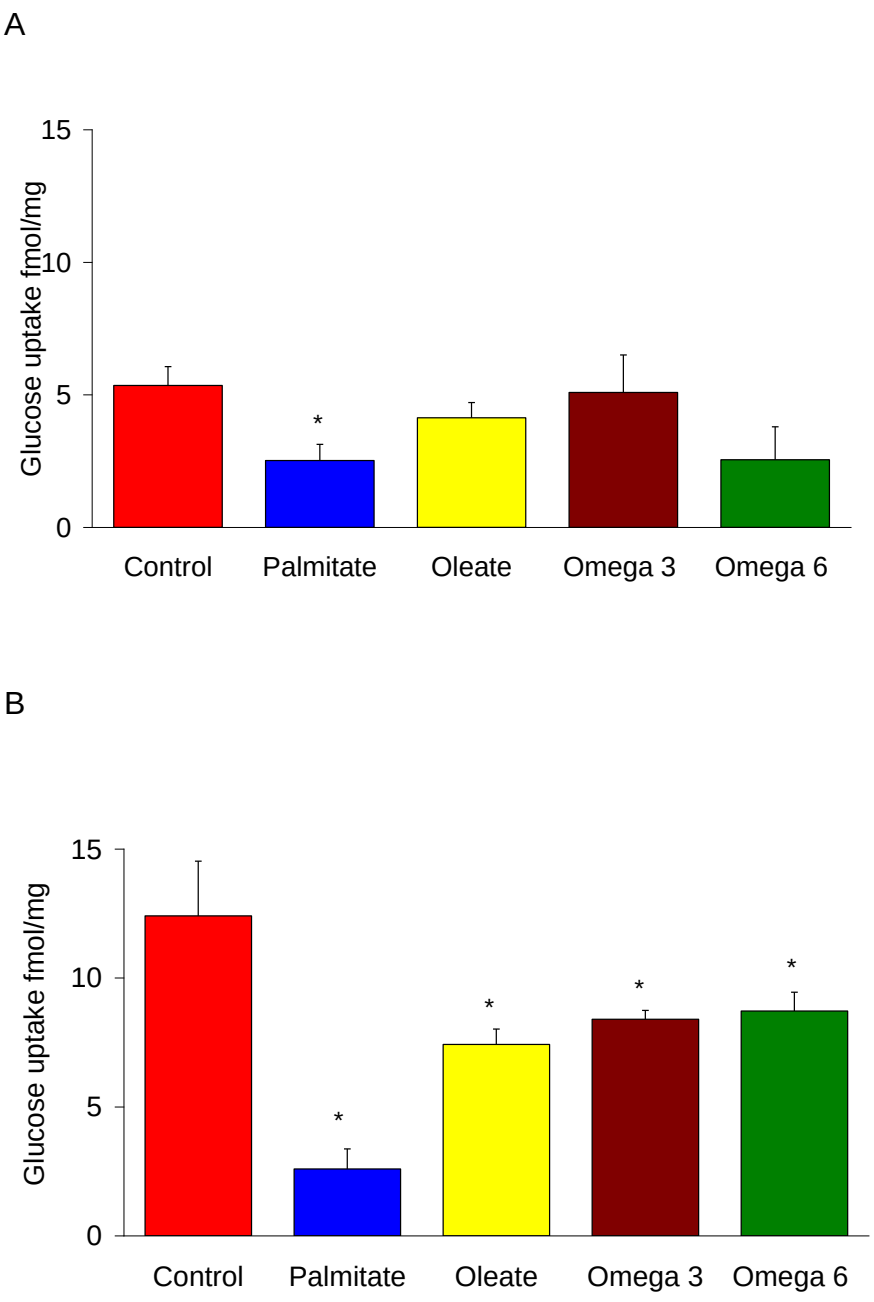

Figure 18. The effect of FFAs on insulin-stimulated glucose uptake in L8 mycocytes. Myocytes were cultured in 5.5 mM (A) or 20 mM (B) glucose and exposed to the indicated FFAs for six hours with insulin stimulation in the last hour. Glucose uptake was measured using the 2-deoxy-[^{3}H]-D-glucose method. Results are expressed as the mean of three independent experiments ± SD; *P < 0.05.

4.6.3 The effect of FFAs on glucose uptake in 3T3-L1 adipocytes

Palmitate, oleate, omega 3 and omega 6 had no effect on basal glucose uptake in adipocytes cultured in 5.5 mM glucose. Similar results were observed when cells were cultured in 20 mM glucose except for palmitate, that reduced basal glucose uptake (17.8 ± 11.7 fmol/mg vs. 9.3 ± 6.4 fmol/mg; p =0.02) (Figure 19).

Palmitate, oleate, omega 3 and omega 6 had no effect on insulin-stimulated glucose uptake in adipocytes cultured in 5.5 mM glucose, however in adipocytes cultured in 20 mM glucose, palmitate significantly reduced insulin-stimulated glucose uptake (27.6 ± 18.0 fmol/mg vs. 10.1 ± 7.1 fmol/mg; p=0.05). Neither oleate nor the essential FFAs, omega 3 and omega 6, significantly affected insulin-stimulated glucose uptake (Figure 20).

A

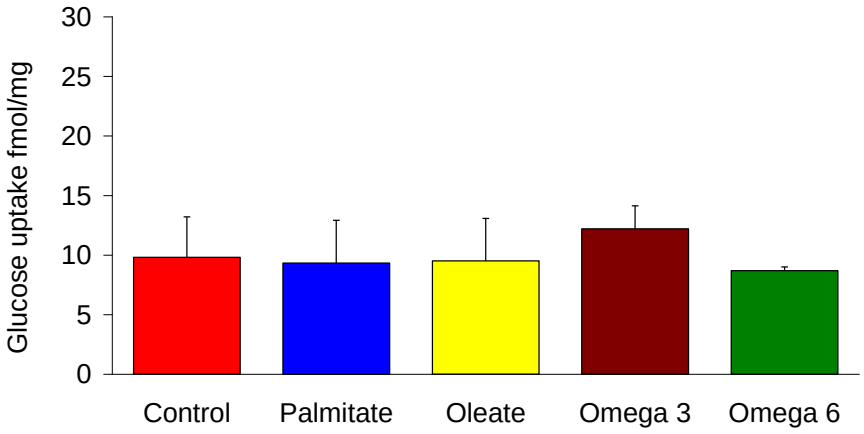

B

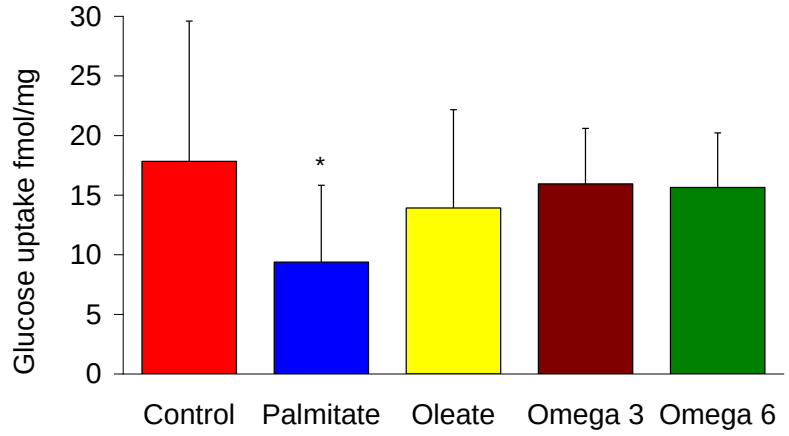

Figure 19. The effect of FFAs on basal glucose uptake in 3T3-L1 adipocytes.
Myocytes were cultured in 5.5 mM (A) or 20 mM (B) glucose and exposed to the indicated FFAs for six hours. Glucose uptake was measured using the 2-deoxy-[3H]-D-glucose method. Results are expressed as the mean of three independent experiments ± SD; *P < 0.05**.**

A

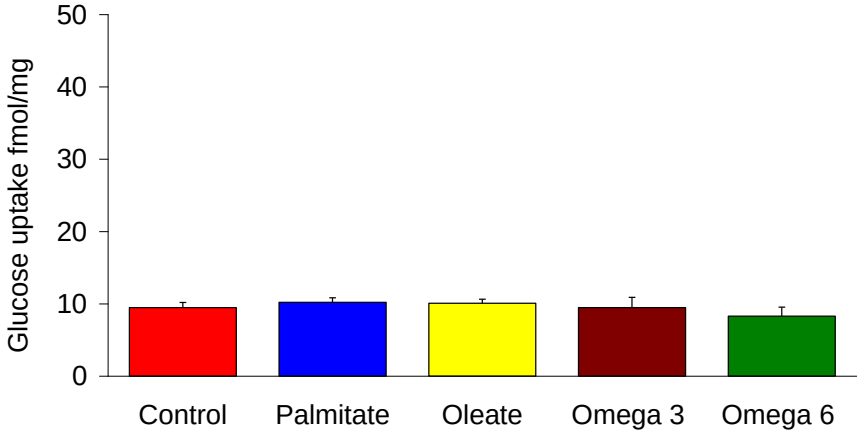

B

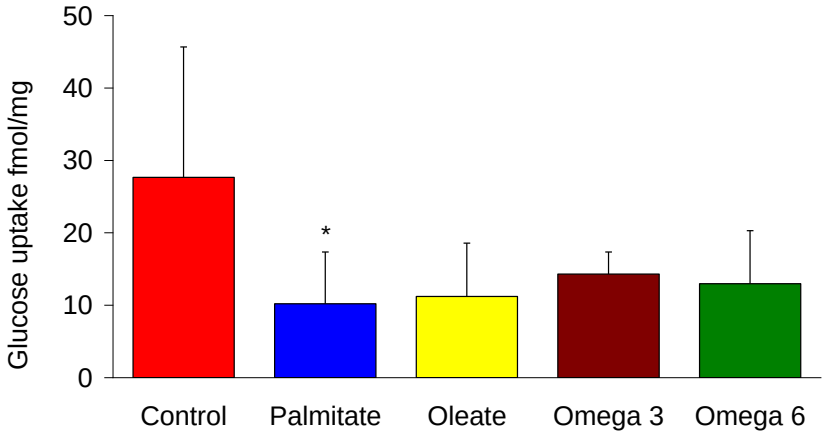

Figure 20. The effect of FFAs on insulin-stimulated glucose uptake in 3T3-L1 adipocytes. Adipocytes were cultured in 5.5 mM (A) or 20 mM (B) glucose and exposed to the indicated FFAs for six hours with insulin stimulation in the last hour. Glucose uptake was measured using the 2-deoxy-[3H]-D-glucose method. Results are expressed as the mean of three independent experiments ± SD; *P < 0.05.

4.7 Glucose utilization in C2C12 and L8 myocytes, and in 3T3-L1 adipocytes

4.7.1 The effect of free fatty acids on glucose-6-phosphate levels in C2C12 myocytes

The conversion of intracellular glucose to G6P by the enzyme hexokinase is a rate limiting step in glycolysis. To investigate the affect of FFAs on G6P concentrations in the cell, myocytes and adipocytes were cultured in 5.5 mM or 20 mM glucose and exposed to the various FFAs (palmitate, oleate, omega 3 and omega 6) at a concentration of 0.75 mM with or without 1 µM insulin stimulation as described in section 3.3.

During basal conditions, palmitate (10.1 ± 1.5 nM/µl vs. 2.9 ± 0.6 nM/µl; p=0.004) and omega 6 (10.1 ± 1.5 nM/µl vs. 1.9 ± 0.4 nM/µl; p=0.05) reduced G6P concentrations in C2C12 myocytes cultured in 5.5 mM glucose. Oleate (10.1 ± 1.5 nM/µl vs. 15.9 ± 0.9 nM/µl; p=0.01) and omega 3 (10.1 ± 1.5 nM/µl vs. 14.7 ± 0.4 nM/µl; p= 0.006) increased G6P concentrations in C2C12 myocytes cultured in 5.5 mM glucose. Similar results were observed in 20 mM glucose, where palmitate (12.1 ± 0.4 nM/µl vs. 3.7 ± 0.2 nM/µl; p=0.03) and omega 6 (12.1 ± 0.4 nM/µl vs. 7.6 ± 0.8 nM/µl; p =0.02) reduced G6P concentrations. However, oleate had no effect when myocytes were cultured in 20 mM, while omega 3 increased G6P concentrations (12.1 ± 0.4 nM/µl vs. 31.0 ± 1.7 nM/µl; p= 0.004) (Figure 21).

During insulin-stimulated conditions, palmitate reduced G6P concentrations in C2C12 myocytes cultured in 5.5 mM glucose (18.0 ± 0.4 nM/µl vs. 2.9 ± 0.0 nM/µl; p=<.0.0001). Similarly in 20 mM glucose, palmitate reduced G6P concentrations (13.0 ± 2.5 nM/µl vs. 4.3 ± 0.43 nM/µl; p=0.04). Oleate did not affect G6P concentrations in myocytes cultured in 5.5 mM glucose, however, oleate significantly increased G6P concentrations in myocytes cultured in 20 mM glucose (13.0 ± 2.56 nM/µl vs. 46.3 ± 0.4 nM/µl; p=0.003). Omega 3 (18.0 ± 0.4 nM/µl vs. 12.2 ± 0.9 nM/µl; p= 0.0007) and omega 6 (18.0 ± 0.4 nM/µl vs. 7.5 ± 0.4 nM/µl; p= 0.0007) decreased G6P concentrations in myocytes cultured in 5.5 mM glucose. In

myocytes that were cultured in 20 mM glucose, omega 3 (13.0 ± 2.5 nM/µl vs. 32.5 ± 3.8 nM/µl; p=0.02) and omega 6 (13.0 ± 2.5 nM/µl vs. 32.0 ± 0.3 nM/µl; p =0.01) increased G6P concentrations (Figure 22).

A

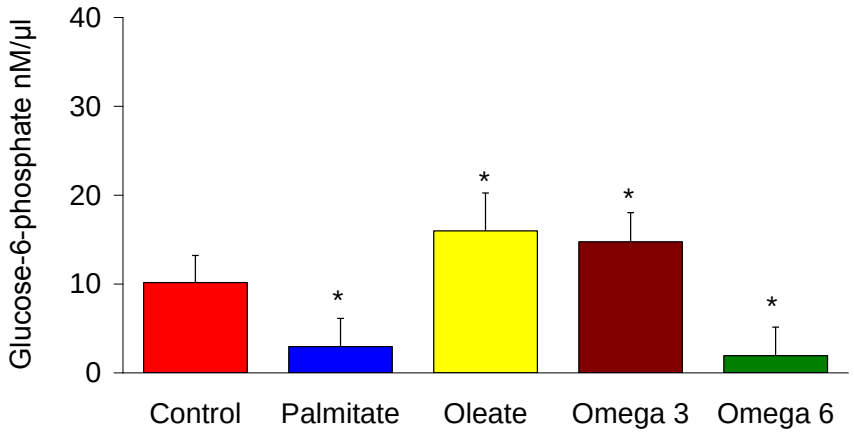

B

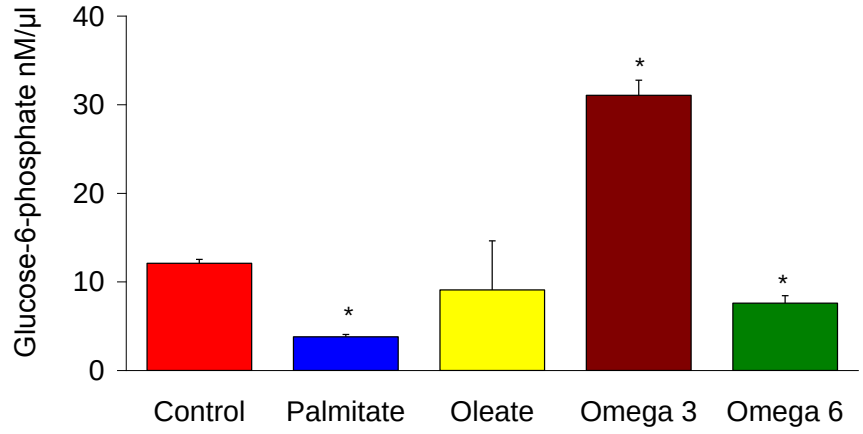

Figure 21. The effect of FFAs on basal glucose-6-phosphate concentrations in C2C12 myocytes.
Myocytes were cultured in 5.5 mM (A) or 20 mM (B) glucose and exposed to the indicated FFAs for six hours. Glucose-6-phosphate concentrations were measured using the glucose-6-phosphate assay kit. Results are representative of three independent experiments ± SD,*P < 0.05.

A

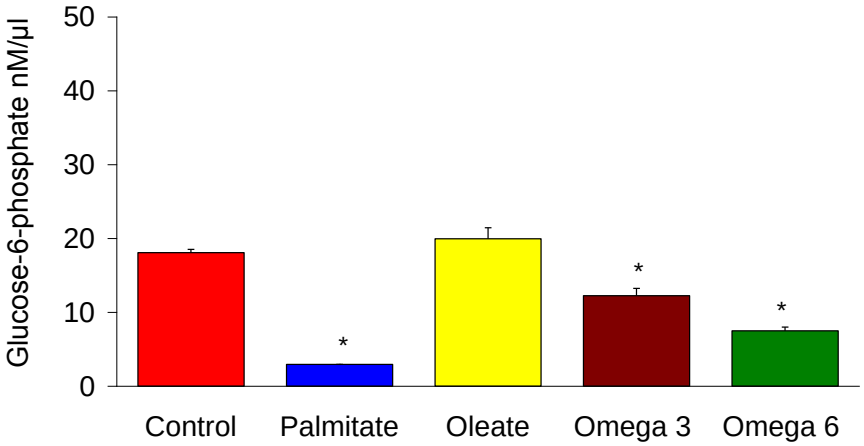

B

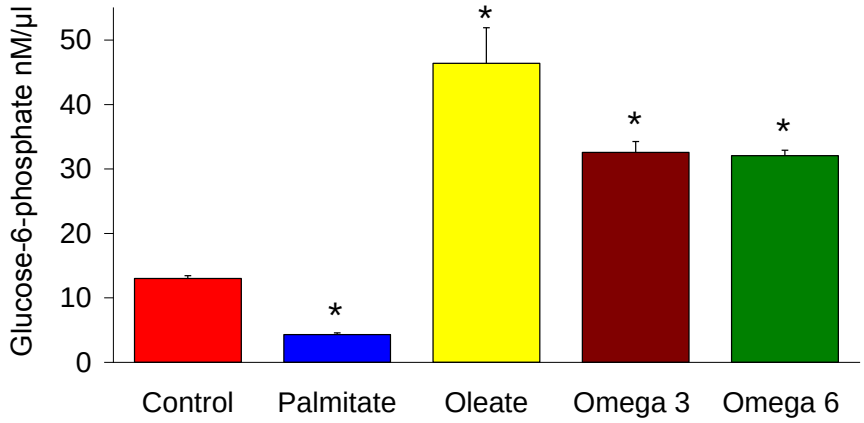

Figure 22. The effect of FFAs on insulin-stimulated glucose-6-phosphate concentrations in C2C12 myocytes.
Myocytes were cultured in 5.5 mM (A) or 20 mM (B) glucose and exposed to the indicated FFAs for six hours with insulin stimulation in the last hour. Glucose-6-phosphate concentrations were measured using the glucose-6-phosphate assay kit. Results are representative of three independent experiments ± SD,*P < 0.05.

4.7.2 The effect of free fatty acids on glucose-6-phosphate concentrations in L8 myocytes

Palmitate reduced basal G6P levels, although not significantly, in L8 myocytes cultured in 5.5 mM glucose (17.3 ± 0.7 nM/µl vs. 8.1 ± 6.1 nM/µl; p =0.1). Oleate (17.3 ± 0.7 nM/µl vs. 8.1 ± 6.1 nM/µl; p= 0.02) and omega 3 (17.3 ± 0.7 nM/µl vs. 8.3 ± 1.9 nM/µl p=0.01) also decreased G6P concentrations when cells were cultured in 5.5 mM glucose. Omega 6 increased G6P concentrations (17.3 ± 0.7 nM/µl vs. 21.9 ± 0.3 nM/µl; p =0.0006) when cultured in 5.5 mM glucose. In L8 myocytes that were cultured in 20 mM glucose, palmitate (27.2 ± 10.1 nM/µl vs. 9.7 ± 1.1 nM/µl; p= 0.01) and oleate (27.2 ± 10.1 nM/µl vs. 9.5 ± 3.1 nM/µl; p= 0.03) significantly reduced G6P concentrations. Omega 3 and omega 6 had no effect on basal G6P concentrations in L8 myocytes (Figure 23).

Palmitate (47.2 ± 0.7 nM/µl vs. 3.7 ± 0.5 nM/µl; p<0.001), oleate (47.2 ± 0.7 nM/µl vs. 10.1 ± 0.8 nM/µl; p<0.001) and omega 3 (47.2 ± 0.7 nM/µl vs. 15.7 ± 2.3 nM/µl; p=0.003) reduced insulin-stimulated G6P in L8 myocytes cultured in 5.5 mM. However, omega 6 had no effect on G6P concentrations. In L8 myocytes cultured in 20 mM glucose palmitate (57.3 ± 5.3 nM/µl vs. 3.7 ± 0.5 nM/µl; p<0.0001), oleate (57.3 ± 5.3 nM/µl vs. 12.7 ± 0.3 nM/µl; p =0.0002), omega 3 (57.3 ± 5.3 nM/µl vs. 12.9 ± 7 nM/µl; p =0.001) and omega 6 (57.3 ± 5.3 nM/µl vs. 13.3 ± 0.3 nM/µl; p= 0.0002) reduced G6P concentrations (Figure 24).

A

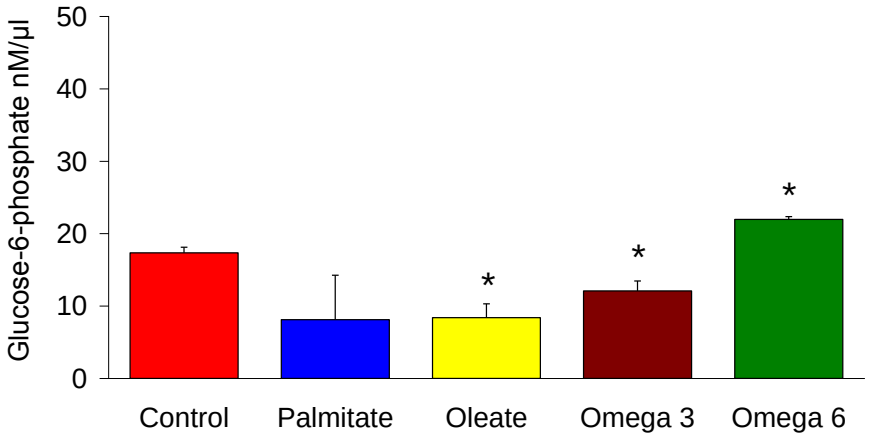

B

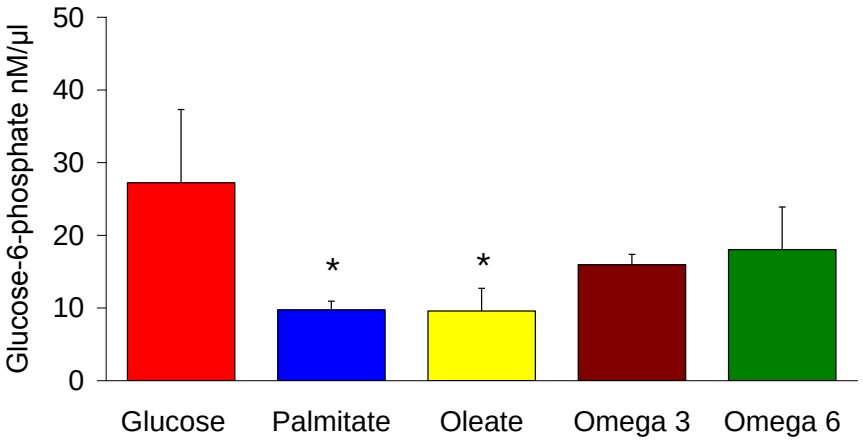

Figure 23. The effect of FFAs on basal glucose-6-phosphate concentrations in L8 myocytes.
Myocytes were cultured in 5.5 mM (A) or 20 mM (B) glucose and exposed to the indicated FFAs for six hours. Glucose-6-phosphate concentrations were measured using the glucose-6-phosphate assay kit. Results are representative of three independent experiments ± SD,*P < 0.05.

A

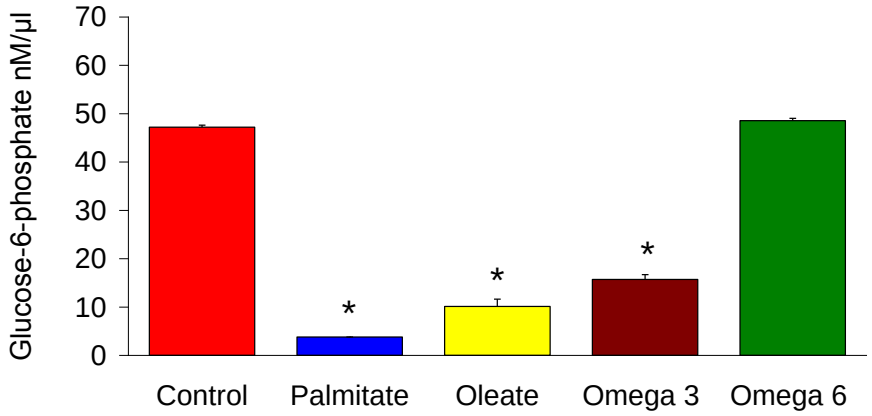

B

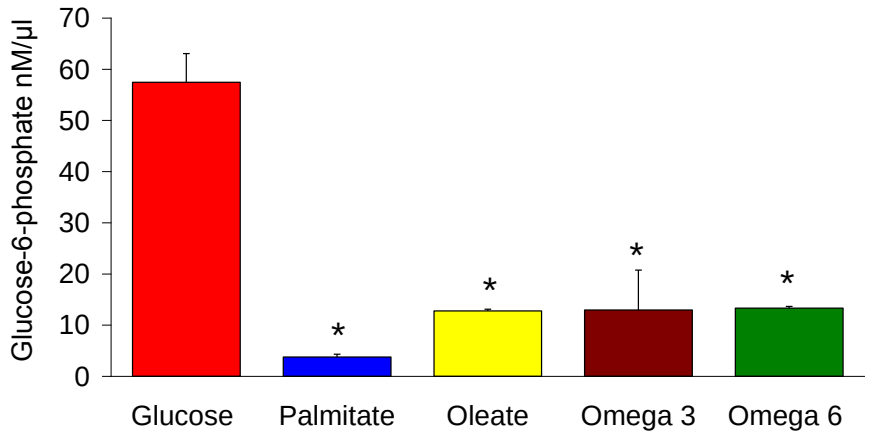

Figure 24. The effect of FFAs on insulin stimulated glucose-6-phosphate concentrations in L8 myocytes.
Myocytes were cultured in 5.5 mM (A) or 20 mM (B) glucose and exposed to the indicated FFAs for six hours with insulin stimulation in the last hour. Glucose-6-phosphate concentrations were measured measured using the glucose-6-phosphate assay kit. Results are representative of three independent experiments ± SD,*P < 0.05.

4.7.3 The effect of free fatty acids on glucose-6-phosphate concentrations in 3T3-L1 adipocytes

Palmitate, oleate and omega 3 had no effect on basal G6P concentrations in adipocytes cultured in 5.5 mM glucose. Although not significant, omega 6 reduced G6P concentrations (47.7 ± 14.0 nM/µl vs. 15.1 ± 5.2 nM/µl; p=0.09). When adipocytes were cultured in 20 mM glucose, palmitate (37.3 ± 0.3 nM/µl vs. 80.7 ± 1.37 nM/µl; p =0.001), oleate, (37.3 ± 0.3 nM/µl vs. 76.8 ± 1.3 nM/µl; p =0.001), omega 3 (37.3 ± 0.3 nM/µl vs. 60.8 ± 2.7 nM/µl; p=0.01) and omega 6 (37.3 ± 0.3 nM/µl vs. 77.8 ± 9.8 nM/µl; p= 0.02) significantly increased G6P concentrations (Figure 25).

Palmitate and oleate had no effect on insulin-stimulated G6P concentrations in adipocytes cultured in 5.5 mM glucose. Omega 3 (71.1 ± 9.6 nM/µl vs. 38.0 ± 0.7 nM/µl; p=0.04) and omega 6 (71.1 ± 9.6 nM/µl vs. 42.9 ± 5.5 nM/µl; p= 0.06) reduced G6P concentrations, although the reduction was not significant. In adipocytes cultured in 20 mM glucose only oleate reduced G6P concentrations (87.0 ± 7.5 nM/µl vs. 53.0 ± 8.9 nM/µl; p=0.05). Palmitate, omega 3 and omega 6 had no effect on insulin stimulated G6P concentrations (Figure 26).

A

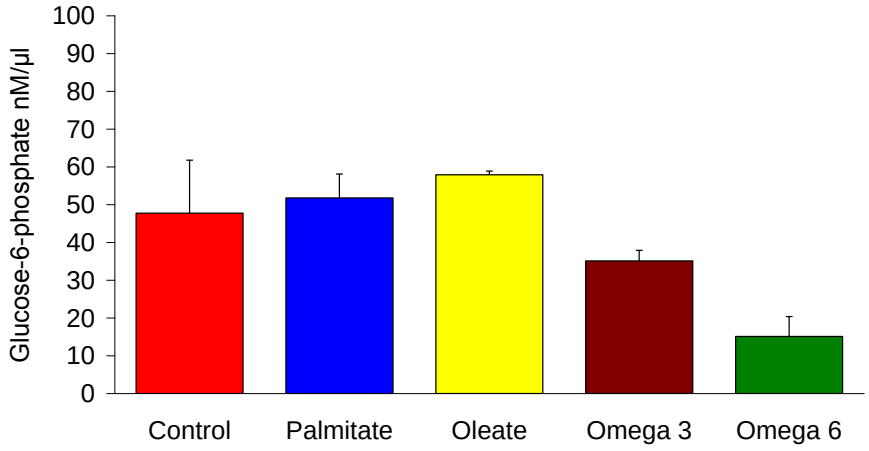

B

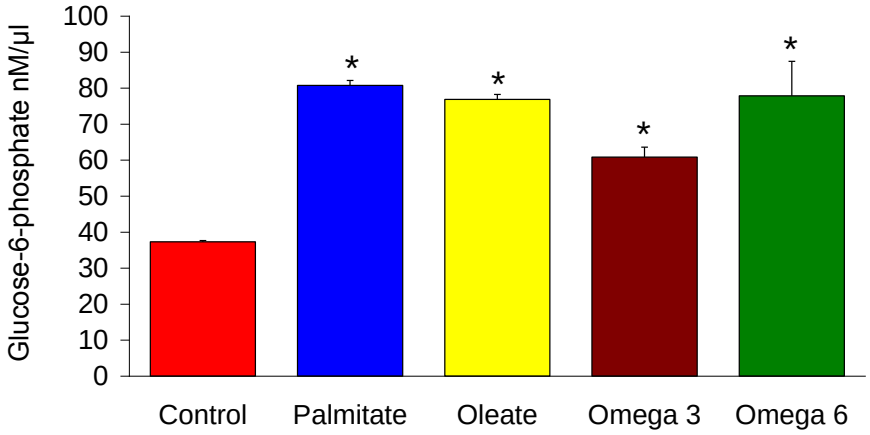

Figure 25. The effect of FFAs on basal glucose-6-phosphate concentrations in 3T3-L1 adipocytes.
Adipocytes were cultured in 5.5 mM (A) or 20 mM (B) glucose and exposed to the indicated FFAs for six hours. Glucose-6-phosphate concentrations were measured using the glucose-6-phosphate assay kit. Results are representative of three independent experiments ± SD,*P < 0.05.

A

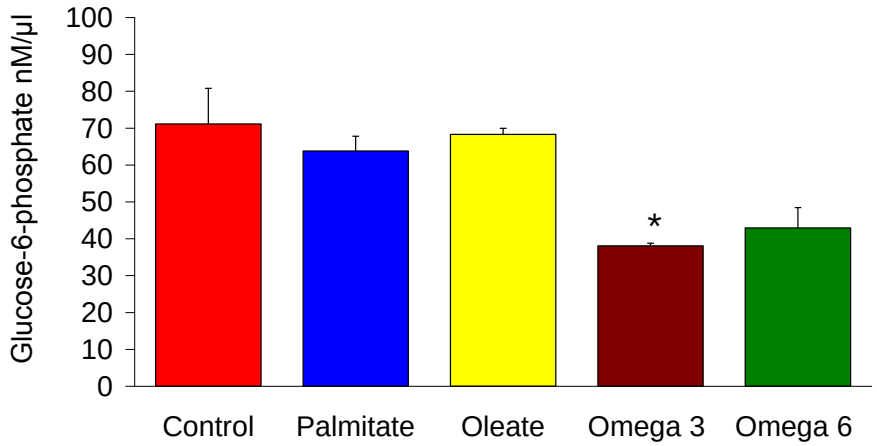

B

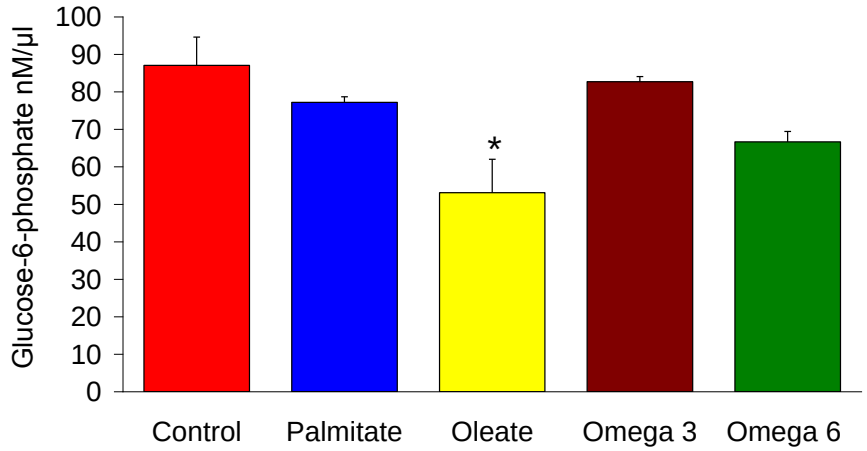

Figure 26. The effect of FFAs on insulin-stimulated glucose-6-phosphate concentrations in 3T3-L1 adipocytes.

Adipocytes were cultured in 5.5 mM (A) or 20 mM (B) glucose and exposed to the indicated FFAs for six hours with insulin stimulation in the last hour. Glucose-6-phosphate concentrations were measured using the glucose-6-phosphate assay kit. Results are representative of three independent experiments ± SD,*P < 0.05.

4.8 The effect of free fatty acids on glycogen content

After entering the muscle cell, glucose can be converted into energy in the form of ATP for short term storage or it can be converted to glycogen or fat for long term energy storage. To determine whether FFA treatment affects glycogen synthesis, intracellular glycogen concentrations were measured using a commercial glycogen assay.

Myocytes and adipocytes were cultured in media containing 5.5 mM or 20 mM glucose, 0.75 mM FFA (palmitate, oleate, omega 3 and omega 6), with or without 1 µM insulin stimulation, as described in section 3.3. Cell lysates were deproteinized to remove proteins that may interfere with the analysis of small molecules in biological samples prior to performing the assay.

4.8.1 The effect of free fatty acids on glycogen content in C2C12 myocytes

None of the FFAs, palmitate, oleate, omega 3 nor omega 6, had an affect on basal or insulin-stimulated glycogen concentrations in C2C12 myocytes cultured in 5.5 mM or 20 mM glucose (Figure 27and 28).

A

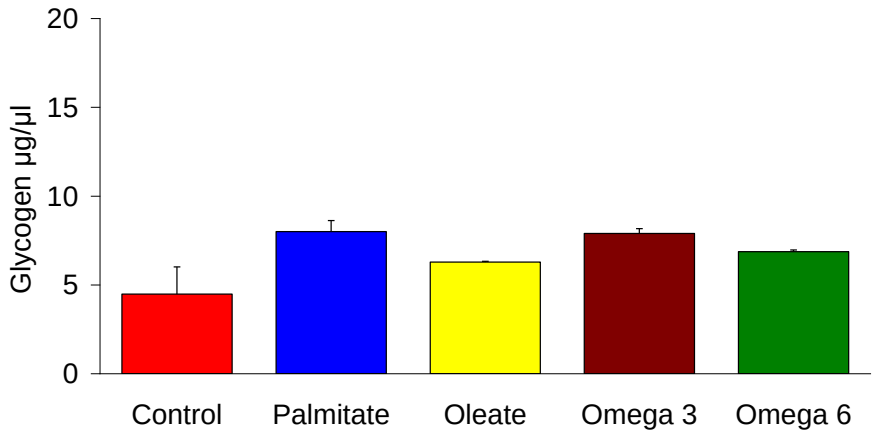

B

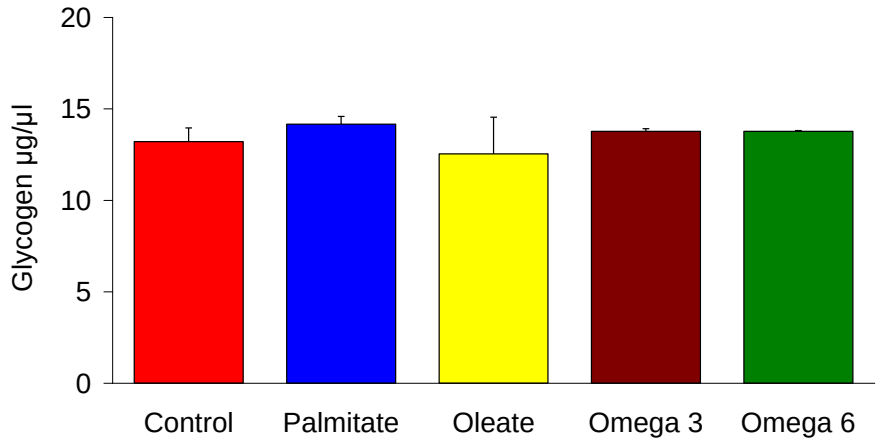

Figure 27. The effect of FFAs on basal glycogen content in C2C12 myocytes.
Myocytes were cultured in 5.5 mM (A) or 20 mM (B) glucose and exposed to the indicated FFAs for six hours. Glycogen concentrations were measured using the glycogen assay kit. Results are representative of three independent experiments ± SD. *P <0.05.

A

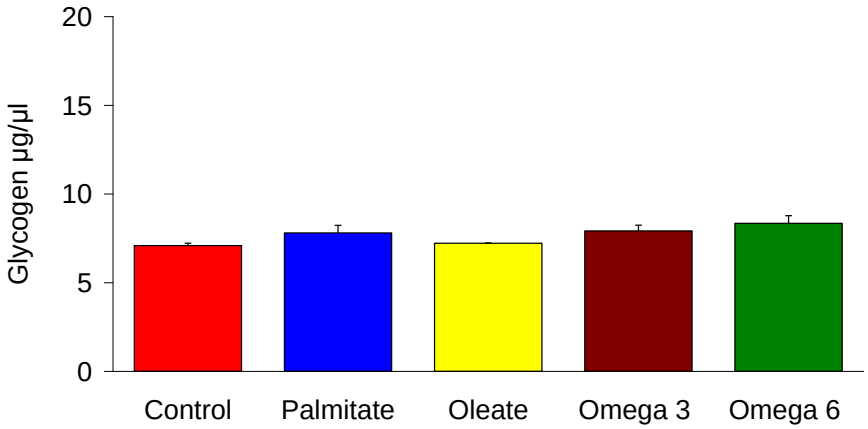

B

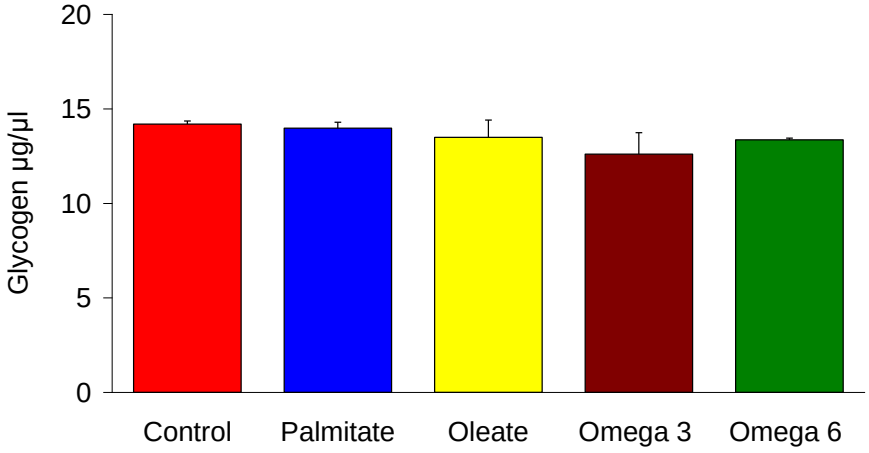

Figure 28. The effect of FFAs on insulin-stimulated glycogen content in C2C12 myocytes. Myocytes were cultured in 5.5 mM (A) or 20 mM (B) glucose and exposed to the indicated FFAs for six hours with insulin stimulation in the last hour. Glycogen concentrations were measured using the glycogen assay kit. Results are representative of three independent experiments ± SD. *P <0.05.

4.8.2 The effect of free fatty acids on glycogen content in L8 myocytes

Under basal conditions, palmitate (9.08 ± 1.4 µg/µl vs. 16.7 ± 2.1 µg/µl; p =0.05), oleate (9.08 ± 1.4 µg/µl vs. 18.3 ± 0.6 µg/µl; p=0.02) and omega 3 (9.08 ± 1.4 µg/µl vs. 16.8 ± 0.4 µg/µl; p=0.004) significantly increased glycogen concentrations in L8 myocytes cultured in 5.5 mM glucose. Although not significant, omega 6 (9.0 ± 1.4 µg/µl vs. 14.6 ± 3.8 µg/µl; p=0.1) also increased glycogen concentrations in L8 myocytes cultured in 5.5 mM glucose.

When myocytes were cultured in 20 mM glucose, palmitate increased glycogen concentrations, although not significantly (7.0 ± 0.5 µg/µl vs. 9.4 ± 0.8 µg/µl; p=0.08). Glycogen levels were increased after exposure to oleate (7.0 ± 0.5 µg/µl vs. 10.1 ± 0.1 µg/µl; p = 0.05), omega 3 (7.0 ± 0.5 µg/µl vs. 14.7 ± 0.7 µg/µl; p= 0.007) and omega 6 (7.0 ± 0.5 µg/µl vs. 15.2 ± 0.04 µg/µl; p=0.001) (Figure 29).

Under insulin-stimulated conditions, none of the FFAs affected glycogen concentrations when mycocytes were cultured in 5.5 mM glucose. However, when L8 myocytes were cultured in 20 mM glucose, glycogen concentrations was reduced after treatment with palmitate (15.1 ± 1.0 µg/µl vs. 8.7 ± 0.8 µg/µl; p= 0.02), oleate (15.1 ± 1.0 µg/µl vs. 9.1 ± 0.9 µg/µl; p= 0.02), omega 3 (15.1 ± 1.0 µg/µl vs. 8.3 ± 3.5 µg/µl; p=0.1) and omega 6 (15.1 ± 1.0 µg/µl vs. 9.0 ± 0.5 µg/µl; p=0.01) (Figure 30).

A

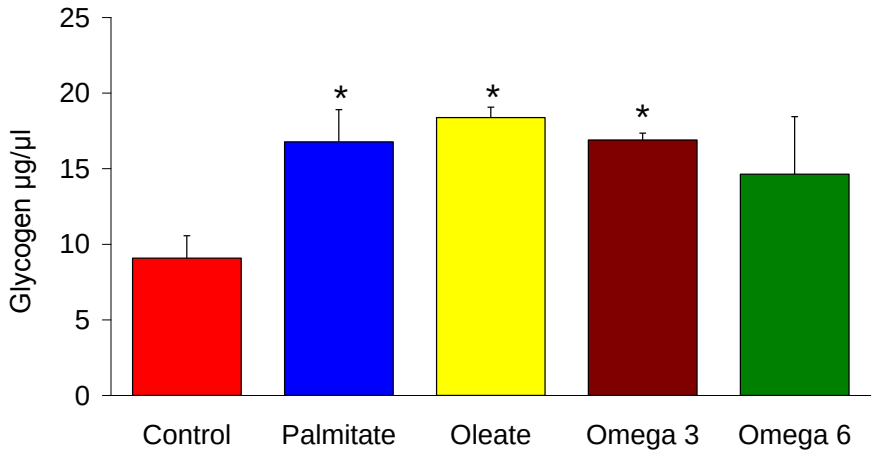

B

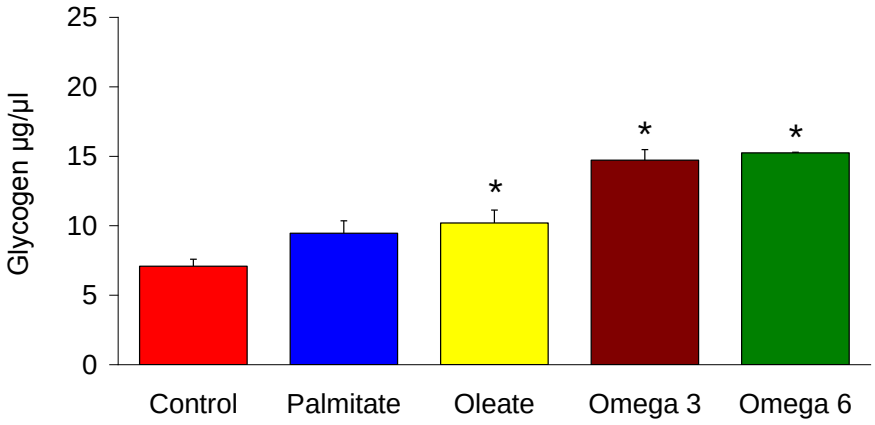

Figure 29. The effect of FFAs on basal glycogen levels in L8 myocytes.
Myocytes were were cultured in 5.5 mM (A) or 20 mM (B) glucose and exposed to the indicated FFAs for six hours. Glycogen concentrations were measured using the glycogen assay kit. Results are representative of three independent experiments ± SD. *P <0.05.

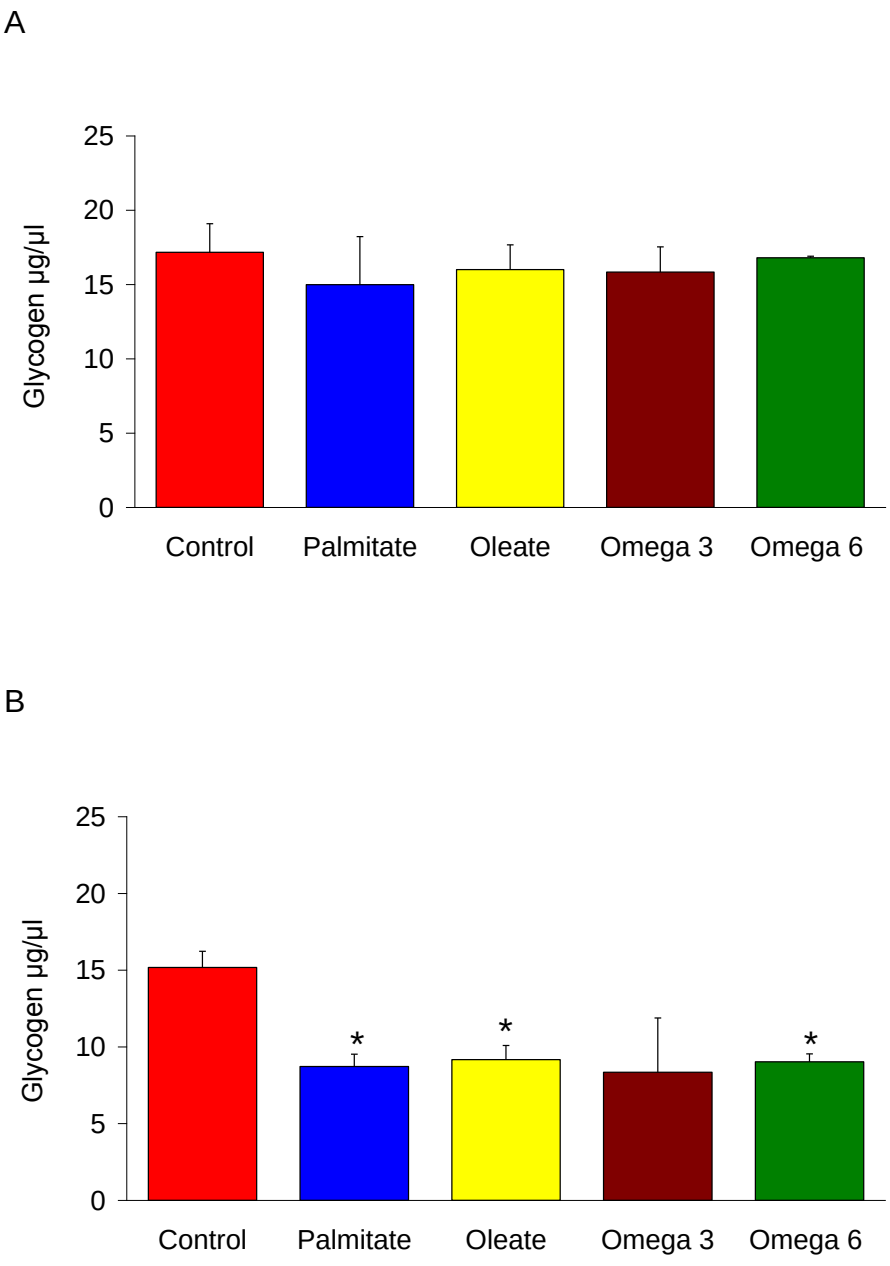

Figure 30. The effect of FFAs on insulin-stimulated glycogen levels in L8 myocytes.
Myocytes were cultured in 5.5 mM (A) or 20 mM (B) glucose and exposed to the indicated FFAs for six hours with insulin stimulation in the last hour. Glycogen concentrations were measured using the glycogen assay kit. Results are representative of three independent experiments ± SD. *P <0.05.

4.8.3. The effect of free fatty acids on glycogen content in 3T3-L1 adipocytes

Under basal conditions at 5.5 mM glucose, palmitate and oleate had no effect on glycogen concentrations. Omega 3 (8.14 ± 1.09 µg/µl vs. 11.37 ± 0.09 µg/µl; p=0.05) and omega 6 (8.14 ± 1.09 µg/µl vs. 11.22 ± 0.01 µg/µl; p=0.1) increased glycogen concentrations. At 20 mM glucose none of the FFAs had an effect on basal glycogen concentrations (Figure 31). Under insulin-stimulated conditions, none of the FFAs affected glycogen concentrations when adipocytes were cultured in 5.5 mM or 20 mM glucose (Figure 32).

A

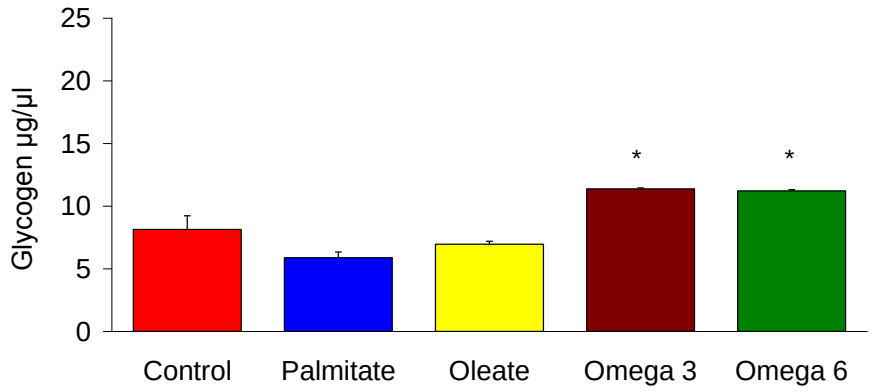

B

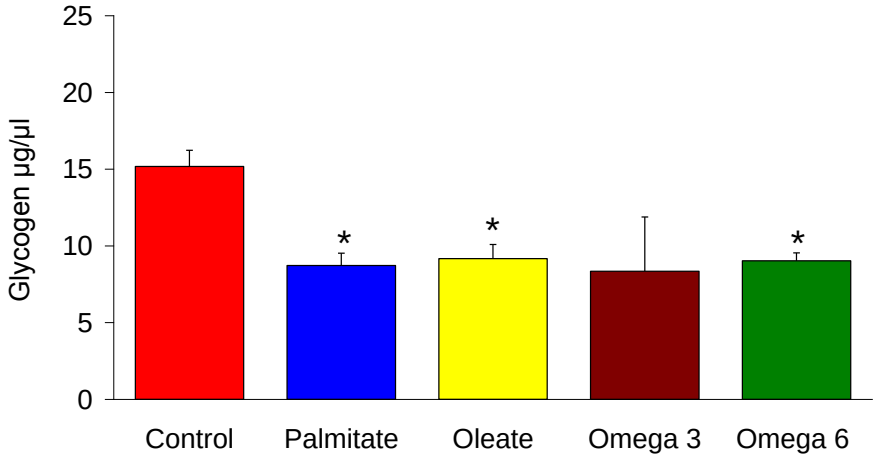

Figure 31. The effect of FFAs on basal glycogen content in 3T3-L1 adipocytes.
Adipocytes were cultured in 5.5 mM (A) or 20 mM (B) glucose and exposed to the indicated FFAs for six hours. Glycogen concentrations were measured using the glycogen assay kit. Results are representative of three independent experiments ± SD. *P <0.05.

A

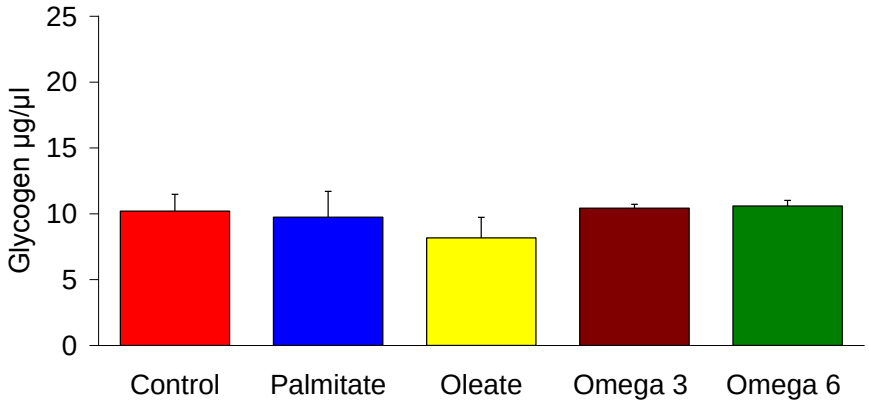

B

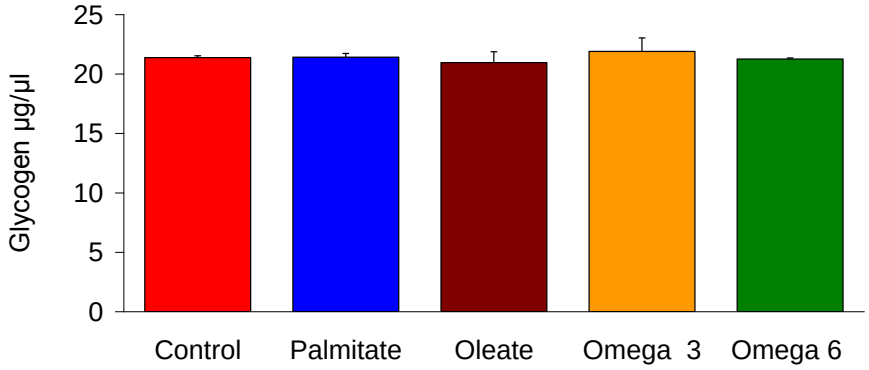

Figure 32. The effect of FFAs on insulin-stimulated glycogen content in 3T3-L1 adipocytes. Adipocytes were cultured in 5.5 mM (A) or 20 mM (B) glucose and exposed to the indicated FFAs for six hours with insulin stimulation in the last hour. Glycogen concentrations were measured using the glycogen assay kit. Results are representative of three independent experiments ± SD. *P <0.05.

4.9 The effect of free fatty acids on glucose oxidation

To examine the effect of FFAs on the rate of glucose oxidation, myocytes and adipocytes were cultured in media containing 5.5 mM or 20 mM glucose, 0.75 mM FFA (palmitate, oleate, omega 3 and omega 6), with or without 1 µM insulin supplementation as described in section 3.3. Thereafter, cells were washed and exposed to media containing 5.5 mM glucose with 0.5 µCi glucose D-[^{14}C (U)] for an hour. After an hour, the filter paper CO_2 trap was removed from the lids of six well plates, placed in a scintillation vial containing 10 ml of scintillation fluid and analysed in a liquid scintillation counter. CO_2 oxidation was reported as the percentage of the relevant glucose control.

4.9.1 The effect of free fatty acids on glucose oxidation in C2C12 myocytes

Palmitate, oleate, omega 3 and omega 6 had no effect on the rate of basal glucose oxidation in C2C12 myocytes cultured in 5.5 mM glucose. However, when these myocytes were cultured in 20 mM glucose, glucose oxidation was reduced after treatment with palmitate (100 ± 1.9% vs. 46.6 ± 0.8%; p=0.02), oleate (100 ± 1.9% vs. 21.0 ± 0.7%; p=0.001), omega 3 (100 ± 1.9% vs. 15.8 ± 0.2%; p=0.0007) and omega 6 (100 ± 1.9% vs.15.6 ± 0.5%; p =0.001) (Figure 33).

Palmitate, oleate, omega 3 and omega 6 had no effect on insulin stimulated glucose oxidation in C2C12 myocytes cultured in 5.5 mM glucose. In myocytes that were cultured in 20 mM glucose, glucose oxidation was reduced after treatment with palmitate (100 ± 3.3% vs. 9.1 ± 0.6%; p=0.01), oleate (100 ± 3.3% vs. 9.7 ± 0.4%; p =0.01), omega 3 (100 ± 3.3% vs. 13.3 ± 0.6%; p= 0.002) and omega 6 (100 ± 3.3% vs. 10.1 ± 0.5%; p= 0.02) (Figure 34).

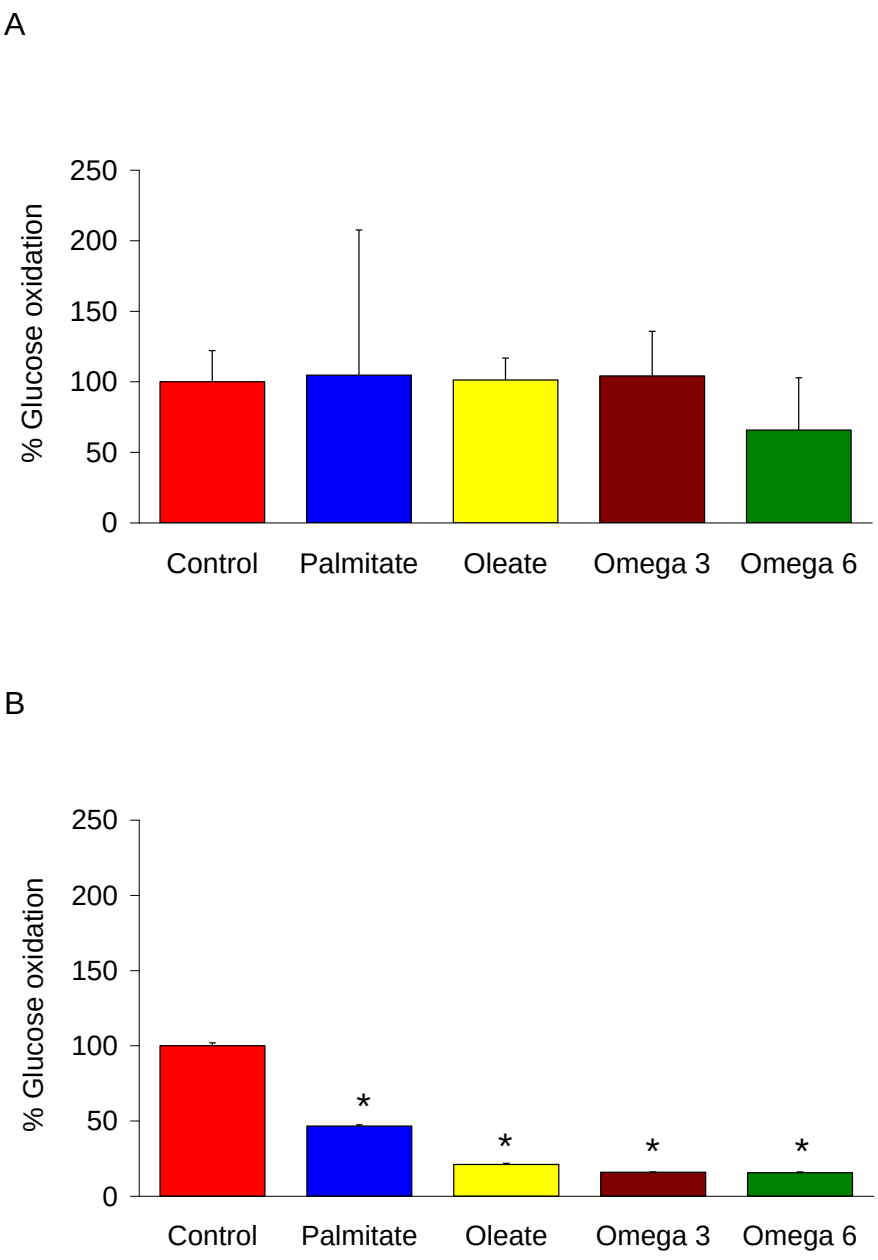

Figure 33. The effect of FFAs on basal glucose oxidation in C2C12 myocytes.
Myocytes were cultured in 5.5 mM (A) or 20 mM (B) glucose and exposed to the indicated FFAs for six hours. Glucose oxidation was measured using glucose D-[^{14}C (U)]. Results are representative of three independent experiments ± SD. *P <0.05.

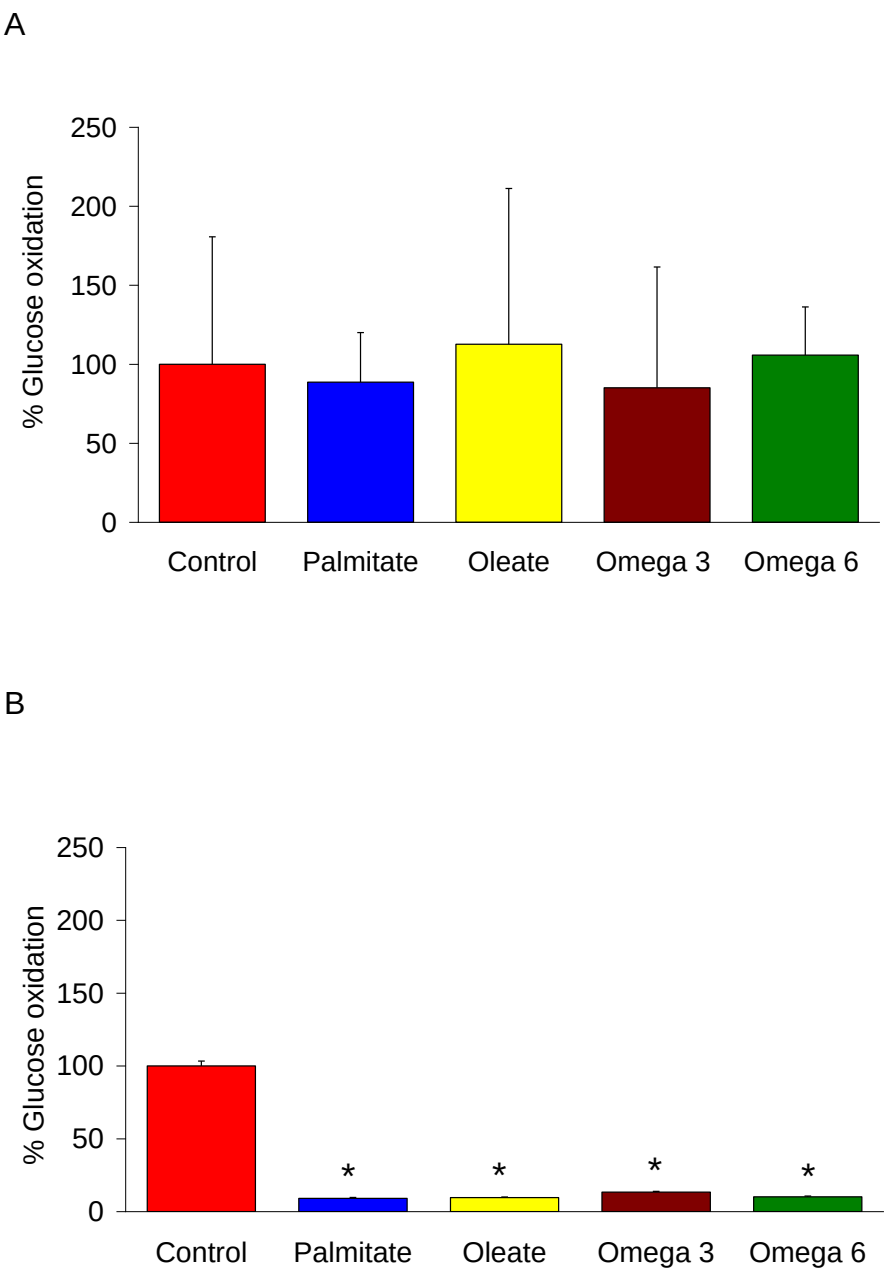

Figure 34. The effect of FFAs on insulin-stimulated glucose oxidation in C2C12 myocytes. Myocytes were cultured in 5.5 mM (A) or 20 mM (B) glucose and exposed to the indicated FFAs for six hours with insulin stimulation in the last hour. Glucose oxidation was measured using glucose D-[^{14}C (U)]. Results are representative of three independent experiments ± SD. *P <0.05.

4.9.2 The effect of free fatty acids on glucose oxidation in L8 myocytes

Palmitate, oleate and omega 3 had no effect on glucose oxidation when L8 myocytes were cultured in 5.5 mM glucose. Omega 6 reduced glucose oxidation (100.0 ± 27.2% vs. 57.5 ± 1.4%; p=0.01). In L8 myocytes cultured in 20 mM glucose basal glucose oxidation was reduced after treatment with palmitate, (100.0 ± 5.6% vs. 26.4 ± 2.6%; p=0.0003), oleate (100.0 ± 5.6% vs. 24.8 ± 0.3%; p=0.002), omega 3 (100.0 ± 5.6% vs. 22.5 ± 3.9 %; p=0.002) and omega 6 (100.0 ± 5.6% vs. 20.9 ± 1.8%; p=0.0002) (Figure 35).

In L8 myocytes cultured in 5.5 mM glucose, insulin-stimulated glucose oxidation was decreased after treatment with palmitate (100.0 ± 26.0% vs. 46.4 ± 3.0%; p=0.001), oleate (100.0 ± 26.0% vs. 63.2 ± 2.8%; p<0.0001), omega 3 (100.0 ± 26.0% vs. 60.1 ± 9.3%; p=0.005) and omega 6 (100.0 ± 26.0% vs. 49.1 ± 8.5%; p=0.02). Similar results were observed in 20 mM glucose. Palmitate (100.0 ± 6.8 % vs. 27.2 ± 3.0%; p=0.0001), oleate (100.0 ± 6.8% vs. 23.4 ± 0.01%; p=0.001), omega 3 (100.0 ± 6.8% vs. 22.8 ± 3.8%; p=0.001) and omega 6 (103.6 ± 6.8% vs. 19.20 ± 3.4%; p=0.001) decreased glucose oxidation (Figure 36).

A

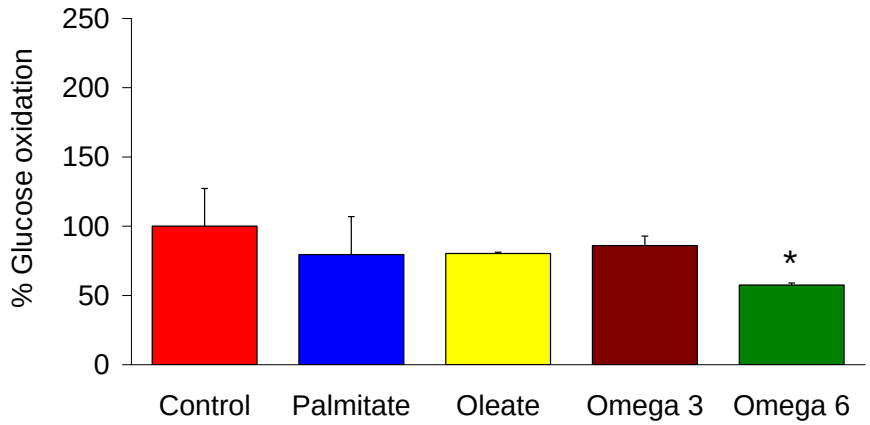

B

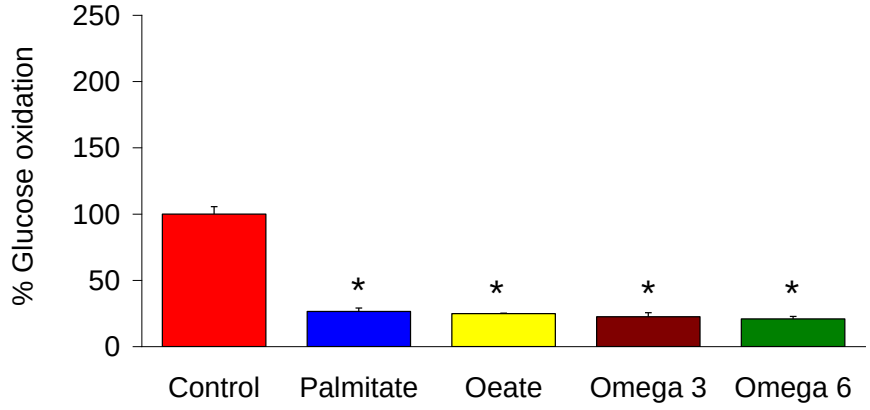

Figure 35. The effect of FFAs on basal glucose oxidation in L8 myocytes.
Myocytes were cultured in 5.5 mM (A) or 20 mM (B) glucose and exposed to the indicated FFAs for six hours. Glucose oxidation was measured using glucose D-[^{14}C (U)]. Results are representative of three independent experiments ± SD. *P <0.05.

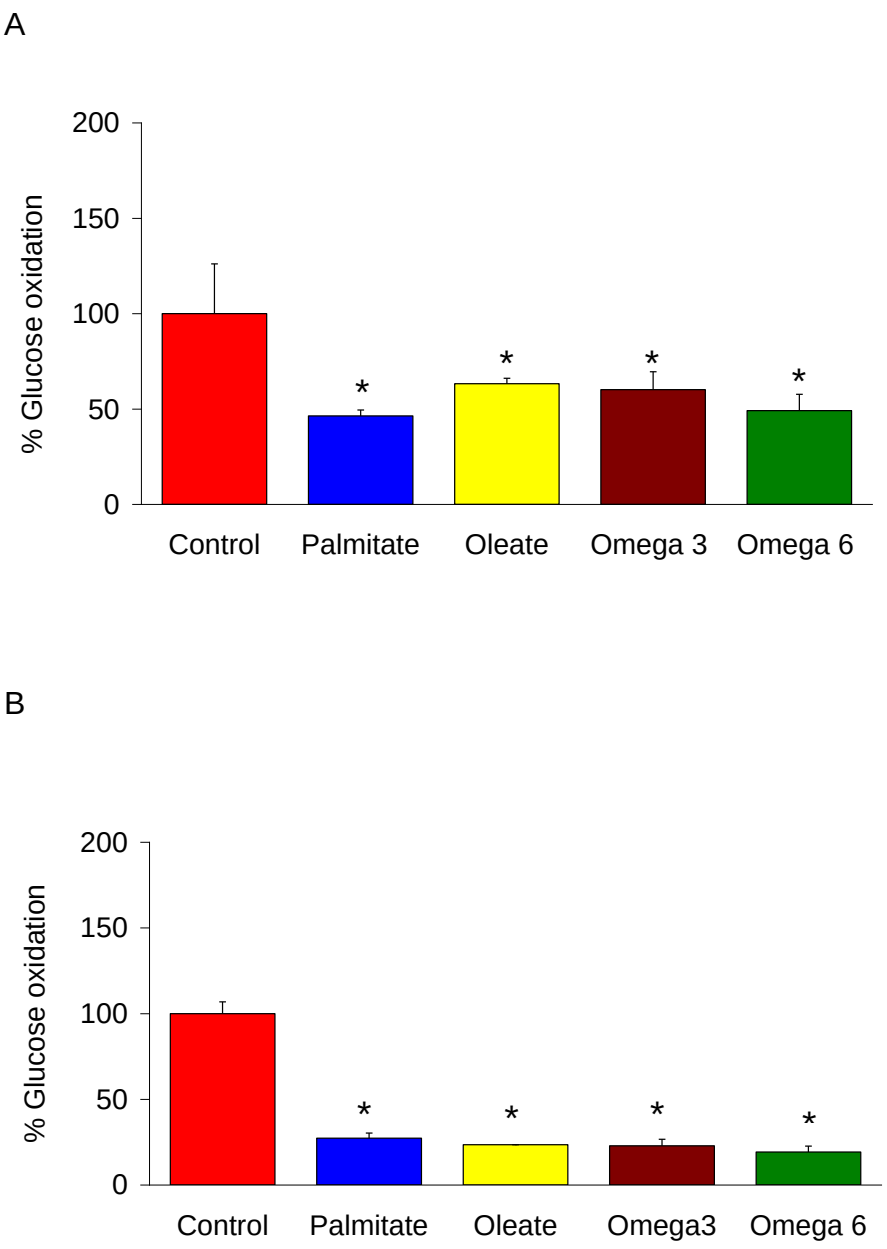

Figure 36. The effect of FFAs on insulin-stimulated glucose oxidation in L8 mycocytes. Myocytes cultured in 5.5 mM (A) or 20 mM (B) glucose and exposed to the indicated FFAs for six hours with insulin stimulation in the last hour. Glucose oxidation was measured using glucose D-[^{14}C (U)]. Results are representative of three independent experiments ± SD. *P <0.05.

4.9.3 The effect of free fatty acids on glucose oxidation 3T3-L1 adipocytes

Palmitate significantly increased basal glucose oxidation in adipocytes cultured in 5.5 mM glucose (100.0 ± 10.0% vs. 357.2 ± 133.8%; p=0.001). Oleate, omega 3 and omega 6 had no effect on basal glucose oxidation in adipocytes. Basal glucose oxidation was reduced by palmitate (100.0 ± 3.2% vs. 84.6 ± 4.6%; p=0.009), oleate (100.0 ± 3.2% vs. 68.7 ± 4.6%; p=0.001), omega 3 (100.0 ± 3.2% vs. 87.1 ± 5.0%; p=0.02) and omega 6 (100.0 ± 3.2% vs. 66.9 ± 0.5%; p=0.009) when cells cultured in 20 mM glucose (Figure 37).

Palmitate (100.0 ± 4.2% vs. 86.1 ± 2.4%; p=0.001), oleate (100.0 ± 4.2% vs. 84.2 ± 1.2%; p<0.0001), omega 3 (100.0 ± 4.2% vs. 76.2 ± 3.2%; p=0.04) and omega 6 (104.7 ± 4.2% vs. 67.7 ± 6.0%; p=0.02) decreased insulin-stimulated glucose oxidation in adipocytes cultured in 5.5 mM glucose. Similary, insulin-stimulated glucose oxidation was reduced in adipocytes cultured in 20 mM glucose by palmitate (100.0 ± 2.8% vs. 78.0 ± 2.8%; p= 0.0004), oleate (100.0 ± 2.8% vs. 74.2 ± 2.9%; p= 0.0002), omega 3 (100.0 ± 2.8% vs. 81.3 ± 4.8%; p=0.003) and omega 6 (100.0 ± 2.8% vs. 62.1 ± 5.9%; p=0.005) (Figure 38).

A

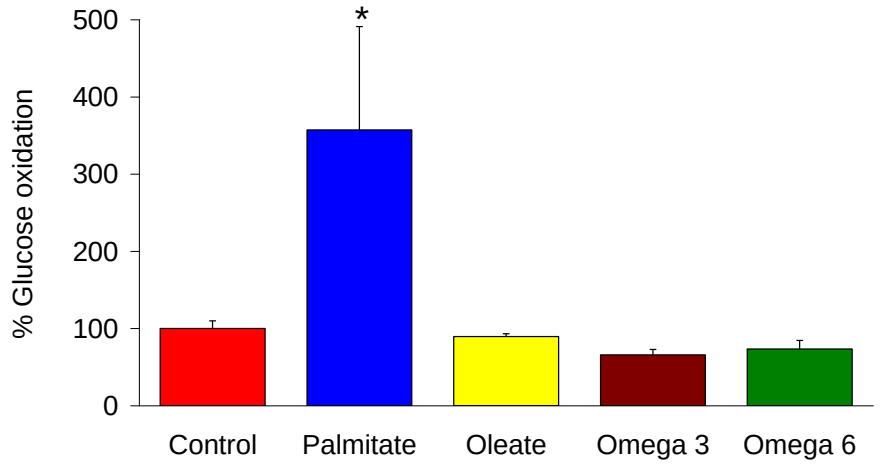

B

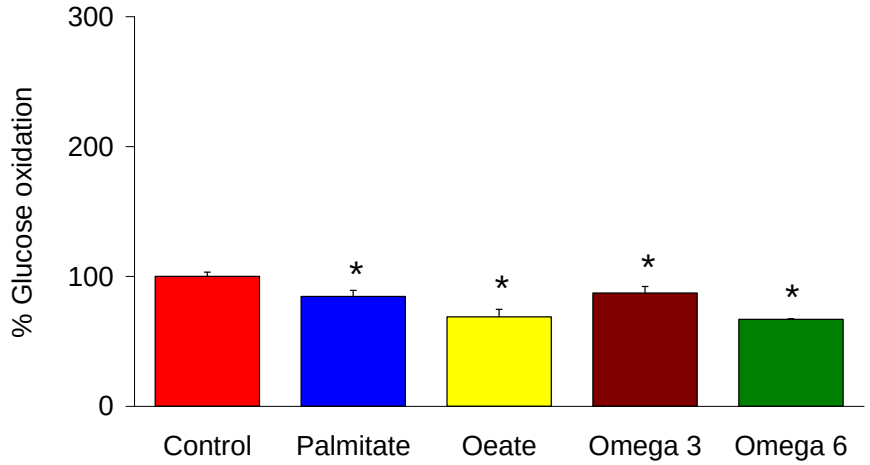

Figure 37. The effect of FFAs on basal glucose oxidation in 3T3-L1 adipocytes.
Adipocytes were cultured in 5.5 mM (A) or 20 mM (B) glucose and exposed to the indicated FFAs for six hours. Glucose oxidation was measured using glucose D-[^{14}C (U)]. Results are representative of three independent experiments ± SD. *P <0.05.

A

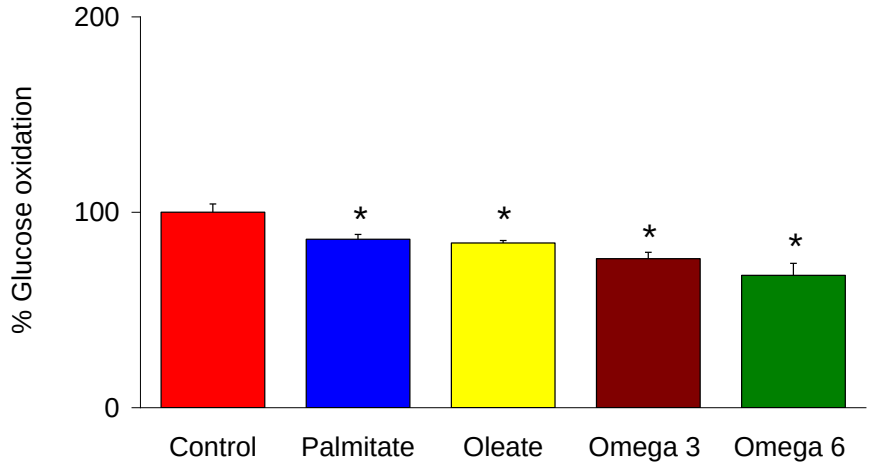

B

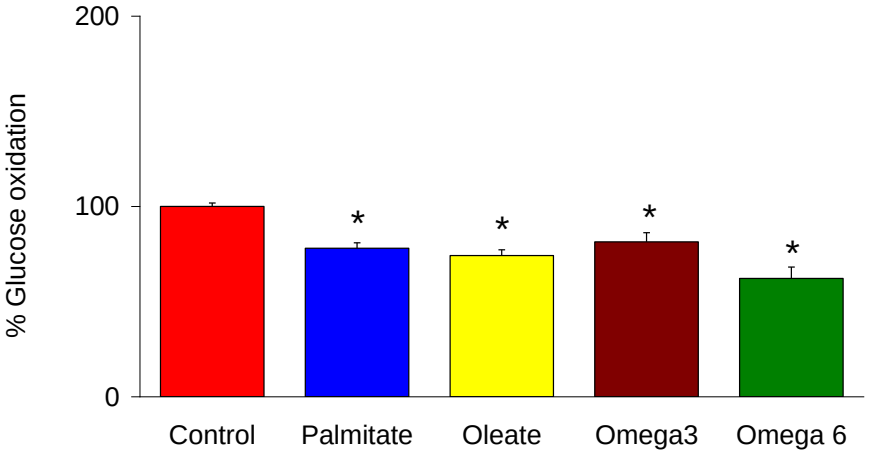

Figure 38. The effect of FFAs on insulin-stimulated glucose oxidation in 3T3-L1 adipocytes.

Adipocytes were cultured in 5.5 mM (A) or 20 mM (B) glucose and exposed to the indicated FFAs for six hours with insulin stimulation in the last hour. Glucose oxidation was measured using glucose D-[^{14}C (U)]. Results are representative of three independent experiments ± SD. *P <0.05.

Table 11. Summary of glucose uptake and metabolism.

Cell line	Palmitate		Oleate		Omega 3		Omega 6	
	Basal	Insulin	Basal	Insulin	Basal	Insulin	Basal	Insulin
Glucose uptake from 5.5 mM glucose								
C2C12	↓	↓	NE	↓	NE	NE	NE	NE
L8	↓	↓	NE	NE	NE	NE	NE	NE
3T3-L1	NE	NE	NE	NE	NE	NE	NE	NE
Glucose uptake from 20 mM glucose								
C2C12	↓	↓	NE	NE	NE	NE	NE	NE
L8	NE	↓	NE	↓	NE	↓	NE	↓
3T3-L1	↓	↓	NE	NE	NE	NE	NE	NE
G6P from 5.5 mM glucose								
C2C12	↓	↓	↑	NE	↑	↓	↓	↓
L8	NS	↓	↓	NE	↓	↓	↑	NE
3T3-L1	NC	↓	NC	NE	NC	↓	NE	NE
G6P from 20 mM glucose								
C2C12	↓	↓	NE	↑	↑	↑	↓	↑
L8	↓	↓	↓	↓	NE	↓	NE	↓
3T3-L1	↑	NE	↑	↓	↑	NE	↑	NE
Glycogen from 5.5 mM glucose								
C2C12	NE	NE	NE	NE	NE	NE	NE	NE
L8	↑	↓	↑	↓	↑	NC	NC	↓
3T3-L1	NE	NE	NE	NE	↑	NE	↑	NE
Glycogen from 20 mM glucose								
C2C12	NE	NE	NE	NE	NE	NE	NC	NE
L8	NE	NE	↑	NE	↑	NE	↑	NE
3T3-L1	NE	NE	NE	NE	NE	NE	NC	NE
$^{14}CO_2$ from 5.5 mM glucose								
C2C12	NE	↓	NE	↑	NE	NE	NE	NE
L8	↓	↓	NE	↓	NE	NE	NE	↓
3T3-L1	↑	↓	NE	↓	NE	NE	NE	↓
$^{14}CO_2$ from 20 mM glucose								
C2C12	↓	↓	↓	↓	↓	↓	↓	↓
L8	↓	↓	↓	↓	↓	↓	↓	↓
3T3-L1	↓	↓	↓	↓	↓	↓	↓	↓

↑indicates an increase from relevant control,
↓ indicates a deacrese from relevant control
NE indicates no effect

4.10 Gene expression analysis

4.10.1 RNA concentrations and purity

RNA was extracted from C2C12 myocytes and 3T3-L1 adipocytes treated with palmitate using Tri reagent and purified using the RNeasy minikit as described in section 3.12. The ratios of absorbance $^{260\ nm}/_{280\ nm}$ and $^{260\ nm}/_{230\ nm}$ indicate the quality and purity of RNA; ratios greater than 1.8 indicate good quality of RNA (Muyal *et al.,* 2009). Results showed that the quality of RNA was within the acceptable range in C2C12 myocytes and in 3T3-L1 adipocytes. Results are illustrated in Table 12.

Table 12. RNA concentrations, total yield and purity.

Sample	Experiment No*	ng/µl[#]	Total yield (µg)[†]	A_{260}/ A_{280}	A_{260}/ A_{230}
C2C12 myocytes					
Control	1	262.83	20.50	1.96	1.64
Control	2	360.38	28.11	2.09	1.72
Control	3	408.40	31.86	2.01	1.84
Control +insulin	1	324.78	25.33	2.03	1.96
Control +insulin	2	371.22	28.96	1.95	1.32
Control +insulin	3	390.39	30.45	2.08	1.71
Palmitate	1	296.46	23.12	1.92	1.49
Palmitate	2	146.86	11.48	2.05	1.49
Palmitate	3	346.72	27.04	2.11	2.01
Palmitate + insulin	1	205.45	16.03	2.04	1.73
Palmitate + insulin	2	154.10	12.02	1.98	1.57
Palmitate + insulin	3	298.36	23.27	2.10	0.75
3T3-L1 adipocytes					
Control	1	646.99	50.46	2.14	1.55
Control	2	420.32	32.78	2.08	2.06
Control	3	570.32	44.48	2.07	1.74
Control +insulin	1	377.76	29.46	2.03	1.96
Control +insulin	2	355.92	27.76	2.09	2.29
Control +insulin	3	303.67	23.68	2.10	2.03
Palmitate	1	533.69	41.62	2.14	2.23
Palmitate	2	274.88	21.44	2.12	2.30
Palmitate	3	432.08	33.70	2.04	2.08
Palmitate + insulin	1	392.23	30.59	2.08	1.99
Palmitate + insulin	2	291.58	22.74	2.10	1.98
Palmitate + insulin	3	504.19	39.32	2.07	1.38

*Experiments were done in triplicate
[#]ng/µl was calculated using the average of three independent Nanodrop measurements
[†]Total Yield was calculated by multiplying ng/µl by the total volume of RNA obtained

4.10.2 Genomic DNA contamination

To remove contaminating genomic DNA, 20 µg of RNA was DNase treated with the TurboDNase kit as described in section 3.13. The percentage of RNA recovered after DNase treatment is indicated in Table 13. The RNA recovered

dropped dramatically in palmitate treated C2C12 myocytes, but not in 3T3-L1 adipocytes. More than 50% RNA was recovered after DNase treatment of untreated myocytes and in adipocytes. Palmitate treated cells yielded less then 50% of RNA after DNase treatment.

Table 13. RNA concentrations obtained after DNase treatment of 20 µg of RNA.

Sample	Experiment No*	µg RNA recovered after treatment[#]	Percentage recovery[†]
C2C12 myocytes			
Control	1	10.31	51.53
Control	2	11.60	58.01
Control	3	12.95	64.73
Control +insulin	1	10.06	50.29
Control +insulin	2	10.62	53.12
Control +insulin	3	13.40	67.00
Palmitate	1	7.79	38.97
Palmitate	2	3.96	19.78
Palmitate	3	12.17	60.84
Palmitate + insulin	1	6.13	30.64
Palmitate + insulin	2	4.59	22.97
Palmitate + insulin	3	10.37	51.85
3T3-L1 adipocytes			
Control	1	17.44	87.21
Control	2	14.39	71.93
Control	3	15.88	79.42
Control +insulin	1	14.11	70.54
Control +insulin	2	12.56	62.82
Control +insulin	3	11.74	58.70
Palmitate	1	17.88	89.42
Palmitate	2	10.12	50.62
Palmitate	3	15.41	77.03
Palmitate + insulin	1	14.70	73.48
Palmitate + insulin	2	10.32	51.62
Palmitate + insulin	3	15.06	75.29

*Experiments were done in triplicate
[#]Concentration of RNA recovered after treatment
[†]Percentage RNA recovery was calculated by dividing total RNA yield after treatment by 20 µg and multiplying by 100

To assess whether genomic DNA was efficiently removed by DNase treatment, reverse transcription reactions containing (plus RT) or without (minus RT) the reverse transcription enzyme were subjected to quantitative real-time PCR. Taq polymerase, the enzyme responsible for the polymerase chain reaction (PCR), will only amplify double stranded DNA, thus RNA must be reverse transcribed before being used as a template in PCR. Amplification in minus RT reactions represents genomic DNA contamination. A Ct difference of more than 10 cycles between the plus and minus RT reactions indicate negligible genomic DNA contamination. cDNA prepared from rat liver RNA (Ambion) was included as a positive control, while water was used as a negative control. As illustrated in Table 14, DNase treatment significantly reduced genomic DNA contamination.

Table 14. Quantitative Real Time PCR analysis of DNase treated RNA

Sample	Experiment No*	Ct# (minus RT)	Ct$ (plus RT)	Ct diff†
C2C12 myocytes				
Control	1	36.53	16.79	19.74
Control	2	>40	17.24	>23
Control	3	>40	16.82	>23
Control +insulin	1	37.48	16.85	20.63
Control +insulin	2	37.63	16.13	21.50
Control +insulin	3	>40	16.66	>23
Palmitate	1	37.64	16.27	21.37
Palmitate	2	36.56	16.90	19.66
Palmitate	3	>40	16.64	>23
Palmitate + insulin	1	39.19	15.92	23.27
Palmitate + insulin	2	36.67	16.52	20.15
Palmitate + insulin	3	36.67	16.52	20.15
Ambion rat liver	-	36.54	17.46	19.08
Water	-	39.52	>40	-
3T3-L1 adipocytes				
Control	1	32.36	16.34	16.02
Control	2	33.08	16.18	16.89
Control	3	32.12	16.07	16.06
Control +insulin	1	32.21	15.98	16.24
Control +insulin	2	32.38	16.99	15.39
Control +insulin	3	35.01	16.84	18.17
Palmitate	1	37.42	16.72	20.70
Palmitate	2	36.20	16.39	19.81
Palmitate	3	35.48	16.27	19.21
Palmitate + insulin	1	37.63	16.26	21.37
Palmitate + insulin	2	37.35	16.36	20.98
Palmitate + insulin	3	36.04	16.32	19.72
Ambion rat liver	-	35.76	16.25	19.52
Water	-			

*Experiments were done in triplicate
Ct minus RT was generated by the PCR ABI 7 500 machine
$ Ct plus RT was generated by the PCR ABI 7 500 machine
† Ct difference was calculated by subtracting Ct minus from Ct plus

4.10.3 PCR efficiency

The slope of a standard curve is used to evaluate the performance of real time PCR reactions and to determine PCR efficiency. Optimal PCR efficiency is indicated by a slope of -3.3. Slopes between -3.1 and -3.6 are acceptable. The slope and R^2 (correlation co-efficient) values obtained for the Taqman® gene expression assays used in this study was calculated using a rat cDNA standard curve (Table 15). The slopes for all the genes to be investigated were within the acceptable range.

Table 15. Slope and R^2 values of the genes investigated in the study.

Gene	Slope	R^2
Insulin receptor substrate 1 (Irs1)	-3.6	0.98
Insulin receptor substrate 2 (Irs2)	-3.4	0.98
Phosphatidylinositol 3 Kinase (Pi3k)	-3.4	0.98
Glucose transporter 4 (Glut4)	-3.6	0.99
Glycogen synthase (Gsy)	-3.3	0.99
Beta actin (ActB)	-3.2	0.99
Glyceraldehyde-3-phosphate dehydrogenase (Gapdh)	-3.4	0.98

4.10.4 The effect of palmitate treatment on gene expression

The effect of palmitate treatment on the expression of Irs1, Irs2, Pi3k, Glut4 and Gsy mRNA in C2C12 myocytes and 3T3-L1 adipocytes, under both basal and insulin-stimulated conditions, was determined using quantitative real time PCR (qRT-PCR). The expression of the reference genes ActB and Gapdh was used to normalize mRNA levels. None of the Taqman® gene expression assays tested yielded positive results in 3T3-L1 adipocytes. Results for gene expression analysis in C2C12 myocytes will be discussed.

Treatment of C2C12 myocytes with palmitate affected the expression of genes similarly during basal and insulin-stimulated conditions. Palmitate treatment reduced Irs1 mRNA expression during basal (2.91 ± 3.38 vs. 1.29 ± 0.46; p=0.4) and insulin-stimulated (1.97± 1.55 vs. 0.99 ± 0.35; p= 0.3) conditions (Figure 39A). Irs2 mRNA expression was upregulated by palmitate during basal (1.16 ± 0.63 vs. 1.83 ± 1.1; p=0.4) and insulin-stimulated (0.42 ± 0.1 vs. 2.3 ± 1.9; p= 0.1) conditions (Figure 39B). Palmitate treatment decreased Glut4 mRNA expression during both basal (0.39 ± 0.35 vs. 0.11 ± 0.03; p= 0.2) and insulin-stimulated (0.33 ± 0.14 vs. 0.14 ± 0.03; p= 0.07) conditions (Figure 39C). Pi3k mRNA expression was downregulated by palmitate during basal (1.41 ± 0.47 vs. 1.04 ± 0.1; p=0.2) and during insulin-stimulated (2.01 ± 1.12 vs. 0.74 ± 0.14; p=0.1) conditions (Figure 39D). Palmitate increased Gsy mRNA expression during basal (13.60 ± 6.2 vs. 19.14 ±0.8; p= 0.2) and insulin-stimulated (12.42 ± 1.65 vs.14.09 ± 2.4; p= 0.3).conditions (Figure 40E). None of these gene expression differences were statistically significant. A summary of the results is shown in Table 16.

Table 16. Summary of results for gene expression.

Genes	Control	Palmitate	P=	Control + insulin	Palmitate + nsulin	P=
Irs1	2.91 ± 3.38	1.29 ± 0.46	0.4	1.97 ± 1.55	0.99 ± 0.35	0.3
Irs2	1.16 ± 0.63	1.83 ± 1.11	0.4	0.42 ± 0.14	2.34 ± 1.99	0.1
Pi3k	1.42 ± 0.47	1.05 ± 0.18	0.2	2.01 ± 1.12	0.74 ± 0.14	0.1
Glut 4	0.39 ± 0.35	0.11 ± 0.03	0.2	0.33 ± 0.14	0.14 ± 0.03	0.07
Gsy	13.6 ± 6.24	19.14 ± 0.82	0.2	12.42 ± 1.65	14.09 ± 2.45	0.3

A

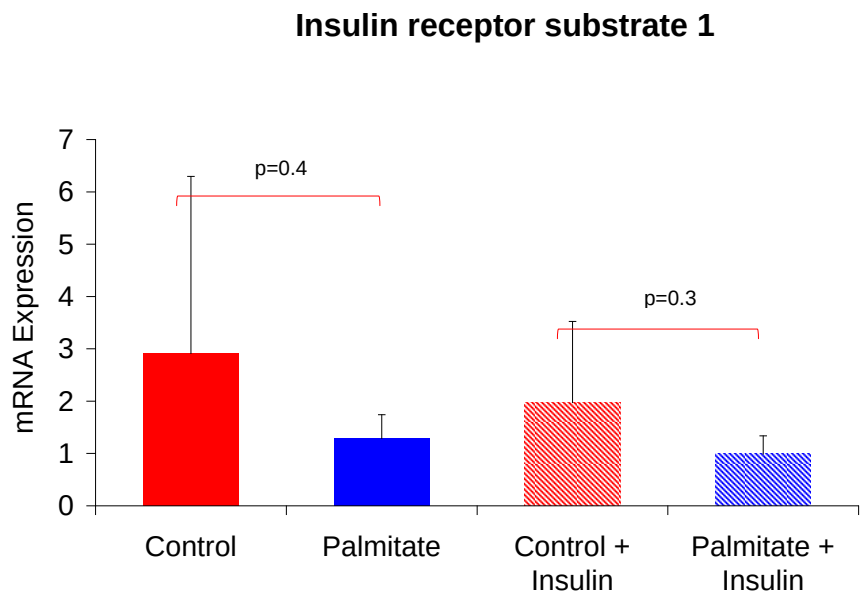
Insulin receptor substrate 1
mRNA Expression
7
6
5
4
3
2
1
0
p=0.4
p=0.3
Control
Palmitate
Control + Insulin
Palmitate + Insulin

B

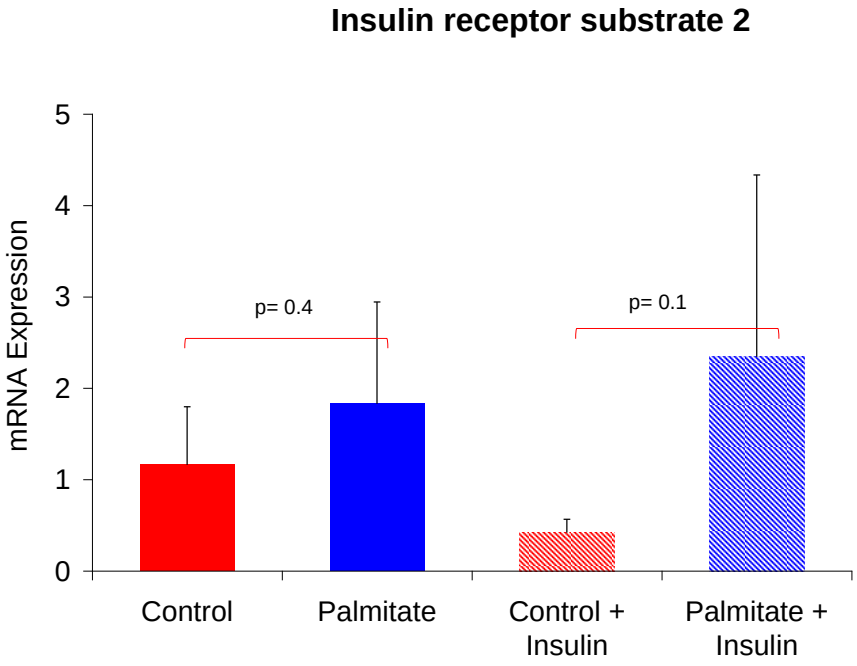
Insulin receptor substrate 2
mRNA Expression
5
4
3
2
1
0
p= 0.4
p= 0.1
Control
Palmitate
Control + Insulin
Palmitate + Insulin

C

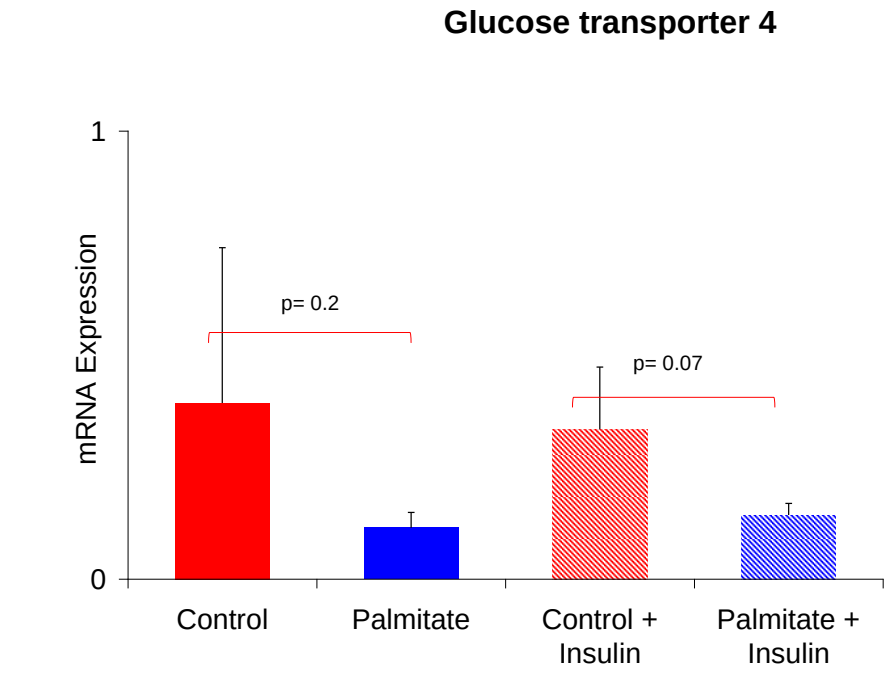
Glucose transporter 4
1
0
mRNA Expression
p= 0.2
p= 0.07
Control
Palmitate
Control + Insulin
Palmitate + Insulin

D

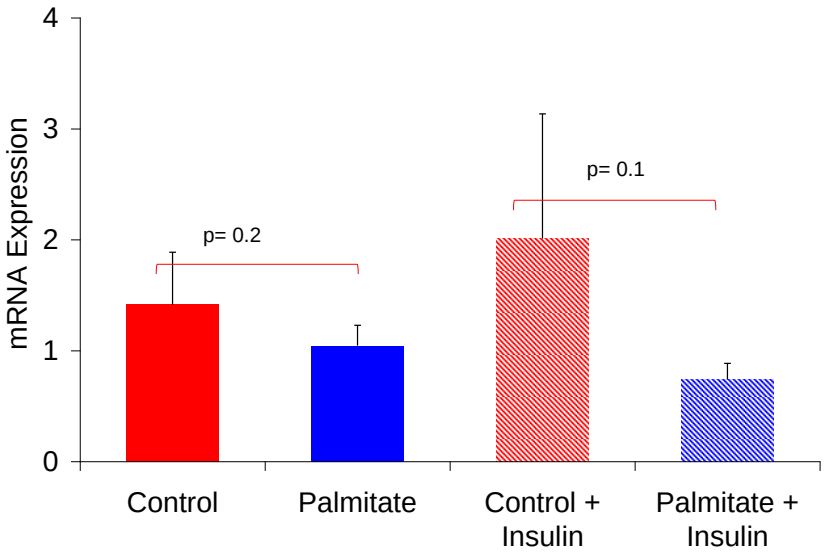
Phosphatidylinositol 3 Kinase
4
3
2
1
0
mRNA Expression
p= 0.2
p= 0.1
Control
Palmitate
Control + Insulin
Palmitate + Insulin

E

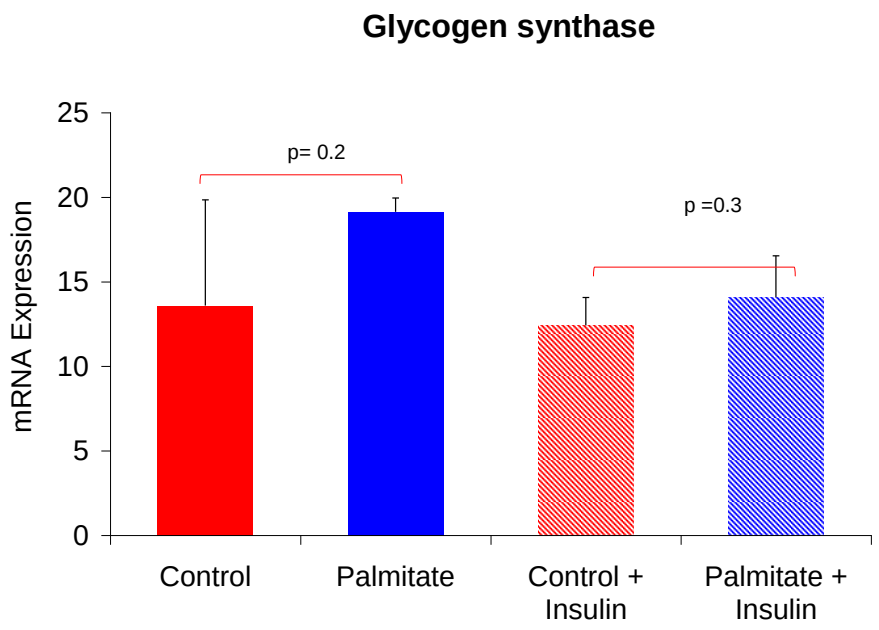

Figure 39. The effect of palmitate treatment on gene expression.
Myocytes were cultured in 5.5 mM glucose and exposed to palmitate for six hours with or without insulin stimulation in the last hour. Messenger RNA levels were determined by quantitative real time PCR. insulin receptor substrate 1 (A), insulin receptor substrate 2 (B), glucose transporter 4 (C), phosphatidylinositol 3 kinase (D) and glycogen synthase (E) mRNA expression were affected similarly during basal and insulin-stimulated culture conditions. Results are expressed as the average of 3 independent experiments ± SD.

Chapter 5

Discussion

5.1 Effect of FFAs on myocytes and adipocytes

In skeletal muscle, elevated plasma FFAs, particularly non-esterified fatty acids (NEFFAs), have been shown to play a direct and indirect role in the pathogenesis of insulin resistance, impaired glucose disposal and to be a risk factor for the development of T2D (Dimopoulos *et al.,* 2006; Haag *et al.,* 2009; Ragheb *et al.,* 2009; Roden *et al.,* 1996). However, the relationship between the type of FFAs, insulin-stimulated glucose uptake and glucose metabolism remains unclear (Dresner *et al.,* 1999; Ruddock *et al.,* 2008). Palmitate, a SFFA, has been associated with insulin resistance, where as certain MUFFAs and PUFFAs (such as oleate, omega 3 and omega 6) are thought to ameliorate insulin resistance (Dimopoulos *et al.,* 2006, Coll *et al.,* 2008).

Skeletal muscle represents 40-50% of total body mass, and accounts for 70-80% of post-prandial insulin-stimulated glucose disposal. Skeletal muscle is therefore essential to maintaining glucose homeostasis (Nedachi *et al.,* 2006). Two skeletal muscle cell lines were used in this study. C2C12 cells are myoblasts originating from mouse satellite cells (Song *et al.,* 1999; Gundry *et al.*, 2009) and L8 cells are derived from fetal rat myoblasts. C2C12 myoblasts have been shown to have lower insulin sensitivity (Ragheb *et al*., 2009; Tortella and Pilch, 2002; Chavez and Summers, 2003); whereas L8 cells are thought to closely mimic the features and responses of normal mammalian skeletal muscle to insulin (Dimopoulos *et al*., 2006; Nedachi *et al.,* 2009).

3T3-L1 derived adipocytes are commonly used to study the cellular mechanisms associated with obesity and diabetes. Adipocytes play a central role in maintaining lipid homeostasis and energy balance in vertebrates by storing triglycerides or releasing free fatty acids in response to changing energy needs (Wu *et al.,* 1999; Chavez and Summers, 2003; Epps-fung *et al.,* 1997).

In the present study, we assessed the basal (unstimulated) and insulin-stimulated effect of the SFFA palmitate, the MUFFA oleate and the essential EFFAs omega 3 and omega 6 on glucose uptake and metabolism.

5.2 Myocytic differentiation of C2C12 and L8 myoblasts

Differentiation of myoblasts to myocytes and myotubules increase *in vitro* glucose uptake and utilization, thereby allowing for *in vitro* experiments that closely mimic normal muscle function. C2C12 and L8 muscle cells were differentiated into myocytes and myotubules by converting confluent cells to low serum medium for two days. Serum deprivation induces cell senescence, myocytic differentiation and the formation of multinucleated myotubules (Oh *et al.,* 2006). Proteomic studies have demonstrated that following serum deprivation, proteins of the Ras-MAPK-mediated myogenic signaling pathway are rapidly upregulated, while signaling pathways known to inhibit myogenic differentiation are downregulated (Kislinger *et al.*, 2005).

In this study, C2C12 myoblasts were more efficient at forming multicellular myotubules than L8 myoblasts. The observations were similar to that observed by Nedachi *et al.,* 2006. They reported that C2C12 myocytes differentiate more efficiently compared to L6 cells in terms of myotubular sarcomere formation. The rapid differentiation of C2C12 myoblasts in comparison to L8 or L6 cells can be ascribed to their different origins. C2C12 myoblasts were derived from mature murine skeletal muscle while L8 or L6 cells originate from newborn rat skeletal muscle (Segarini *et al.,* 1992).

Myotubule formation, a measure of contractibility and normal muscle function, can be used as a morphological measure of myocytic differentiation. At a functional level, apart from an increase in myogenic contractile proteins, levels of intracellular metabolic enzymes such as pyruvate kinase, creatine kinase, ATP-

synthase, acyl-coenzyme A oxidase and 3-hydroxyacyl-coA dehydrogenase are increased (Kislinger *et al.*, 2005).

At a molecular level, myotubule formation is associated with increased Glut4 mRNA expression and insulin-stimulated glucose utilization (Richardson and Pessin, 1993; Hommelberg *et al.,* 2010). Differentiation of C2C12 myoblasts to myotubules increases their Glut4 mRNA expression by 3-4 fold. However, these levels are still substantially lower than that of normal skeletal muscle *in vivo* (Richardson and Pessin, 1993). In contrast to C2C12 myoblasts, undifferentiated L8 myoblasts, express high levels of Glut4 mRNA and are responsive to insulin stimulation regardless of their differentiation status (Oh *et al.,* 2006).

5.3 Adipocytic differentiation of 3T3-L1 fibroblasts

Chronic exposure of 3T3-L1 fibroblasts to Dex, IBMX and insulin, change the fibroblastic phenotype to an adipocytic phenotype. To induce these phenotypic changes, 3T3-L1 fibroblasts need to undergo at least two cell divisions in a differentiation media containing Dex, IBMX and insulin. Thereafter, transformed 3T3-L1 fibroblasts start to accumulate fat (adipogenesis) (Sakaue *et al.,* 2002; Wu *et al.,* 1999). In this study, five days after Dex, IBMX and insulin treatment fat accumulation could be microscopically observed in the cells, thereby confirming that the cells were successfully transformed into adipocytes.

5.4 Selection of optimal free fatty acid concentrations in C2C12 myocytes and 3T3-L1 adipocytes

An initial glucose uptake screen was used to determine the concentration of FFA that elicited the greatest effect on basal glucose uptake in C2C12 myocytes and 3T3-L1 adipocytes. In C2C12 myocytes palmitate, omega 3 and omega 6 were shown to maximally reduce basal glucose uptake at a concentration of 0.75 mM without affecting mitochondrial dehydrogenase activity, as measured by the MTT assay. Oleate had no effect on glucose uptake in C2C12 myocytes. In 3T3-L1

adipocytes, palmitate and oleate had no effect, while omega 3 and omega 6 increased glucose uptake.

Epps-Fung *et al.,* 1997 reported a maximal effect on glucose uptake after 16 hours exposure to 0.3 mM palmitate in 3T3-L1 adipocytes. In similar studies, Dimopoulos *et al.,* 2006, reported that 0.75 mM palmitate and oleate had a maximal effect on glucose uptake after exposing L6 myocytes to these two FFAs for 16 hours. These findings were confirmed by Chavez and Summers, 2003, who reported a maximal effect of palmitate on glucose metabolism in C2C12 myocytes and 3T3-L1 adipocytes that were pre-exposed to palmitate for 16 hours followed by a further three hours exposure during the assay.

For consistency, in this study, it was therefore decided to use a FFA concentration of 0.75 mM for all subsequent assays. In addition, using equimolar concentrations of FFAs allows for direct comparisons between respective FFAs. To maximize the effect of FFA on glucose uptake and metabolism, it was decided to pre-expose the C2C12 and L8 myocytes and 3T3-L1 adipocytes to the relevant FFA for 24 hours, followed by a further six hours of exposure on the day of the assay.

5.5 Glucose uptake

5.5.1. Effect of insulin stimulation on glucose uptake in C2C12 and L8 myocytes, and 3T3-L1 adipocytes

Myocytes, in contrast to myoblasts, are characterized by increased expression of the insulin sensitive glucose transporter GLUT4 (Nedachi *et al.,* 2009; Ragheb *et al.,* 2009). Insulin-stimulated glucose uptake involves the translocation of GLUT4 from the cytoplasm to the plasma membrane.

In comparison to L6 myocytes glucose uptake in C2C12 myocytes is less responsive to insulin stimulation (Nedachi *et al.,* 2009; Nedachi and Kanzaki,

2006). Nedachi and Kanzaki, 2006 showed that decreased insulin sensitivity of C2C12 myocytes is due to decreased insulin-stimulated translocation of GLUT4 to the plasma membrane. Futhermore, C2C12 myocytes express increased amounts of GLUT1 which increases basal glucose uptake that could mask insulin-stimulated glucose uptake, especially at high glucose concetrations. In addition, basal glucose uptake is autoregulated by the extracellular glucose concentration (Nedachi *et al.,* 2009).

In this study insulin-stimulation significantly increased glucose uptake by 61% when C2C12 myocytes were cultured in 5.5 mM glucose. However insulin-stimulation had no effect at 20 mM glucose. A plausible explanation for the decreased insulin-stimulated glucose uptake at high glucose concentrations may be due to autoregulation of basal glucose uptake by GLUT1, as reported by Nedachi *et al.,* 2009.

In L8 myocytes and 3T3-L1 adipocytes insulin stimulation did not significantly increase glucose uptake.

5.5.2 Effect of free fatty acids on glucose uptake in C2C12 and L8 myocytes

Palmitate reduced basal glucose uptake in C2C12 myocytes cultured in both 5.5 mM and 20 mM glucose, and in L8 myocytes cultured in 5.5 mM glucose only. From these results it appears that palmitate effects basal glucose uptake more in C2C12 myocytes than in L8 myocytes, which were resistant to the effects of palmitate at the higher 20 mM glucose concentration.

Insulin-stimulated glucose uptake was adversely affected by palmitate in both C2C12 and L8 myocytes cultured in 5.5 mM and 20 mM glucose concentrations. These findings are consistent with various other studies. Ragheb *et al.,* 2009 and Schmitz-Peiffer *et al.,* 1999, reported a decrease in both basal and insulin-stimulated glucose uptake in C2C12 cells exposed to 0.75 mM and 1.0 mM palmitate for 16 hours. Lennon *et al.,* 2009 also reported a decrease in basal and

insulin-stimulated glucose uptake in human podocytes cultured with 0.75 mM palmitate for 24 hours. Powell *et al.,* 2004 reported a decrease in both basal and insulin-stimulated glucose uptake in L6 myocytes cultured in 25 mM glucose and exposed to 0.75 mM palmitate for 16 hours. Findings in L8 myocytes is in agreement with Hajduch *et al.,* 2001, who implicated intracellular ceramide concentrations with the inhibition of insulin-stimulated glucose uptake in L6 myocytes. They found that ceramides did not inhibit IR, IRS1, PI3k or PDK-1 activation but rather caused the downstream disruption of PKB activation. The intracellular accumulation of ceramide, a metabolite of palmitate, is thought to be directly involved with the inhibition of PKB and glycogen synthase kinase 3 (GSK3). Schmitz-Peiffer *et al.,* 1999 reported that exposure of C2C12 myocytes to palmitate for 18 hours increased the intracellular ceramide content two-fold.

Oleate had no effect on basal glucose uptake in C2C12 and L8 myocytes cultured in 5.5 mM and 20 mM glucose. In contrast to these findings, other studies reported an increase in basal glucose uptake in C2C12 and L6 myocytes cultured with 0.75 mM oleate for 16 hours (Cazzolli *et al.,* 2002; Dimopoulos *et al.,* 2006; Ragheb *et al.,* 2009).

Insulin-stimulated glucose uptake was reduced in C2C12 cells cultured in 5.5 mM glucose media. At the higher glucose concentration of 20 mM, a similar but non-significant trend was evident. These findings are similar to those of Ragheb *et al.,* 2009 and Schmitz-Peiffer *et al.,* 1999.

In L8 myocytes, insulin-stimulated glucose uptake was not affected by oleate at 5.5 mM glucose. However, insulin-stimulated glucose uptake was reduced at the higher concentration of 20 mM glucose. This finding is in contrast with that of Gao *et al.,* 2009 who reported that oleate, at a concentration range of 0.5 mM-0.75 mM for six hours had no affect on insulin-stimulated glucose uptake in L6 myocytes. Findings of this study are consistent with the Randle theory (Randle *et*

al., 1964) where the addition of FFA to high glucose concentrations affects glucose utilization by the cell.

Omega 3 and omega 6 had no effect on both basal and insulin-stimulated glucose uptake in C2C12 and L8 myocytes cultured at both 5.5 mM and 20 mM glucose.

From these results, it is clear that palmitate has a profound effect on both basal and insulin-stimulated glucose uptake in muscle. The association between palmitate and insulin resistance is well established (Dimopoulos *et al.,* 2006; Ragheb *et al.,* 2009). The interaction between extracellular glucose and lipid concentrations play opposing, yet well synchronised roles in normal muscle energy physiology. *In vivo*, muscle cells switch between lipid and glucose as the main source of energy. As postprandial glucose levels rise, insulin stimulates glucose uptake and metabolism, while lipolysis is inhibited and the utilization of FFAs as a major source of energy decreases (Bouche *et al.,* 2004).

5.5.3 Effect of free fatty acid on glucose uptake in adipocytes

In 3T3-L1 adipocytes, FFAs had no effect on basal glucose uptake when adipoctes were cultured in 5.5 mM glucose but decreased glucose uptake at 20 mM glucose. Similary, palmitate decreased insulin-stimulated glucose uptake at 20 mM glucose only. Similar results have been reported by Epps-Fung *et al.,* 1997, who reported decreased glucose uptake in adipocytes that were treated with 25 mM glucose and 0.3 mM palmitate. The other FFAs (oleate and essential fatty acids, omega 3 and omega 6) had a non-significant lowering effect on insulin-stimulated glucose uptake when adipocytes were cultured in 20 mM glucose.

5.6 Glucose-6-phosphate

5.6.1 Effect of free fatty acids on glucose-6-phosphate in C2C12 and L8 myocytes

Palmitate and omega 6 reduced basal G6P concentrations in C2C12 myocytes cultured in 5.5 mM or 20 mM glucose. Oleate increased basal G6P concentrations in C2C12 myocytes cultured in 5.5 mM glucose but had no effect at 20 mM glucose. Omega 3 increased basal G6P concentrations at both glucose concentrations. Palmitate reduced insulin-stimulated G6P concentrations in C2C12 myocytes cultured in 5.5 mM or 20 mM glucose. Oleate increased insulin-stimulated G6P concentrations at 20 mM glucose. Omega 3 and omega 6 decreased G6P concentrations at 5.5 mM glucose but increased G6P concentrations at 20 mM glucose.

In L8 myocytes, palmitate decreased basal G6P concentrations at 20 mM glucose. Oleate decreased G6P concentrations at both 5.5 mM and 20 mM glucose. Omega 3 decreased G6P concentrations at 5.5 mM while omega 6 increased G6P concentrations at 5.5 mM glucose. Palmitate, oleate and omega 3 decreased insulin-stimulated G6P concentrations at both 5.5 mM and 20 mM glucose, while omega 6 decreased G6P concentrations at 20 mM glucose.

As far back as 1964 Randle demonstrated that G6P concentrations increase in the presence of elevated FFAs due to the inhibition of phosphofructokinase (PFK). Phosphorylation of glucose to G6P by hexokinase confines the movement of glucose from the cytoplasm to the extracellular space. This study showed that palmitate decreased insulin-stimulated G6P concentrations in C2C12 and L8 myocytes cultured in 5.5 mM and 20 mM glucose. These results are contradictory to Randle's theory but are similar to the findings of Roden *et al.,* 1996 and Krebs *et al.,* 2000 who demonstrated lowered intracellular insulin-stimulated G6P concentrations in humans after lipid infusion.

What is not clear is whether palmitate affects G6P concentrations by reducing glucose uptake at the transporter level or by inhibiting hexokinase activity.

Oleate increased insulin-stimulated G6P concentrations in C2C12 myocytes cultured in 20 mM glucose while it decreased G6P concentrations in L8 myocytes cultured at both 5.5 mM and 20 mM glucose. This finding underlines one of the differences between the two cell lines, where C2C12 myocytes exposed to elevated FFAs accumulate G6P as suggested by Randle 1964, while in L8 myocytes reduced G6P concentrations is consistant with the findings of Roden *et al.,* 1996.

The essential FFAs, omega 3 and omega 6 decreased insulin-stimulated G6P concentrations at 5.5 mM but increased insulin-stimulated G6P concentrations at 20 mM glucose in C2C12 myocytes. In L8 myocytes, omega 3 decreased insulin-stimulated G6P concentrations at 5.5 mM however, at 20 mM glucose both omega 3 and omega 6 decreased insulin-stimulated G6P concentrations.

Decreased G6P concentrations in C2C12 cultured at 5.5 mM glucose could be due to increased G6P clearance by increased glycogen synthase activity or increase glucose metabolism. Alternatively, insulin-stimulated glucose uptake via GLUT4 or hexokinase activity could be affected. At 20 mM glucose the essential FFAs decrease G6P concentrations, suggesting substrate inhibition. Similar effects are observed during hyperglycemia and hyperlipidemia (Garcia-Ocana and Alonso, 2010). As described previously for C2C12 myocytes, the reduction in insulin-stimulated G6P concentrations in L8 myocytes could be due to reduced glucose uptake and hexokinase activity.

5.6.2. Effect of free fatty acids on G6P in adipocytes

Insulin-stimulated G6P concentrations were reduced by omega 3 in adipocytes cultured in 5.5 mM glucose. Oleate decreased insulin-stimulated G6P concentrations at 20 mM glucose. An interesting finding was that at the high

glucose concentration of 20 mM all FFAs increased basal G6P concentrations, but not during insulin-stimulation. Reduction of the intracellular accumulation of G6P is consistent with insulin inhibiting lipolysis and thereby increasing glucose metabolism. This is important as it demonstrates the relationship between insulin resistance and the accumulation of fat via glucose metabolites (Krebs *et al.,* 2000).

5.7 Glycogen content

5.7.1 Effect of free fatty acid on glycogen content in C2C12 and L8 myocytes

In C2C12 myocytes, none of the FFAs affected insulin-stimulated glycogen concentrations at 5.5 mM or 20 mM glucose. In L8 myocytes, palmitate, oleate and omega 6 decreased insulin-stimulated glycogen concentrations at 20 mM glucose. This corresponds with the decreased insulin-stimulated G6P results observed in L8 myocytes.

In normal muscle cells during normoglycemia, insulin concentrations are low, glucose is used equally for glucose oxidation and glycogen synthesis. During the post-prandial state, plasma insulin increases in response to increasing glucose concentrations and glycogen synthesis predominates (Schmitz-Peiffer, 2000). In this study reduced glycogen concentrations were observed in L8 myocytes; this can be explained by reduced G6P concentrations and therefore substrate availability for glycogen syntheses.

The discrepancy between L8 and C2C12 myocytes glycogen concentrations, can at least in part, be explained by differences in their glycogen synthesis physiology. In C2C12 myocytes the rate of glucose uptake is 10-fold higher than the rate of glycogen synthesis and therefore insulin stimulation and FFAs has a minimal effect on the glycogen synthesis (Park *et al.,* 1998; Cazzolli, *et al.,* 2002).

5.7.2 Effect of free fatty acids on glycogen content 3T3-L1 adipocytes

At both glucose concentrations none of the FFAs had an affect on insulin-stimulated intracellular glycogen levels. In contrast to muscle, the primary function of adipocytes is lipid synthesis and storage. Adipocytes only contain small amounts of glycogen. In contrast to muscle where glycogen is stored for energy, in adipocytes the precise physiological role of glycogen remains unclear (Markan *et al.,* 2010).

5.8 Glucose oxidation

5.8.1 Effect of free fatty acid on glucose oxidation in C2C12 and L8 myocytes

In C2C12 myocytes all FFA decreased insulin-stimulated glucose oxidation at 20 mM glucose; while in L8 myocytes insulin-stimulated glucose oxidation was reduced at both 5.5 mM and 20 mM glucose concentrations. These findings are consistent with the Randle theory whereby lipid and glucose metabolites compete for mitochondrial oxidation (Randle, 1964; Hue and Taegtmeyer, 2009). Belfort *et al.,* 2005 reported a decrease in glucose oxidation after exposure of human muscle to high levels of FFAs, futher supporting for these findings.

5.8.2 Effect of free fatty acids on glucose oxidation in 3T3-L1 adipocytes

In 3T3-L1 adipocytes, insulin-stimulated glucose oxidation was reduced by all FFAs at 5.5 mM and 20 mM glucose concentration. Although these decreases were significant, the actual fold decreases, compared to myocytes, were less. These results demonstrate that 3T3-L1 adipocytes, in terms of glucose uptake and metabolism, are not as sensitive to extracellular FFAs concentrations compared to myocytes, as reported by other studies (Wu *et al.,* 2006; Gross *et al.,* 2008).

5.9The effect of palmitate on messenger RNA expression of genes involved in the insulin signaling pathway

The SFFA, palmitate decreased glucose uptake during insulin-stimulated conditions in C2C12 and L8 myocytes cultured in both 5.5 mM and 20 mM glucose. In 3T3-L1 adipocytes, palmitate decreased glucose uptake in cells cultured in 20 mM glucose only. Due to these findings, C2C12 myocytes exposed to palmitate were used to investigate messenger RNA expression of genes involved in the insulin signaling pathway.

Palmitate treatment caused no statistically significant change in mRNA expression of the genes investigated. The expression of the insulin signaling genes was similarly regulated during basal and insulin-stimulated conditions. During basal conditions cells were cultured without exogenous insulin. Muscle cells do not secrete insulin, thus genes involved in the insulin signalling pathway are not expected to be regulated during basal conditions. These findings are consistent with others who have reported that palmitate regulates insulin-stimulated glucose uptake post Pi3k (Schmitz-Peiffer *et al*., 1999). However, contradictory findings have been reported by Dresner *et al.*, 1999 who showed that lipid infusion decreased Irs1 and Pi3k mRNA in humans.

Although palmitate treatment decreased Glut4 mRNA levels during basal and insulin-stimulated conditions, only the reduction after insulin treatment was significant at a 90% confidence interval (p=0.08). Similar results were reported by Jové *et al*., 2006. These authors showed that palmitate treatment in C2C12 cells increased activation of protein kinase C thetha (PKCθ), which in turn activated NFκβ leading to increased mRNA levels of the proinflammatory cytokine, tumour necrosis factor alpha (TNFα) and decreased Glut4 mRNA levels. These findings confirm reports by Griffin *et al.,* 1999 who showed increased levels of FFAs induced insulin resistance by activating PKCθ

Schmitz-Peiffer *et al*., 1999 showed that palmitate treatment decreased insulin-stimulated glycogen synthesis in C2C12 cells. Results of this study failed to show

an affect at the level of glycogen synthase (Gsy) mRNA expression consistent with intracellular glycogen concentrations.

The discrepancies between these results and those reported in the literature could be due to several reasons. It could due to different experimental models used. In this study the C2C12 muscle cell line was used while other studies have used human or animals muscle, or other *in vitro* muscle cell lines. Cell culture conditions can lead to varying results; in this study cells were pre-exposed to palmitate for 24 hour thereafter for six hours on the day of the assay. Different times of insulin stimulation could futher contribute to varying results between studies. In this study cells were stimulated with insulin for one hour while Dresner *et al.,* 1997 use 15 minutes. Song *et al.,* 1999 showed that insulin-stimulation of skeletal muscle cells increased or decreased IRS1 and IRS2 phosphorylation in time dependant manner over a 40 minute period.

Investigation of proteins involved in the insulin signaling pathway may be regulated at the post-transcriptional, translation or post-translational levels. Several lines of evidence have suggested that phosphorylation events are the major form of regulation. Thus, changes in the expression or activity of these proteins may not be evident at the mRNA level. Several studies have provided support for this. Chavez *et al.,* 2003 reported that palmitate inhibited AKT/PKB phosphorylation within two to four hours at a concentration of 0.25 mM. Ragheb *et al.,* 2009 reported a reduction in PKB in palmitate treated cells.

This study showed that insulin-stimulation down regulated Irs1, Glut4 and Pi3k mRNA levels, although the decrease was not statistically significant. Irs2 mRNA levels were increased, possibly suggesting that Irs2 activity may compesate for decreased Irs1 activity. This has been described previously (Yang *et al.,* 2010).

5.10 Conclusion

The addition of FFAs to myocytes and adipocytes, *in vitro,* had varying effects on glucose uptake and metabolism. Palmitate, a SFFA reduced insulin-stimulated glucose uptake at both 5.5 mM and high 20 mM glucose concentrations in myocytes, while only affecting glucose uptake in adipocytes at the glucose concentration of 20 mM. These findings support the hypothesis that adipocytes in contrast to myocytes retain their insulin sensitivity when exposed to palmitate at normoglycemic conditions (5.5 mM). Glucose utilization is reduced at hyperglycemic conditions which suggest that 3T3-L1 adipocytes, as with myocytes, autoregulate glucose uptake in response to extracellular glucose concentrations.

In terms of basal and insulin-stimulated glucose uptake in myocytes, this study confirmed that, compared to oleate, omega 3 and omega 6, palmitate had the worse affect on glucose uptake. As the FFAs were used at equimolar concentrations, it is reasonable to conclude that palmitate apart from competition for substrate with glucose, has additional effects on insulin-stimulated glucose uptake. This finding is consistent with other studies that have linked the palmitate metabolites DAG and ceramide to insulin resistance in myocytes.

In contrast to other studies reporting that UFFAs improved insulin sensitivity and glucose uptake in myocytes and adipocytes, this study showed that neither oleate, omega 3 nor omega 6 improved basal or insulin-stimulated glucose uptake in C2C12 myocytes. In L8 myocytes, oleate, omega 3 and omega 6 reduced insulin-stimulated glucose uptake in 20 mM glucose. However the decreases were not as marked as palmitate. In 3T3-L1 adipocytes, oleate, omega 3 and omega 6 had no effect on glucose uptake.

Palmitate decreased G6P concentrations in insulin-stimulated myocytes cultured at 5.5 mM and 20 mM glucose concentrations. However, palmitate had no effect on the insulin-stimulated G6P concentrations in 3T3-L1 adipocytes. The

decrease in G6P concentrations induced by palmitate in myocytes, together with the decrease in glucose uptake is consistent with reduced glucose influx into the cell due to the inhibition of GLUT4 translocation to the plasma membrane or the rate limiting effect of hexokinase. These findings are similar to what has been described in diabetics.

Free fatty acids exerted a minimal effect on insulin-stimulated glycogen content in myocytes and adipocytes. This suggests that FFAs affect glucose utilization (oxidation) rather than glycogen synthesis.

In support of the Randle theory, whereby FFAs and glucose compete for the same mitochondrial substrate, all the FFAs reduced basal and insulin-stimulated glucose oxidation at 20 mM glucose concentration.

The induction of insulin resistance in C2C12 myocytes by palmitate was confirmed at the molecular level, with mRNA expression of key genes involved in insulin signaling, (Irs1, Pi3k and Glut4).

5.11 Shortcomings of the study

Due to budget restrictions, mRNA expression of the genes involved in insulin signaling was only performed on C2C12 myocytes, treated with palmitate. This should be expanded to the other cell lines and FFAs in future. Although the aim of the study was to investigate the effect of FFAs on insulin-stimulated glucose uptake and metabolism, it would have been beneficial to study FFA uptake and metabolism using radiolabelled FFAs. This would elucidate the interaction between FFAs and glucose metabolism. In addition, the quantification of the intracellular FFAs metabolites such as DAG, and ceramide could have further clarify the underlining differences that saturated and unsaturated FFAs have on glucose metabolism.

5.12 Future Studies

Future studies using radiolabelled FFAs would provide valuable information about the relationship between glucose and fat metabolism. In addition, it would be interesting to investigate the relationship of FFAs in combination i.e. saturated in combination with mono-unsaturated or poly-unsaturated FFAs *in vitro*. The study should be expanded to include an *in vivo* model whereby FFA concentrations are increased either by diet or by intravenous administration of specific FFAs. In terms of insulin signaling, apart from gene expression studies, the activation of key regulatory enzymes of the insulin stimulatory pathway such as IRS1/2, PI3K and GLUT4 as well as other regulators of metabolism eg. AMPK could be determined using a western blot method.

Chapter 6

References

Abdul-Ghani MA and DeFronzo RA. Pathogenesis of insulin resistance in skeletal muscle. Journal of Biomedicine and Biotechnology 2010; 2010: 1-19.

Aronoff SL, Berkowitz K, Shreiner B and Want L. Glucose metabolism and regulation: beyond insulin and glucagon. Diabetes Spectrum 2004; 17(3): 183-190.

Belfort R, Mandarino L, Kashyap S, Wirfel K, Pratipanawatr T, Berria R, DeFronzo RA, and Cusi K. Dose-response effect of elevated plasma free fatty acid on insulin signalling. Diabetes 2005; 54(6): 1640-1648.

Bergman RN and Ader M. Free fatty acids and pathogenesis of type 2 diabetes mellitus. Trends in Endocrinology and Metabolism 2000; 11(9): 351-356.

Binnert C, Koistinen H, Martin MKG, Andreelli F, Ebeling P, Koivisto VA, Laville M, Auwerx J and Vidal H. Fatty acid transport protein-1 mRNA expression in skeletal muscle and in adipose tissue in humans. American Journal of Physiology Endocrinology and Metabolism 2000; 279: 1072-1079.

Blin C, Panserat S, Médale F, Gomes E, Brèque J, Kaushik S and Krishnamoorthy R. Teleost liver hexokinase- and glucokinase-like enzymes: partial cDNA cloning and phylogenetic studies in rainbow trout (Oncorhynchus mykiss), common carp (Cyprinus carpio) and gilthead seabream (Sparus aurata). Fish Physiology and Biochemistry 1999; 21(2): 93-102.

Bouche C, Serdy S, Kahn CR and Goldfine AB. The cellular fate of glucose and its relevence in type 2 Diabetes. Endocrine Reviews 2004; 25(5): 807-830.

Bouzakri K, Zachrisson A, Al-Khalili L, Zhang BB, Koistinen HA, Krook A and Zierath JR. siRNA-based gene silencing reveals specialized roles of IRS-1/Akt2

and IRS-2/Akt1 in glucose and lipid metabolism in human skeletal muscle. Cell Metabolism 2006; 4(1): 89-96.

Brown GK. Glucose transporters: structure, function and consequences of deficiency. Journal of Inherited Metabolic Disease 2000; 23(3): 237-246.

Broydell M, Mazzuca DM, Kudo PA and LO TCY. The role of the GLUT4 transporter in regulating rat myoblast glucose transport processes. Biochimica Et Biophysica Acta1998; 1371(2): 295-308.

Buchakjian MR and Kornbluth S. The engine driving the ship: metabolic steering of cell proliferation and death. Nature Reviews Molecular Cell Biology 2010; 11: 715-727.

Buzzi F, Xu L, Zuellig RA, Boller SB, Spinas GA, Hynx D, Chang Z, Yang Z, Hemmings BA, Tschopp O and Niessen M. Differential effects of protein kinase B/Akt isoforms on glucose homeostasis and islet mass. Molecular and Cellular Biology, 2010; 30(3): 601-612.

Calvo MB, Figueroa A, Pulido EG, Campelo RG and Aparicio LA. Potential role of sugar transporters in cancer and their relationship with anticancer therapy. International Journal of Endocrinology 2010; 2010: 1-14.

Cazzolli R, Craig DL, Biden TJ and Schmitz-Peiffer C. Inhibition of glycogen synthesis by fatty acid in C2C12 muscle cells in independent of PKC-α, -ϵ, and –θ. American Journal of Physiological Endocrinology and Metabolism 2002; 282: E1204-E1213.

Chan BT and Lee AV. Insulin receptor substrates (IRSs) and breast tumorigenesis. Journal of Mammary Gland Biology and Neoplasia 2008; 13(4): 415-422.

Chan WAY. Cardiac mitochondrial respiration in two rodent models of obesity, thesis for the degree of Master of Science in Medicine 2006, Faculty of Health Sciences, UCT.

Chavez JA and Summers SA. Characterising the effects of saturated fatty acid on insulin signaling, ceramide and diacylglycerol accumulation in 3T3-l-1 adipocytes and C2C12 myotubes. Archives of Biochemistry and Biophysics. 2003; 419: 101-109.

Chavez JA, Knots TA, Wang L, Li G, Dobrowsky TR, Florant GL and Summers SA. A role for ceramide but not diacylglycerol in the antagonism of insulin signal transduction by saturated fatty acid. The American Society for Biochemistry and Molecular biology 2003; 278: 10297-10303.

Coll T, Eyre E, Calvo RR, Palomer X, Sanchec RM, Merlos M, Laguna JC and Carrera MV. Oleate reverses palmitate-induced insulin resistance and inflamation in skeletal muscle cells. The Journal of Biological Chemistry 2008; 283: 11107-11116.

Cooney GJ, Lyons RJ, Crew AJ , Jensen TE, Molero JC, Mitchel CJ, Biden TJ, Ormandy CJ, James DE and Daly RJ. Improved glucose homeostasis and enhanced insulin signalling in Grb14-deficient mice. The EMBO Journal 2004; 23: 582 -593.

Cooper GM. The cell: a molecular approach. 2nd edition: Sunderland (MA): Sinauer Associates; 2000.

Corpeleijn E, Saris WHM and Blaak EE. Metabolic flexibility in the development of insulin resistance and type 2 diabetes: effects of lifestyle. Obesity Reviews 2009; 10(2): 178- 193.

Criddle DN, Sutton R and Petersen OH. Role of Ca2+ in pancreatic cell death induced by alcohol metabolites. Journal of Gastroenterology and Hepatology 2006; 3: 14-17.

Da Poian AT, El-Bacha T and Luz MRMP. Nutrient utilization in humans: metabolism pathways. Nature Education 2010; 3(9): 11.

Davidoff F. Blood sugar, disease, and non disease. Annals of Internal Medicine 1997; 127(3): 235-237.

De Santa Olalla LM, Sàchez Muniz FJ and Vaquero MP. N-3 fatty acids in glucose metabolism and insulin sensitivity. Nutricion Hospitalaria 2009; 24:113-127.

Diel P, Baadners D, Schlüpmann K, Velders M and Schwarz JP. C2C12 myoblastoma cell differentiation and proliferation is stimulated by androgens and associated with a modulation of myostatin and Pax7 expression. Journal of Molecular Endocrinology 2008; 40: 231-241.

Dietschy JM and Spady DK. Measurement of rates of cholesterol synthesis using tritiated water. Journal of Lipid Research 1984; 25: 1469-1476.

Dimopoulos N, Watson M, Sakamoto K and Hundal HS. Differential effects of palmitate and palmitoleate on insulin action and glucose utilisation in rat L6 skeletal muscle cells. Biochemical Journal 2006; 399: 473-481.

Dresner A, Laurent D, Marcucci M, Griffin ME, Dufour S, Cline GW, Slezak LA, Anderson DK, Hundal RS, Rothman DL, Peterson FK and Shulman GI. Effects of free fatty acid on glucose transport and IRS-1- associated phosphatidylinositol 3 kinase activity. The Journal of Clinical Investigation 1999; 103(2): 253-259.

Dupont J, Tesseraud S and Simon J. Insulin signalling in chicken liver and muscle. General and Comparative Endocrinology 2009; 163(1-2): 52-57.

Dutta-Roy AK. Cellular uptake of long-chain fatty acids: role of membrane-associated fatty-acid-binding/transport proteins. Cellular and Molecular Life Sciences 2000; 57(10): 1360-1372.

Epps-Fung M, Williford J, Wells A and Hardy RW. Fatty acid-induced insulin resistance in adipocytes. Endocrinology 1997; 138: 4338-4345.

Foster LJ, Li D, Randhawa VK and Klip A. Insulin accelerate inter-endosomal GLUT4 traffic via phosphatidylinositol 3-kinase and protein kinase B. The Journal of Biological Chemistry 2001; 276: 44212-44221.

Gao D, Bailey CJ and Griffiths HR. Metabolic memory effect of the saturated fatty acid, palmitate in monocytes. Biochemical and Biophysical Research Communications 2009; 388: 278-282.

Garcia-Ocana A and Alonso LC. Glucose Mediated Regulation of Beta Cell Proliferation. The open Endocrinology Journal 2010; 4: 55-56.

Garrett R and Grisham CM. Biochemistry. Third edition. Blemont, CA: Thomson Brooks/ Cole; 2005 p.584.

Glatz JFC, Luiken JJFP, and Bonen A. Membrane fatty acid transporters as regulators of lipid metabolism: implications for metabolic disease. Physiological Reviews 2010; 90(1): 367-417.

Goalstone ML and Draznin B. Insulin signaling. Western Journal of Medicine 1997; 167: 166-173.

Gomez O, Ballester-Lurbe B, Poch E, Mesonero JE and Terrado J. Developmental regulation of glucose transporters GLUT3, GLUT4 and GLUT8 in the mouse cerebellar cortex. Journal of Anatomy 2010; 217: 616-623.

Gorovits N and Charron MJ. What we know about facilitative glucose transporters: Lessons from cultured cells, animal models, and human studies. Biochemistry and Molecular Biology Education 2003; 31(3): 163-172.

Griffin ME, Marcucci MJ, Cline GW, Bell K, Barruci N, Lee D, Goodyear LJ, Kraegen EW, White MF and Shulman GI. Free fatty acid–induced insulin resistance is associated with activation of protein kinase C and alterations in the insulin signalling cascade. Diabetes 1999; 48: 1270-1274.

Gross DN, van den Heuvel APJ and Birnbaum MJ. The role of FOXO in the regulation of metabolism role of FOXO in the regulation of metabolism. Oncogene 2008; 24: 2320-2336.

Gundry RL, Raginski K, Tarasova YT, Tchernyshyov I, Bausch-Fluck D, Elliott ST, Boheler KR, Jennifer E, Van Eyk JE and Wollscheid B. The Mouse C2C12 myoblast cell surface N-Linked glycoproteome. Molecular and Cellular Proteomics 2009; 8: 2555–2569.

Guo CS, Degnin C, Fiddler TA, Stauffer D and Thayer MJ. Regulation of MyoD activity and muscle cell differentiation MDM2, pRb, and Sp1. Journal of Biological Chemistry 2003; 278(25): 22615-2222.

Haag M, Malipa ACS, Van papendorp DH, Stivaktas PI, Alummoottil S and Koorts AM. Short-term fatty acid effects on adipocytes glucose uptake: mechanistic insights. Postglandins Leukotrines and Essential Fatty acid 2009; 80: 247-253.

Hajduch E, Balendran A, Batty IH, Litherland GJ, Blair AS, Downes CP and Hundal HS. Ceramide impairs the insulin-dependent membrane recruitment of protein kinase B leading to a loss in downstream signaling in L6 skeletal muscle cells. Diabetologia 2001; 44: 173-183.

Han CY, Kargi AY, Omer M, Chan CK, Martin M, O'Brien KD, Wight TN and Chait A. Differential effect of saturated and unsaturated free fatty acids on the generation of monocyte adhesion and chemotactic factors by adipocytes: dissociation of adipocyte hypertrophy from inflammation. Diabetes 2009; 23: 2-17.

Hartshorne GM, Lyrakou S, Hamoda H, Oloto E and Ghafari F. Oogenesis and cell death in human prenatal ovaries: what are the criteria for oocyte selection? Molecular Human Reproduction 2009; 15(12) 805-819.

Hays NP, Galassetti PR, and Coker RH. Prevention and treatment of type 2 diabetes: current role of lifestyle natural product, and pharmacological interventions. Pharmacology and Therapeutics 2008; 118(2): 181-191.

Hediger MA, Romero MF, Peng J, Rolfs A, Takanaga H and Bruford EA. The European Journal of Physiology 2004; 447: 465-468.

Heilig CW, Liu Y, England RL, Freytag SO, Gilbert JD, Heiling KO, Zhu M, Concepcion LA and Brosius FC. D-glucose stimulates mesangial cell GLUT1 expression and basal and IGF-I-sensitive glucose uptake in rat mesangial cells: implications for diabetic nephropathy. Diabetes 1997; 46(6): 1030-1039.

Holland WL, Knotts TA, Chavez JA, Wang L, Hoehn KL, and Summers SA. Lipid mediators of insulin resistance. Nutrition Reviews 2007; 65(1): 39-46.

Hommelberg PPH, Plat J, Remels AHV, Essen ALM , Kelders MCJM, Mensink RP, Schols AMWJ and Langen RCJ . Trans-10, cis-12 conjugated linoleic acid inhibits skeletal muscle differentiation and GLUT4 expression independently from NF-κB activation. Molecular Nutrition and Food Research 2010; 54(12): 1763-1772.

Hu FB, Van Dam RM and Liu S. Diet and risk of T2D: the role of type of fat and carbohydrates. Diabetologia 2001; 44: 804- 817.

Hue L and Taegtmeyer H. The Randle cycle revisited: a new head for an old hat. American Journal of Physiology-Endocrinology and Metabolism 2009; 297(3): E578-E591.

Hui TY and Bernlohr DA. Fatty acid transporters in animal cells. Frontiers in Bioscience 1997; 2: 222-231.

Imai K, Hamaguchi M, Mori K, Takeda N, Fukui M, Kato T, Kawahito Y, Kinoshita S and Kojima T. Metabolic syndrome as a risk factor for high-ocular tension. International Journal of Obesity 2010; 34: 1209-1217.

Isharwal S, Misra A, Wasir JS and Nigam P. Diet and insulin resistance: a review and Asian Indian perspective. Indian Journal of Medical Research 2009; 129: 485-499.

Jain SS, Chabowski A, Laelie A. Snook LA, Schwenk RW, Jan FC, Glatz JFC, Luiken JJFP and Bonen A. Additive effects of insulin and muscle contraction on fatty acid transport and fatty acid transporters, FAT/CD36, FABPpm, FATP1, 4 and 6. Febs letters 2009; 583(13): 2294-2300.

Jovè M, Planavila A, Sánchez RM, Merlos M, Laguna JC and Vázquez-Carrera M. Palmitate induces tumor necrosis factor-α expression in C2C12 skeletal muscle cells by a mechanism involving protein kinase C and nuclear factor-kB activation. Endocrinology 2006; 147 (1): 552-561.

Kahn BB. Facilitative glucose transporters: regulatory mechanisms and dysregulation in diabetes. The American Society for Clinical Investigation 1992; 89: 1367-1374.

Kanzaki M and Pessin JE. Insulin-stimulated GLUT4 translocation in adipocytes is dependant upon cortical actin remodeling. Journal of Biological Chemistry 2001; 276(45): 42436-42444.

Karnieli E and Armoni M. Transcriptional regulation of the insulin-responsive glucose transporter GLUT4 gene: from physiology to pathology. American Journal of Physiology Endocrinology and Metabolism 2008; 295(1): 38-45.

Kelley DE and Mandarino LJ. Fuel selection in human skeletal muscle in insulin resistance. Diabetes 2000; 49: 677-683.

Kerner J and Hoppel C. Fatty acid import into mitochondria. Molecular and Cell Biology of Lipids 2000; 1486(1): 1-17.

Khan A and Pessin J. Insulin regulation of glucose uptake: a complex interplay of intracellular signalling pathways. Diabetologia 2002; 45(11): 1475-1483.

Kido Y, Nakae J, and Accil D. The insulin receptor and its cellular targets. Clinical Endocrinology and Metabolism 2001; 86(3): 972-979.

Kim JA, Wei Y and Sowers JR. Role of mitochondrial dysfunction in insulin resistance. Circulation Research 2008; 102: 401- 414.

Kislinger T, Gramolini AO, Yan Pan Y, Rahman K, MacLennan DH, and Emili A. Proteome dynamics during C2C12 myoblast differentiation. Molecular and Cellular Proteomics 2005; 4: 887-901.

Knight JB, Eyster CA, Griesel BA and Olson AL. Regulation of the human GLUT4 gene promoter: interaction between a transcriptional activator and myocyte enhancer factor. Proceedings of the National Academy of Sciences 2003; 100(25): 14725-14730.

Koivisto UM, Martinez-Valdez H, Bilan PJ, Burdett E, Ramlal T and Klip A. Differential regulation of the GLUT-1 and GLUT-4 glucose transport systems by glucose and insulin in L6 muscle cells in culture. The Journal of Biological Chemistry 1991; 266(4): 2615-2621.

Koonen DPY, Glatz JFC, Bonen A and Luiken JJFP. Long-chain fatty acid uptake and FAT/CD36 translocation in heart and skeletal muscle. Biochimica et Biophysica Acta 2005; 1736 : 163-180.

Krebs M, Krssak M, Nowotny P, Weghuber D, Gruber S, Mlynarik V, Bischof M, Stingl H, Furnsinn C, Waldhäusl W and Roden M. Free fatty acids inhibit the glucose-stimulated increase of intramuscular glucose-6-phosphate concentration in humans. The Journal of Cinical Endocrinology and Metabolism 2000; 86(5): 2153-2160.

Kumar A and Singh V. Atherogenic dyslipidemia and diabetes mellitus: what's new in the management arena? Vascular Health and Risk Management 2010; 6: 665-669.

Lennon R, Pons D, Sabin MA, Wei C, Shield JP, Coward RJ, Tavare JM, Mathieson PW Saleem MA and Welsh GI. Saturated fatty acid induces insulin resistace in human podocytes: implications for diabetic nephropathy. Nephorology Dialysis Transplantion 2009; (24): 3288-3296.

Li R, Thorens B and Loeken MR. Expression of the gene encoding the high-Km glucose transporter 2 by the early postimplantation mouse embryo is essential for neural tube defects associated with diabetic embryopathy. Diabetologia 2007; 50(3) 682-689.

López-Solache I, Marie V, and Vignault E. Regulation of uncoupling protein-2 m I: thiazolidinediones stimulate uncoupling requiring ongoing protein synthesis. Endocrine 2002; 19(2): 197-208.

Mann GE, Yudilevich DL and Sobrevia L. Regulation of amino acid and glucose transports in endothelial and smooth muscle cells. The American Physiological Society 2003; 83: 183-252.

Marcel YL and Suzue G. Kinetic studies on the specificity of long chain acyl coenzyme A synthetase from rat liver microsomes. Journal of Biological Chemistry 1972; 247: 4539-4542.

Markan KR, Jurczak MJ and Brady MJ. Stranger in a strange land: Roles of glycogen turnover in adipose tissue metabolism. Molecular and Cellular Endocrinology 2010; 318: 54-60.

Mau M, Kalbe C, Viergutz T, Nürnberg G and Rehfeldt C. Effects of dietary isoflavones on proliferation and DNA integrity of myoblasts derived from newborn piglets. Pediatric Research 2008; 63(1): 39-45.

Mauseth JD. Botany: an introduction to plant biology. Fouth edition. Philadelphia: Jones and Bartlett Publishers; 2009 p. 264.

Medina RA and Owen GI. Glucose transporters: expression, regulation and cancer. Biological Research 2002; 35(1): 9-26.

Moller DE, Chang PY, Yaspelkis BB, Flier JS, Wallberg-Henriksson H and Ivy JL. Transgenic mice with muscle-specific insulin resistance develop increased adiposity, impaired glucose tolerance, and dyslipidemia. Endocrinology 1996; 137: 2397-2405.

Montel-Hagen A, Marc S and Naomi T. Erythroid glucose transporters. Current Opinion in Hematology 2009; 16 (3): 165-172.

Morganstein DL, Christian M, Turner JJO, Parker MG and White R. Conditionally immortalized white pre-adipocytes: a novel adipocyte model. The Journal of Lipid Research 2008; 49: 676-685.

Mozaffarian D, Pischon T, Hankinson SE, Rifai N, Joshipura K, Willett WC and Rimm EB. Dietary intake of trans fatty acids and systemic inflammation in women. American Journal of Clinical Nutrition 2004; 79 (4): 606-612.

Mueckler M. Facilitative glucose transporters. European Journal of Biochemistry 1994; 219(3): 713-725.

Mursula A. ∆3-∆2-Enoyl-CoA isomerase from the yeast saccharomyces cerevisiae. Academic dissertation submitted at University of Oulu for public discussion in Kajaaninsali Oulu 2002.

Muyal JP, Muyal V, Kaistha BP, Seifart C, Fehrenbach H. Systematic comparison of RNA extraction techniques from frozen and fresh lung tissues: checkpoint towards gene expression studies. Diagnostic Pathology 2009; 24: 4-9.

Nair S and Wilding JPH. Sodium glucose cotransporter 2 inhibitors as a new treatment for diabetes mellitus. The Journal of Clinical Endocrinology and Metabolism 2010; 95(1): 34-42.

Nandi A, Wang X, Accili D and Wolgemuth DJ. The effect of insulin signaling on female reproductive function independent of adiposity and hyperglycemia. Endocrinology 2010; 151(4): 1863-71.

Nedachi T and Kanzaki M. Regulation of glucose transporters by insulin and extracellullar glucose in C2C12 myotubes. The American Journal Physiology of Endocrinology Metabolism 2006; 291: 817-828.

Nedachi T, Hatakeyama H, Kono T, Sato M and Kanzaki M. Characterisation of contraction-inducible CXC chemokines and their roles in C2C12 myocytes. The American Journal of Physiological Society 2009; 297: E866-E878.

Nolan JJ. O'Halloran D, McKenna TJ, Firth R and Redmond S. The cost of treating type 2 diabetes. Irish Medical Journal 2006; 99(10): 307-310.

Nualart F, García MDA, Rodolfo A, Medina RA and Owen GI. Glucose transporters in sex steroid hormone related cancer. Current Vascular Pharmacology 2009; 7: 534-548.

O'Boyle RN and Beamish FWH. Growth and intermediary metabolism of larval and metamorphosing stages of the landlocked sea lamprey, Petromyzon marinus L. Environmental Biology of Fishes 1977; 2(2):103-120.

Odegaard ML. Shared metabolic pathways in fuel-stimulated insulin secretion, Dissertation submitted in partial fulfillment of the requirements for the degree of Doctor of Philosophy in the Department of Pharmacology and Cancer Biology 2009, Graduate School of Duke University.

Oh YS, Cho KA, Ryu SJ, Khil LY, Jun HE, Yoon JW and Park SC. Regulation of insulin response in skeletal muscle cell by caveolin status. The Journal of Cellular Biochemistry 2006; 99(3): 747-758.

Olalla LMD, Muniz FJS and Vaquero MP. N-3 fatty acids in glucose metabolism and insulin sensitivity. Nutrición Hospitalaria 2009; 24 (2):113-127.

Olson AL and Knight JB. Regulation of Glut4 expression in vivo and in vitro. Frontiers in Bioscience 2003; (8): 401-409.

Olson AL, Pessin JE. Structure, function, and regulation of the mammalian facilitative glucose transporter gene family. Annual Review of Nutrition. 1996; 16: 235-256.

Park JY, Kim CH, Hong SK, Suh KI and Lee KU. Effects of FFA on insulin-stimulated glucose fluxes and muscle glycogen synthase activity in rats. The American Physiological Society 1998; 275: E338-E344.

Pessin JE and Saltiel AR. Signaling pathways in insulin action: molecular targets of insulin resitance. The Journal of Clinical Investigation 2000; 106(2): 165-169.

Peterson JM, Wang Y, Bryner RW, Williamson DL and Always SE. Bax signaling

regulates palmitate-mediated apoptosis in C2C12 mtoyubes. The American Journal Physiology of Endocrinology Metabolism 2008; 295: 1307-1314.

Piro S, Maniscalchi ET, Monello A, Pandini G, Mascali LG, Rabuazzo AM and Purrell F. Palmitate affects insulin receptor phosphorylation and intracellular insulin signal in a pancreatic α-Cell Line. Endocrinology 2010; 151(9): 4197-4206.

Powell DJ, Turban S, Gray A, Hajduch E and Hundal HS. Intracellular ceramide synthesis and protein kinase Cζ activation play an essential role in palmitate-induced insulin resistance in rat L6 skeletal muscle cells. Biochemistry Journal 2004; 382: 619 – 629.

Prashanth M, Ganesh HK , Vimal MV, John M , Bandgar T, Joshi SR and Shah SR. Prevalence of nonalcoholic fatty liver disease in patients with Type 2 diabetes mellitus. Journal of the Association of Physicians of India 2009; 57: 205-210.

Puig O and Tjian R. Transcriptional feedback control of insulin receptor by dFOXO/FOXO1. Genes and Development 2005; 19: 2435-2446.

Ragheb R, Shanab GML, Medhat AM, Seoudi DM, Adeli K and Fantus IG. Free fatty acid-induced muscle insulin resistance and glucose uptake dysfunction: Evidence for PKC activation and oxidative stress-activated signalling pathways.

The Biochemical and Biophysical Research Communications 2009; 389: 211-216.

Räisänen U, Bekkers M, Bonddigton P, Sarangi S and Clarke A. The causation of disease – the practical and ethical consequences of competing explanations. Medicine, Health Care and Philosophy 2008; 9(3): 293-306.

Randle PJ, Newsholme EA and Garland PB. Effect of fatty acid, ketone bodies and pyruvate and of alloxan diabetes and starvation on the uptake and metabolic fate of glucose in rat heart and diaphragm muscle. Biochemical Journal 1964; 93: 652-665.

Randle PJ. Regulatory interactions between lipids and carbohydrates: the glucose fatty acid cycle after 35 years. Diabetes Metabolism Review 1998; 14(4): 263-283.

Rasmussen BB and Wolfe RR. Regulation of fatty acid oxidation in skeletal muscle. Annual Review of Nutrition 1999; 19: 463-484.

Richardson JM and Pessin JE. Identification of a skeletal muscle-specific regulator domain in the rat GLUT4/muscle-fat gene. Journal of Biological Chemistry 1993; 268(28): 21021-21027.

Risérus U. Fatty acid and insulin sensitivity. Current Opinion in Clinical Nutrition and Metabolic Care 2008; 11(2): 100-1055.

Roden M, Price TB, Perseghin G, Pertersen KF, Rothman DL, Cline GW and Shulman GI. Mechanism of free fatty acid-induced insulin resistance in humans The American society for Clinical Investigation 1996; 97(12): 2859-2865.

Rosen ED, Walkey CJ, Puigserver P and Spiegelman BM. Transcriptional regulation of adipogenesis. Genes and Development 2000; 14: 1293-1307.

Rosenbloom AL, Silverstein JH, Amemiya S, Zeitler P, Klingensmith, G. Type 2 diabetes in the child and adolescent. Pediatric Diabetes 2009; 10(12): 17-32.

Ruddock MW, Stein A, Landaker E, Park J, Cooksey RC, McClain D and Patti ME. Saturated fatty acids inhibit hepatic insulin action by modulating insulin receptor expression and post-receptor signalling. The Journal of Biochemistry. 2008; 144: 599-607.

Saini V. Molecular mechanism of insulin resistance in type 2 diabetes mellitus. World Journal of Diabetes 2010; 1(3): 68-75.

Sakaue H, Konishi M, Ogawa W, Asaki T, Mori T, Yamasaki M, Takata M, Ueno H, Kato S, Kasuga M and Itoh N. Requirement of fibroblast growth factor 10 in development of white adipose tissue. Genes and Development 2002; 16: 908-912.

Schenck FW. Ullmann's Encyclopedia of Industrial Chemistry.Verlag: Willey-VCH; 2006 DOI: 10.1002/14356007.a12_457.pub2.

Schmitz-Peiffer C. Signalling aspects of insulin resistance in skeletal muscle: mechanisms induced by lipid oversupply. Cellular Signalling 2000; 12: 583-594.

Schmitz-Peiffer CS, Craig DL and Boden TJ. Ceramide generation is sufficient to account for the inhibition of the insulin stimulated PKb pathway in C2C12 skeletal muscle cells pretreated with palmitate. The Journal of Biological Chemistry 1999; 274(34): 24202-24210.

Schreyer S, Ledwig D, Rakatzi I, Klöting I and Eckel J. Insulin receptor substrate-4 is expressed in muscle tissue without acting as a substrate for the insulin receptor. Endocrinology 2003; 144(4): 1211-1218.

Sebastián D, Guitart M, García-Martínez C, Mauvezin C, Orellana-Gavaldà JM, Dolors Serra D, Gómez-Foix AM, Hegardt FG, and Asin G. Novel role of FATP1

in mitochondrial fatty acid oxidation in skeletal muscle cells. The Journal of Lipid Research 2009; 50(9): 1789–1799.

Segarini PR, Ziman JM, Kane CJM, and Dasch JR. Two novel patterns of transforming growth factor-β (TGF-β) binding to cell surface proteins a re dependent upon the binding of TGF-Pl and indicate a mechanism of positive cooperativity. The Journal of Biological Chemistry 1992; 261(2): 1048-1053.

Seino Y, Nanjo K, Tajima N, Tajima N, Kadowaki T, Kashiwagi A, Araki E, Ito C, Inagaki N, Iwamoto N, Kasuga M, Hanafusa T, Haneda M and Ueki K. Report of the committee on the classification and diagnostic criteria of diabetes mellitus. Journal of Diabetes Investigation 2010; 1(5): 212-228.

Seki Y, Sato K and Akiba Y. Changes in muscle mRNA for hexokinase, phosphofructokinase-1 and glycogen synthase in acute and persistent hypoglycemia induced by tolbutamide in chickens. Comparative Biochemistry and Physiology 2005; 142: 201-208.

Shaw JE, Sicree RA and Zimmet PZ. Global estimated of the prevalence of diabetes for 2010 and 2030. Diabetes Research and Clinical Practise 2010; 87: 4-14.

Shulman GI. Cellular mechanism of insulin resistance. The Journal of Clinical Investigation 2000; 106(2): 171-175.

Silberstein L, Webster SG, Travis M and Blau HM. Developmental progression of myosin gene expression in cultured muscle cells. Cell 1986; 46(7): 1075-1081.

Skyler JS. Prediction and prevention of type 1 diabetes: progress, problems, and prospects. Clinical Pharmacology and Therapeutics 2007; 81: 768-771.

Song XM, Ryder JW, Kawano Y, Chibalin AV, Krook A and Zierath JR. Muscle fiber type specificity in insulin signal transduction. American Journal of Physiology 1999; 277(46): 1690-1696.

Sztalryd C, Komaromy MC, and Kraemer FB. Overexpression of hormone-sensitive lipase prevents triglyceride accumulation in adipocytes. The Journal of Clinical Investigation 1995; 95: 2652-2661.

Taniguchi CM, Emanuelli B and Kahn CR. Critical nodes in signalling pathways: insights into insulin action. Nature Reviews Molecular Cell Biology 2006; 7: 85-96.

Teusink B, Voshol PJ, Dahlmans VEH, Rensen PCN, Pijl H, Romijn JA and Havekes LM. Contribution of fatty acids released from lipolysis of plasma triglycerides to total plasma fatty acid flux and tissue-specific fatty acid uptake. Diabetes 2003; 52(3): 614-620.

Thevonod F. Frontiers in Diabetes. Basel: Karger; 2008; Vol 19: p.1-18.

Thompson AL, Lim-Fraser MYC, Kraegen EW and Cooney GJ. Effects of individual fatty acid on glucose uptake and glycogen sythesis in soleuse muscle *in vitro*. The American Physiological society 2009; 2: 56-68.

Thorell A, Hirshman MF, Nygren J, Jorfeldt L, Wojtaszewski JFP, Dufresne SD, Horton ES, Ljungqvist O and Goodyear LJ. Excersize and insulin cause GLUT-4 translocation in human skeletal muscle. The American Journal Physiology Endocrinology and Metabolism 1999; 277: E733-E741.

Tortella LL and Pilch PF. C2C12 myocytes lack an insulin-responsive vesicular compartment despite dexamethasone-induced GLUT4 expression. The American Journal of Physiology-Endocrinology Metabolism 2002; 283: 514-524.

Tozzo E, Gnudi L and Kahn BB. Overexpression of GLUT4 driven by an adipose-specific promoter amelioration of insulin resistance in streptozotocin diabetic mice by transgenic. Endocrinology 1997; 138: 1604-1611.

Treadway JL, Hargrove DM, Nardone NA, McPherson RK, Russo JF, Milicig AJ, Stukenbrokg HA, Gibbs EM, Stevenson RW, and Pessinn JE. Enhanced peripheral glucose utilization in transgenic mice expressing the human GLUT4 gene. The Journal of Biological Chemistry 1994; 269(47): 29956-29961.

Tsao TS, Stenbit AE, Factor SM, Chen W, Rossetti L and Charron MJ. Prevention of insulin resistance and diabetes in mice heterozygous for GLUT4 ablation by transgenic complementation of GLUT4 in skeletal muscle. Diabetes 1999; 48: 775-782.

Vakili S and Coudilli MA. Personalized Nutrition: nutritional genomics as a potential tool for targeted medical nutrition therapy. Nutrition Reviews 2007; 65(7): 301-315.

Van der Heiden MG, Cantley LC, and Thompson CB. Understanding the Warburg effect: the metabolic requirements of cell proliferation. Science 2009; 324(5930): 1029-1033.

Wang C, Liu M, Riojas RA, Xin X, Gao Z, Zeng R, Wu J, Watson RT, Kazanki M and Pessin JE. Regulated membrane trafficking of the insulin responsive glucose transporter 4 in adipocytes. The Endocrine Society 2004; 25(2): 177-204.

Watson RT and Pessin JE. GLUT4 translocation: the last 200 nanometres. Cellular Signalling 2007; 19: 2209-2217.

Watson RT and Pessin JE. Bridging the GAP between insulin signalling and GLUT4 translocation. Trends in Biochemical Science 2006; 31(4): 215-222.

Watt MJ, Steinberg GR, Chen ZP, Kemp BE and Febbraio MA. Fatty acids stimulate AMP-activated protein kinase and enhance fatty acid oxidation in L6 myotubes. Journal of Physiology 2006; 574(1):139-147.

Wauman J, De Smet AS, Catteeuw D, Belsham D, and Tavernier J. Insulin receptor substrate 4 couples the leptin receptor to multiple signaling pathways. Molecular Endocrinology 2008; 22: 965–977.

Weigert C, Klopfer K, Kausch C, Brodbeck K, Stumvoll M, Harring HU and Scheleicher ED. Palmitate-induced activation of the hexosamine pathway in human myotubes. Diabetes 2003; 52: 650-656.

White M. Regulating insulin signalling and β cell function through IRS proteins. Canadian Journal of Physiology and Pharmacology 2006; (84): 725-737.

Wild S, Roglic G, Green A, Sicree R, and King H. Global prevalence of diabetes. Diabetes Care 2004; 27(5): 1047-1053.

Wu Q, Ortegon AM, Tsang B, Doege H, Feingold KR and Stahl A. FATP1 is an insulin-sensitive fatty acid transporter involved in diet-induced obesity. Molecular and Cellular Biology 2006; 26(9): 3455-3467.

Wu Z, Rosen ED, Brun R, Hauser S, Adelmant G, Troy AE, McKeon C, Darlington GJ, and Spiegelman BM. Cross-regulation of C/EBPα and PPARγ controls the transcriptional pathway of adipogenesis and insulin sensitivity. Molecular Cell 1999; 3:151-1589.

Wymann MP and Bulgarelli-leva G. Wortmannin inactivates phosphoinositide 3-

kinase by covalent modification of lys-802, a residue involved in the phosphate transfer reaction. Molecular and Cellular Biology 1996; 16(4): 1722-1733.

Yamamoto Y, Yoshimasa Y, Koh M, Suga J, Masuzaki H, Ogawa Y, Hosoda K, Nishimura H, Watanabe Y, Inoue G, and Nakao K. Constitutively active mitogen-activated protein kinase kinase increases GLUT1 expression and recruits both GLUT1 and GLUT4 at the cell surface in 3T3-L1 adipocytes. Diabetes 2000; 49: 332-339.

Yamamoto Y, Yoshimasa Y, Koh M, Suga J, Masuzaki H, Ogawa Y and Yang J. Role of clusters in insulin-regulated GLUT4 trafficking in adipose cells: A new paradigm? International Journal of Biological Science 2010; 6: 716-718.

Yang X, Nath A, Opperman MJ and Chan C. The double-stranded RNA-dependent protein kinase differentially regulates insulin receptor substrates 1 and 2 in HepG2 cells. Molecular Biology of the Cell 2010; 21(19): 3449-3458.

Youngren, J. Regulation of insulin receptor function. Cellular and Molecular Life Sciences 2007; 64 (7-8): 873-891.

Zmuda EJ, Qi L, Zhu MX, Mirmira RG, Montminy MR and Hai T. The roles of ATF3, an adaptive-response gene, in high-fat-diet-induced diabetes and pancreatic β-cell dysfunction. Molecular Endocrinology 2010; 24 (7): 1423-1433.

Appendix 1

List of reagents

Product name	Catalogue number	Supplier and country
2-deoxy-[3H]-D-glucose	TRK672	AEC-Amersham, JHB, SA
3-(4, 5-dimethylthiazol-2-yl)-2, 5-diphenyl tetrazolium bromide (MTT)	M2003	Sigma, St Louise, MO, USA
3-isobutyl-1-methylxanthine (IBMX)	I5879	Sigma, St Louise, MO, USA
Bio Rad Bradford Protein assay kit	500-0201	Bio-Rad, USA
Biovision glucose kit	K646	Biovision, USA
Bovine serum albumin (BSA)	100-10SB	Sigma, St Louise, MO, USA
CELLBIND - 24 well plates	3337	Corning, MA, USA
CELLBIND - 6 well plates	3335	Corning, MA, USA
CELLBIND - 96 well plates	3300	Corning, MA, USA
Cryotubes	430659	Corning, MA, USA
D(U-14C) glucose	NEC042x05 50uCi	PerkinElmar AU,USA
Deprotenizing kit	K808-200	Biovision,USA
Dexamethasone	D4902	Sigma, St Louise, MO, USA
Dimethyl sulfoxide (DMSO)	276855-1L	Sigma, St Louise, MO, USA
Dulbecco's Modified Eagle's Medium DMEM	12-604F	Lonza, Walkersville, MD,USA
Dulbecco's Modified. Eagle's Medium.DMEM without glucose	51442C	Sigma, St Louise, MO, USA
Dulbecco's phosphate buffered saline (DPBS)	17513-F	Lonza, Walkersville, MD,USA
Eppendorf tubes	0030123.301	Sigma, St Louise, MO, USA
Ethanol	2875	Sigma, St Louise, MO, USA
Ethanol absolute,200 proof for molecular	E7023-500	Sigma, St louise, MO,USA
Fetal calf serum FCS	306	Highveld biological,SA
Flask - 75 cm	658 175	Greiner bio-one, Frickenhausen, Germany
Glucose 6 phosphate	K657-100	Biovision, USA
Glucose assay kit	K 606-100	Biovision,USA

Glucose powder	G7021	Sigma, St Louise, MO,USA
Glycogen assay kit	K646-100	Biovision,USA
High capacity cDNA kit	Am 197	Ambion, USA
Horse serum	308	Highveld biological,SA
Insulin	I 6634	Sigma, St Louise, MO,USA
Isopropanol	I9516	Sigma, St Louise, MO,USA
Micro AMP optical 96-well plates reaction plate 15ml	N801-0560	Applied biosystems, Foster city USA
Nuclease free water	AM 9937	Ambion,USA
Oleate	O1383	Sigma, St Louise, MO, USA
Omega 3(Alpha linolenic acid)	L2376	Sigma, St Louise, MO, USA
Omega 6(Linoleic acid)	L1012	Sigma, St Louise, MO, USA
Palmitate	P 5585/P0500	Sigma, St Louise, MO,USA
Pasteur pipettes	612 361	Greiner bio-one, Frickenhausen, Germany
Penicillin and streptomycin	214	Highveld biological,USA
Ready gel Ultima Gold	6013329	Separation Scientific
Rnase free water	AM9937	Ambion,USA
Rnase zap solution	7000	Molecular Bioproducts,INC Sandigo CA
Rneasy mini kit	74106	Qiagen, Hilden
Scintillator vials	566740	Beckman Couter JHB,SA
Serological pipettes - 10ml	4101	Corning, MA, USA
Serological pipettes - 50ml	4490	Corning, MA, USA
Serological pipettes -25ml	4251	Corning, MA, USA
Serological pipettes -5ml	4051	Corning, MA, USA
Sodium bicarbonate (NaHCO3	M2645	Sigma, St louise, MO,USA
Sodium dodecyl sulfate	L3771	Sigma, St louise, MO,USA
Sodium hydroxide (NaOH)/	109140	Merck, SA
Taqman Gene expression master mix	4369016	Applied biosystems, Foster city USA
Tri reagent	T3809	Sigma, St louise, MO,USA

Trypan blue	T8154-20ML	Sigma, St Louise, MO, USA
Trypsin/versene	15050-065	Invitrogen, Carlsbad, CA USA
TURBo DNA-free kit	AM 1907	Ambion,USA
Wortmannin	w 1628	Sigma, St Louise, MO, USA

Appendix 2

Preparation of reagents

Sorenson's buffer

The Sorenson's buffer was prepared by dissolving 0.1 M glycine (0.751 g in 100 ml distilled water) and 0.1 M NaCl (0.584 g in 100ml), thereafter equilibrate pH to 10.5 with NaOH (4 g in 100ml).

0.3 M sodium hydroxide and 1% SDS lysis buffer

A 0.3 M NaOH solution was prepared by dissolving (12 g in 1L distilled water) and adding 1% SDS (1:10 dilution of 10% stock).

FFA (Palmitate FW256.43)

To prepare a 75 mM stock solution, 19.23 mg palmitate was dissolved in 1ml absolute ethanol heated to 90°C. From the stock, a 1:100 dilution was done to yield

Oleate FFA FW282.47

To prepare a 75 mM stock solution, 21.18 mg oleate was dissolved in 1ml absolute ethanol heated to 90°C. From the stock, a 1:100 dilution was done to yield a 0.75 mM oleate solution a 0.75 mM palmitate solution.

Omega 3 (linolenic) (FW278.44)

To prepare a 75 mM stock solution, 20.88 mg omega 3 was dissolved in 1ml absolute ethanol heated to 90°C. From the stock, a 1:100 dilution was done to yield a 0.75 mM omega 3 solution a 0.75 mM palmitate solution.

Omega 6 (linoleic) FW 280.46

To prepare a 75 mM stock solution, 21.03 mg omega 6 was dissolved in 1ml absolute ethanol heated to 90°C. From the stock, a 1:100 dilution was done to yield a 0.75 mM omega 6 solution a 0.75 mM palmitate solution.